

Electronic Supplementary Information for:

Redox and Photocatalytic Properties of a Ni^{II} Complex with a Macrocyclic Biquinazoline (Mabiq) Ligand

Michael Grübel, Irene Bosque, Philipp J. Altmann, Thorsten Bach,* and Corinna R. Hess*

Department of Chemistry and Catalysis Research Center (CRC)
Technische Universität München, 85747 Garching, Germany

Table of Contents

Experimental	2
Materials	2
Physical Measurements	2
Crystallographic Data	3
Density Functional Theory Calculations	4
Photochemical experiments	5
General method for the photocatalytic cyclization	6
Performance of the photocatalytic cyclization using different amines	7
Stoichiometric reaction of 2 with 3	8
Syntheses	9
Molecular Structures	24
Molecular Structure of Ni(Mabiq)OTf (1)	24
Molecular structure of Ni(Mabiq) (2)	27
Molecular structure of Cy ₂ NCH ₂ Mes (6f)	30
EPR Data for Ni(Mabiq) (2)	34
DFT Computational Data	35
ESI-MS of Ni(Mabiq)OTf (1) after the photocatalytic reaction	43
Cyclic Voltammetry (CV) experiments	44
Cyclic Voltammogram of Ni(Mabiq)OTf (1)	44
Cyclic Voltammograms for Amines 6a to 6n	45
Chemical actinometry: Determination of the photon-flux	53
Emission spectra of the LED (455 nm)	57
Determination of the quantum yield for the photoconversion of 1 to 2	58
Determination of the quantum yield for the photocatalytic conversion of 3 to 4	63
Absorption spectra of Ni(Mabiq)OTf (1) in the presence of Et ₃ N (6a) or Cy ₂ NCH ₂ Mes (6f)	65
NMR Spectra	66
References	100

Experimental

Materials

Chemicals were purchased from *Sigma Aldrich* and used without further purification, unless otherwise mentioned. Nickel containing compounds were synthesized and handled under Argon atmosphere, using Schlenk techniques or in a glovebox, using anhydrous solvents. Tetrahydrofuran (THF), diethyl ether (Et₂O), pentane (P) and dichloromethane (DCM) were purified using a MBSPS 800 *MBraun* solvent purification system. All solvents were deoxygenized via freeze-pump-thaw procedure prior to use. Dimethylformamide (DMF; 99.8% stored over molecular sieves) and Triethylamine (TEA; >99.5% BioUltra) (**6a**) were purchased as anhydrous grade from *Sigma Aldrich*. *N,N*-dimethylbenzylamine (**6h**) was purchased from *Sigma Aldrich*. Tetrabutylammonium hexafluorophosphate was recrystallized four times from EtOH before use. Ferrocene was sublimed before use.

Physical Measurements

Solution state NMR spectra were recorded at room temperature on a *Bruker* AVA 400. ¹H-NMR spectra were calibrated to the residual solvent signal of chloroform-d₁ (CHCl₃ δ = 7.26 ppm). ¹³C-NMR spectra were calibrated to the ¹³C-D triplet of CDCl₃ (δ = 77.16 ppm). The following abbreviations for single multiplicities were used: s-singlet, d-doublet, t-triplet, q-quartet, quin.-quintet. X-band EPR spectra were recorded on a JEOL JES-FA 200 spectrometer. Electronic spectra were measured on a Shimadzu UV-3600 Plus UV-vis-NIR spectrophotometer or an Agilent Cary 60 UV-vis spectrophotometer.

ESI mass spectra were measured on a Thermo Scientific™ UltiMate™ 3000 HPLC System using loop mode. Microanalyses were carried out at the Technische Universität München. Electrochemical measurements were carried out with an EmStat³⁺ potentiostat using a three-electrode cell equipped with glassy carbon working and counter electrode and a Ag/AgNO₃ or a Pt wire as reference electrode. Potentials are reported with reference to an internal standard of ferrocenium/ferrocene (Fc^{+/0}). Infrared spectra were recorded on a PerkinElmer IR 4100 spectrometer directly measuring in substance via a total reflexion method (ATR). Intensities are assigned as: w = weak, m = medium, s = strong. GC analysis was performed on an Agilent 7890B instrument (FID) with a HP 5 column (30 mm × 320 μm, 0.25 μm).

Crystallographic Data

Data were collected on an X-ray single crystal diffractometer equipped with a CMOS detector (Bruker Photon-100), a IMS microsource with MoK α radiation ($\lambda = 0.71073 \text{ \AA}$) and a Helios mirror optic by using the APEX III software package.^[1] The measurements were performed on a single crystal coated with perfluorinated ether. The crystal was fixed on top of a micro-sampler, transferred to the diffractometer and frozen under a stream of cold nitrogen. A matrix scan was used to determine the initial lattice parameters. Reflections were merged and corrected for Lorentz and polarization effects, scan speed, and background using SAINT.^[2] Absorption corrections, including odd and even ordered spherical harmonics, were performed using SADABS.^[2] Space group assignments were based upon systematic absences, E statistics, and successful refinement of the structures. Structures were solved by direct methods with the aid of successive difference Fourier maps, and were refined against all data using SHELXLE^[3] in conjunction with SHELXL-2014^[4]. Hydrogen atoms were assigned to ideal positions and refined using a riding model with an isotropic thermal parameter 1.2 times that of the attached carbon atom (1.5 times for methyl hydrogen atoms). If not mentioned otherwise, non-hydrogen atoms were refined with anisotropic displacement parameters. Full-matrix least-squares refinements were carried out by minimizing $\sum w(F_o^2 - F_c^2)^2$ with SHELXL-97^[5] weighting scheme. Neutral atom scattering factors for all atoms and anomalous dispersion corrections for the non-hydrogen atoms were taken from International Tables for Crystallography.^[6] Images of the crystal structures were generated by PLATON.^{[7]-[8]}

Density Functional Theory Calculations

Density Functional Theory (DFT) calculations were performed with the ORCA program package.^[9] Geometry optimizations of the complexes were performed at either the BP86^{[10]-[11]} (1) or the B3LYP^{[12]-[14]} (2) level of DFT. The all-electron Gaussian basis sets were those developed by the Ahlrich's group.^{[15]-[16]} Triple- ζ quality basis sets (TZV(P)) with one set of polarization functions on the metals and on the atoms directly coordinated to the metal center were used.^[16] For the carbon and hydrogen atoms, slightly smaller polarized split-valence SV(P) basis sets were used that were of double- ζ quality in the valence region and contained a polarizing set of d functions on the non-hydrogen atoms. Auxiliary basis sets used to expand the electron density in the resolution-of-the-identity (RI) approach were chosen,^{[17]-[18]} where applicable, to match the orbital basis. SCF calculations were tightly converged (1×10^{-8} Eh in energy, 1×10^{-7} Eh in the density change, and 1×10^{-7} Eh in maximum element of the DIIS error vector). Geometry optimizations were carried out in redundant internal coordinates without imposing symmetry constraints. In all cases the geometries were considered converged after the energy change was less than 5×10^{-6} Eh, the gradient norm and maximum gradient element were smaller than 1×10^{-4} and 3×10^{-4} Eh Bohr⁻¹, respectively, and the root-mean square and maximum displacements of all atoms were smaller than 2×10^{-3} and 4×10^{-3} Bohr, respectively. Orbital/spin density plots were created using GaussView.^[19]

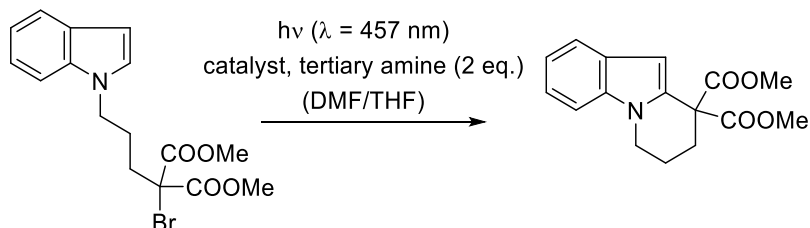
TD-DFT calculations were performed on the optimized using the B3LYP functional (Triple- ζ quality basis sets (def2-TZVP) were used for all atoms), with dichloromethane as the solvent. The conductor like screening model (COSMO) was used for all calculations and RIJCOSX approximation^[20] combined with appropriate Ahlrichs auxiliary basis sets were routinely employed to speed up the calculations.^{[17],[21]} Relativistic effects were accounted for using the zero order regular approximation (ZORA).^[22] The first 40 states were calculated, whereas the maximum dimension of the expansion space in the Davidson procedure (MAXDIM) was set to 400. The full width at half maximum (FWHM) was set to 3000 cm⁻¹.

Photochemical experiments

All photochemical experiments were carried out using the set-up previously described.^[23]

Photoconversion experiments using a LED were carried out in a preheated Schlenk tube (diameter 1 cm) with a polished quartz rod as an optical fiber, which was roughened by sandblasting at one end. 20.0 mg (267 μ mol) of [Ni(Mabiq)]OTf were dissolved in 5.0 ml of a solvent mixture (TEA/MeCN/THF: 2/2/1 or TEA/DMF: 1/4). The reaction mixture was deoxygenated once via a *freeze-pump-thaw* cycle and the glass rod was placed inside the solution under an Ar atmosphere. The solution was protected from light and the LED was switched on.

General method for the photocatalytic cyclization



A flame dried Schlenk-tube was charged with 90.7 μmol (1.00 eq.) of dimethyl 2-(3-(1H-indol-1-yl)propyl)-2-bromomalonate, 1.81 μmol (0.02 eq.) or 0.91 μmol (0.01 eq.) of catalyst and 0.18 mmol, (2.00 eq.) of the corresponding tertiary amine in 3.0 ml of a solvent mixture of THF/DMF (4/1 or 2/1). The mixture was deoxygenated three times by the freeze-pump-thaw procedure. The Schlenk-tube was equipped with the LED and the reaction was irradiated for 13 h. The reaction was stopped by addition of 5.0 ml water and 10 ml Et_2O . The aqueous phase was extracted with Et_2O (3 x 15 ml). The combined organic layers were dried over Na_2SO_4 and the solvent removed under vacuum. The residue subsequently was purified by chromatography on SiO_2 (20:1, P/EtOAc).

TLC: R_f (EtOAc/Pentane 1:4) 0.38 [UV]

The NMR data for the product are in agreement with literature values.^[24]

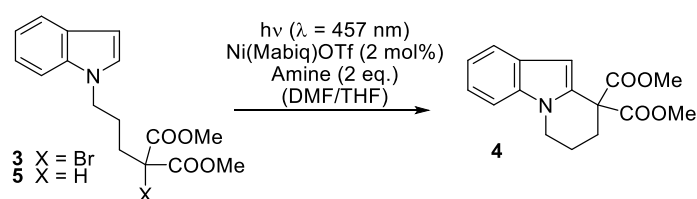
^1H NMR (400 MHz, CDCl_3 , 300K): δ (ppm) = 7.60 (dt, $^3J = 8.0, 1.0 \text{ Hz}$, 1H), 7.29 (dq, $^3J = 8.1, 0.9 \text{ Hz}$, 1H), 7.21 (ddd, $^3J = 8.2, 7.0, 1.2 \text{ Hz}$, 1H), 7.12 (ddd, $^3J = 8.0, 7.0, 1.1 \text{ Hz}$, 1H), 6.60 (d, $^3J = 0.9 \text{ Hz}$, 1H), 4.08 (t, $^3J = 6.2 \text{ Hz}$, 2H), 3.80 (s, 6H), 2.57 – 2.51 (m, 2H), 2.17 – 2.08 (m, 2H).

^{13}C NMR (101 MHz, CDCl_3 , 300K): δ (ppm) = 170.4, 136.4, 131.0, 127.6, 121.8, 120.8, 120.2, 109.2, 102.2, 56.2, 53.3, 42.0, 28.9, 19.9.

Performance of the photocatalytic cyclization using different amines

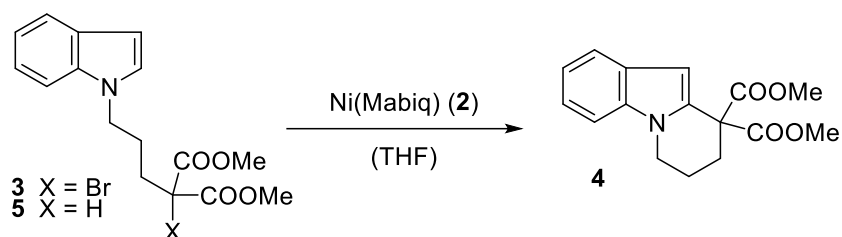
The oxidation potentials of the various amines were measured by cyclic voltammetry (see Figures S9-S22) and the photocatalytic cyclization was performed using the amines as sacrificial donors following the general method described above. The yields of **4** + **5** were obtained after column chromatography in a ratio of 95:5 cyclized to hydro-de-brominated product as determined by ¹H-NMR.

Table S1: Yields of the photocatalytic reaction using different amines with varied oxidation potentials.



Amine	$E_{1/2}$ (V vs. SCE)	Yield 4+5 [%]	Amine	$E_{1/2}$ (V vs. SCE)	Yield 4+5 [%]
	0.78 V	84%		1.22 V	84%
	0.83 V	84%		1.25 V	95%
	0.93 V	97%		1.41 V	40%
	0.99 V	89%		1.43 V	65%
	1.05 V	91%		1.59 V	20%, 21% (2 runs)
	1.05 V	97%		1.61	32%
	1.08 V	90%			
	1.20 V	85%			

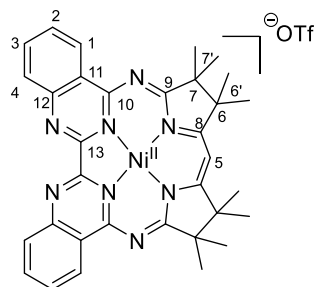
Stoichiometric reaction of **2** with **3**



In a Schlenk tube, 13.7 mg (22.8 μmol , 1.00 eq.) of **2** and 8.40 mg (22.8 μmol , 1.00 eq.) of **3** were each dissolved in 5 ml anhydrous THF. The substrate was added to the catalyst and the mixture was stirred for three hours. The reaction was stopped by adding 5 ml water. The aqueous phase was extracted with Et₂O (3 x 10 ml), the organic phase dried over Na₂SO₄ and the solvents were removed under vacuum. 3.21 mg (11.2 μmol , 49 %) of the product mixture of **4** and **5** was obtained after chromatography on SiO₂ (20:1, P/EtOAc).

Syntheses

[Ni^{II}(Mabiq)]OTf (1)



C₃₄H₃₃F₃N₈NiO₃S
Mw: 749.44 g/mol

Ni(OTf)₂ (98.6 mg, 276 μmol, 1.00 eq.) was added in one portion to a solution containing 150 mg (276 μmol, 1.00 eq.) HMabiq in 10.0 ml EtOH and 40.2 μL (290 μmol, 1.10 eq.) NEt₃. The reaction mixture was stirred for 48 h at 60°C, during which time the product precipitated as a yellow powder. The suspension was cooled to ambient temperature, and the solution was filtered. Diffusion of hexane into a solution of the crude product in DCM, yielded 175 mg (84 %, 0.23 mmol) of **1** as yellow needles suitable for X-ray analysis.

¹H NMR (400 MHz, CDCl₃, 300K): δ (ppm) = 9.15 (ddd, ³J = 8.3, ⁴J = 1.5, ⁵J = 0.59 Hz, 2H, H1), 8.50 (ddd, ³J = 8.4, ⁴J = 1.1, ⁵J = 0.6 Hz, 2H, H4), 8.20 (ddd, ³J = 8.4, ³J = 7.0, ⁴J = 1.5 Hz, 2H, H3), 7.95 (ddd, ³J = 8.3, ³J = 7.04, ⁴J = 1.1 Hz, 2H, H2), 6.77 (s, 1H, H5), 1.46 (s, 24H, H6' & H7').

¹³C NMR (101 MHz, CDCl₃, 300K): δ (ppm) = 186.8 (C8), 179.2 (C9), 155.8 (C10), 153.3 (C13), 150.2 (C11), 136.7 (C3), 130.6 (C2), 129.3 (C4), 127.2 (C1), 123.1 (C12), 97.5 (C5), 52.1 (C6), 51.8 (C7), 24.6 (C7'), 23.8 (C6')

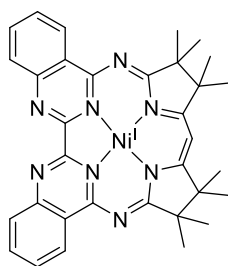
Anal. Calcd for C₃₄H₃₃F₃N₈NiO₃S (*M_r* = 749.44 g mol⁻¹): C, 54.49; H, 4.44; N, 14.95; S, 4.28 %. Found: C, 54.42; H, 4.31; N, 14.97; S, 4.21 %.

FTIR: ν cm⁻¹: 2978 (w, L), 2293 (w), 1603 (m), 1578 (m), 1562 (m), 1508 (m), 1467 (s), 1368 (m), 1262 (s, OTf), 1239 (m), 1220 (m), 1029 (s, OTf), 775 (s).

UV-Vis (in CH₂Cl₂): λ / nm 310 (ε = 44500 M⁻¹ cm⁻¹), 366 (ε = 16300 M⁻¹ cm⁻¹), 414 (ε = 13600 M⁻¹ cm⁻¹), 437 (ε = 16400 M⁻¹ cm⁻¹), 457 (ε = 22300 M⁻¹ cm⁻¹).

ESI-MS *m/z* (rel. Int. %): 599.63 (100) [⁵⁸M-OTf]⁺, 601.48 [⁶⁰M-OTf]⁺.

[Ni^I(Mabiq)] (2)



C₃₃H₃₃N₈Ni
Mw: 600.38 g/mol

A mixture of 50.0 mg (66.7 μmol , 1.00 eq.) **1** and 12.6 mg (66.7 μmol , 1.0 eq.) CoCp₂ in 10 ml MeCN was stirred for 12 h at room temperature. A distinct colour change from yellow to green was observed directly after addition of the solvent. The mixture was filtered, the solid was washed three times with 2.0 ml MeCN, and the solvent removed under reduced pressure, affording 34 mg (85 %, 56.6 μmol) of crude **2** as a green powder. Single crystals suitable for X-ray diffraction were obtained via diffusion from THF/Hexane, yielding 24 mg (62 %, 41.6 μmol) of **2**.

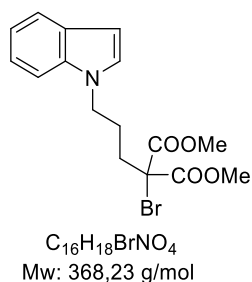
Anal. Calcd for C₃₃H₃₃N₈Ni ($M_r = 744.17 \text{ g mol}^{-1}$): C, 66.02; H, 5.54; N, 18.66; %. Found: C, 65.48; H, 5.60; N, 18.39 %.

FTIR: $\nu \text{ cm}^{-1}$: 3066 (w), 2969 (s), 2905 (m), 2863 (m), 2549 (m), 1581 (m), 1561 (m), 1525 (s), 1483 (s), 1466 (s), 1439 (s), 1387 (m), 1360 (s), 1336 (m), 1326 (m), 1313 (m), 1273 (m), 1233 (s), 1183 (m), 1151 (m), 1132 (s), 1111 (m), 1084 (m), 1067 (m), 1031 (m), 1016 (m), 966 (m), 957 (m), 932 (m), 906 (m), 870 (m), 862 (m), 848 (m), 825 (m), 796 (w), 790 (w), 766 (s), 739 (m), 726 (s), 689 (m), 675 (s), 654 (m).

UV-Vis (in THF): λ / nm : 297 ($\epsilon = 23300 \text{ M}^{-1} \text{ cm}^{-1}$), 329 ($\epsilon = 26200 \text{ M}^{-1} \text{ cm}^{-1}$), 435 ($\epsilon = 9200 \text{ M}^{-1} \text{ cm}^{-1}$), 474 ($\epsilon = 2700 \text{ M}^{-1} \text{ cm}^{-1}$), 641 ($\epsilon = 1400 \text{ M}^{-1} \text{ cm}^{-1}$), 711 ($\epsilon = 3500 \text{ M}^{-1} \text{ cm}^{-1}$), 801 ($\epsilon = 5400 \text{ M}^{-1} \text{ cm}^{-1}$).

ESI-MS m/z (rel. Int. %): 599.59 (100) [⁵⁸M]⁺, 601.51 [⁶⁰M]⁺.

Dimethyl 2-(3-(1H-indol-1-yl)propyl)-2-bromomalonate (**3**)



The compound was synthesized according to literature procedure, with the following modification.^[24] NaH was used, instead of NaHMDS, in the reaction procedure. A reaction mixture of 260 mg (0.89 mmol, 1.00 eq.) dimethyl 2-(3-(1H-indol-1-yl)propyl)-malonate, 41.3 mg (1.03 mmol, 1.15 eq.) NaH and 175 mg (0.98 mmol, 1.1 eq.) NBS in 50 ml dry THF afforded 300 mg (91 %, 0.82 mmol) **3** after purification by chromatography on SiO₂ (9:1, Pentane/EtOAc) (5 h reaction time)

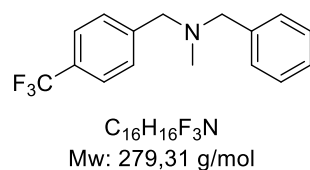
TLC: R_f (EtOAc/Pentane 1:4) 0.41 [UV]

The NMR data matched reported literature values.^[24]

¹H NMR (400 MHz, CDCl₃, 300K): δ (ppm) = 7.63 (d, ³J = 7.7 Hz, 1H), 7.32 (d, ³J = 8.3 Hz, 1H), 7.21 (t, ³J = 7.7 Hz, 1H), 7.13 – 7.08 (m, 2H), 6.50 (d, ³J = 3.1 Hz, 1H), 4.18 (t, ³J = 6.9 Hz, 2H), 3.71 (s, 6H), 2.34 – 2.25 (m, 2H), 2.06 – 1.94 (m, 2H).

¹³C NMR (101 MHz, CDCl₃, 300K): δ (ppm) = 167.2, 135.9, 128.8, 127.7, 121.7, 121.2, 119.5, 109.3, 101.5, 62.0, 54.0, 45.7, 35.7, 26.3.

***N*-benzyl-*N*-methyl-(4-trifluoromethyl)benzylamine (6b)**



To a solution of 500 mg (2.09 mmol, 1.00 eq.) 4-(Trifluoromethyl)-benzylbromide in 4.00 ml anhydrous THF, 270 μ L (253 mg, 2.09 mmol, 1.00 eq) of *N*-benzylmethylamine was added dropwise. The reaction mixture was stirred for 16 h at room temperature. The suspension was diluted in 10 mL EtOAc and treated with saturated $NaHCO_3$ solution (10 ml). The aqueous phase was extracted with EtOAc (3 x 10 ml), the combined organic phases were dried over Na_2SO_4 and the solvent was removed under reduced pressure. Purification by column chromatography (P/EtOAc 10/1 – 4/1) afforded the product. 422 mg (72%, 1.51 mmol) of the product was obtained as a yellow oil.

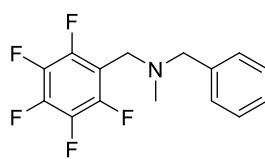
TLC: R_f (EtOAc/Pentane 1:4) 0.62 [UV]

1H NMR (400 MHz, CD_2Cl_2 , 300K): δ (ppm) = 7.59 (d, $^3J = 8.1$ Hz, 1H), 7.52 (d, $^3J = 8.1$ Hz, 1H), 7.41 – 7.29 (m, 2H), 7.28 – 7.22 (m, 1H), 3.57 (s, 1H), 3.54 (s, 1H), 2.17 (s, 2H).

^{13}C NMR (101 MHz, CD_2Cl_2 , 300K): δ (ppm) = 144.8, 139.9, 129.6, 129.4, 128.8, 127.6, 125.6 (q, $^1J = 3.9$ Hz), 62.5, 61.7, 42.6.

HRMS (ESI): $[M+H]^+$ calculated for $C_{16}H_{16}F_3N$: 280.1308; found: 280.1308.

***N*-benzyl-*N*-methyl-2,3,4,5,6-pentafluorobenzylamine (6c)**



C₁₅H₁₂F₅N
Mw: 301,26 g/mol

To a solution of 500 mg (1.92 mmol, 1.00 eq.) 2,3,4,5,6-pentafluorobenzylbromide in 4.00 ml anhydrous THF, 247 μ L (232 mg, 1.92 mmol, 1.00 eq) of *N*-benzylmethylamine was added dropwise. The reaction mixture was stirred for 16 h at room temperature. The suspension was diluted in 10 mL EtOAc and treated with saturated NaHCO₃ solution (10 ml). The aqueous phase was extracted with EtOAc (3 x 10 ml), the combined organic phases were dried over Na₂SO₄ and the solvent was removed under reduced pressure. Purification by column chromatography (P/EtOAc 10/1 – 4/1) afforded the product. 434 mg (75%, 1.44 mmol) of the product was obtained as a yellow oil.

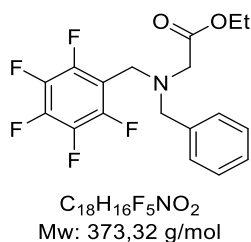
TLC: R_f (EtOAc/Pentane 1:4) 0.64 [UV]

¹H NMR (400 MHz, CD₂Cl₂, 300K): δ (ppm) = 7.35 – 7.22 (m, 5H), 3.71 (s, 2H), 3.56 (s, 2H), 2.17 (s, 3H).

¹³C NMR (101 MHz, CD₂Cl₂, 300K): δ (ppm) = 139.4, 129.4, 128.7, 127.7, 62.3, 48.6, 41.8.

HRMS (ESI): [M+H]⁺ calculated for C₁₅H₁₂F₅N: 302.0963; found: 302.0963.

Ethyl *N*-benzyl-*N*-(2,3,4,5,6-pentafluoro)benzylglycinate (**6d**)



To a flame dried 25 mL round-bottom flask containing 242 mg (2.3 mmol, 1.10 equiv.) of Na_2CO_3 , were added 5 mL of THF followed by 300 mg (1.04 mmol, 1.00 equiv.) of *N*-benzyl-2,3,4,5,6-pentafluorobenzylamine. The mixture was stirred at room temperature for 10 min. Then, 128 μ L of ethyl bromoacetate (1.15 mmol, 1.10 equiv.) were added and the reaction mixture was stirred at room temperature for 12 h. The heterogeneous mixture was filtered and the filtrate was concentrated and the crude product was purified by column chromatography (95:5 to 9:1 hexane:EtOAc) to give 356 mg of product (91% yield) as a colorless oil.

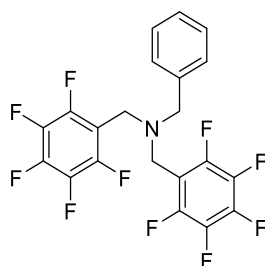
TLC: R_f (EtOAc/Pentane 1:4) 0.51 [UV]

1H NMR (400 MHz, $CDCl_3$, 400K): δ (ppm) = 7.37 – 7.27 (m, 4H), 7.30 – 7.21 (m, 1H), 4.19 (q, $^3J = 7.1$ Hz, 2H), 4.08 (s, 2H), 3.92 (s, 2H), 3.33 (s, 2H), 1.30 (t, $^3J = 7.1$ Hz, 3H).

^{13}C NMR (101 MHz, $CDCl_3$, 300K): δ (ppm) = 170.9, 145.7 (d, $^1J = 247.1$ Hz), 140.6 (d, $^1J = 253.3$ Hz), 138.3, 137.2 (d, $^1J = 252.8$ Hz), 128.7, 128.3, 127.4, 111.9 (t, $^1J = 19.0$ Hz), 60.4, 57.9, 53.1, 44.9, 14.2.

HRMS (ESI): $[M+H]^+$ calculated for $C_{18}H_{16}F_5NO_2$: 374.1174; found: 374.1174.

***N,N*-bis-(2,3,4,5,6-pentafluorobenzyl)benzylamine (6e)**



C₂₁H₁₁F₁₀N
Mw: 467,31 g/mol

To a flame dried 25 mL round-bottom flask containing 439 mg (8.4 mmol, 2.10 equiv.) of Na₂CO₃, were added 5 mL of THF followed by 1.25 mL (8.4 mmol, 2.10 equiv.) of 2,3,4,5,6-pentafluorobenzyl bromide. The mixture was stirred at room temperature for 10 min. 440 μL (4.02 mmol) of benzylamine were added and the reaction mixture was stirred at room temperature for 12 h. The heterogeneous mixture was filtered and the filtrate was concentrated. The crude product was purified by column chromatography (95:5 to 9:1 hexane:EtOAc) to give 1.30 g of an inseparable 1:2 mixture of desired product and 2,3,4,5,6-pentafluorobenzyl bromide as a colorless oil, and 509 mg (44% yield) of *N*-benzyl-*N*-(2,3,4,5,6-pentafluorobenzyl)amine as a white solid. The desired product was separated from the excess 2,3,4,5,6-pentafluorobenzyl bromide by the addition of this mixture to a stirred mixture of 316 μL (2.9 mmol, 1 equiv. with respect to the remaining 2,3,4,5,6-pentafluorobenzyl bromide) of benzylamine and 307 mg (2.9 mmol, 1 equiv. with respect to the remaining 2,3,4,5,6-pentafluorobenzyl bromide) of Na₂CO₃ in 5 mL of THF. The reaction mixture was stirred for 12 h and subsequently filtered. The filtrate was evaporated and the crude material was purified by column chromatography (95:5 to 9:1 hexane:EtOAc) to give 660 mg of **6e** (37% yield after the two steps) as a colorless oil, and 631 mg (76% yield) of *N*-benzyl-*N*-perfluorobenzylamine as a white solid.

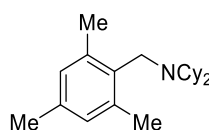
TLC: R_f (EtOAc/Pentane 1:9) 0.62 [UV]

¹H NMR (400 MHz, CDCl₃, 300K): δ (ppm) = 7.38 – 7.11 (m, 5H), 3.78 (s, 4H), 3.64 (s, 2H).

¹³C NMR (101 MHz, CDCl₃, 300K): δ (ppm) 145.63 (d, ¹J = 240.1 Hz), 140.7 (d, ¹J = 254.0 Hz), 137.9, 137.3 (d, ¹J = 253.0 Hz), 128.3, 128.1, 127.4, 111.7 (t, ¹J = 17.3 Hz), 58.3, 45.7.

HRMS (ESI): [M+H]⁺ calculated for C₂₁H₁₁F₁₀N: 468.0805; found: 468.0804.

***N*-(2,4,6-trimethylbenzyl)dicyclohexylamine (6f)**



$C_{22}H_{35}N$
Mw: 313,28 g/mol

To a suspension of 400 mg (2.9 mmol, 2.90 eq.) in 2.00 ml anhydrous DMF in a pressure tube, 600 μ L (3.00 mmol, 3.00 eq) of dicyclohexylamine were added followed by 169 mg (1.00 mmol, 1.00 eq) of 2,4,6-trimethylbenzyl chloride. The tube was sealed and the reaction mixture was stirred for 72 h at 140 °C. The mixture was allowed to reach room temperature and the suspension was diluted in 10 mL EtOAc and filtered. The filtrate was concentrated under reduced pressure. Purification by column chromatography (pentane/EtOAc 40:1) afforded 131 mg of product (42%, 0.42 mmol) as a white solid. Further recrystallization from DMF afforded the product as colorless needles.

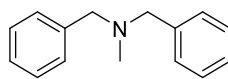
TLC: R_f (pentane/EtOAc 30:1) 0.48 [UV]

1H NMR (400 MHz, $CDCl_3$, 300K): δ (ppm) = 6.78 (s, 2H), 3.72 (s, 2H), 2.44 – 2.37 (m, 2H), 2.36 (s, 6H), 2.25 (s, 3H), 1.78 – 1.64 (m, 8H), 1.60 – 1.52 (m, 2H), 1.49 – 1.29 (m, 4H), 1.25 – 0.96 (m, 6H).

^{13}C NMR (101 MHz, $CDCl_3$, 300K): δ (ppm) = 138.3, 135.5, 133.8, 128.9, 56.5, 43.7, 32.1, 26.68, 26.3, 20.8, 20.3.

HRMS (ESI): $[M+H]^+$ calculated for $C_{22}H_{36}N$: 314.2842; found: 314.2841.

***N*-benzyl-*N*-methylbenzylamine (6g)**



C₁₅H₁₇N
Mw: 211,31 g/mol

To a solution of 347 μ l (500 mg, 2.92 mmol, 1.00 eq.) benzylbromide in 4.00 ml anhydrous THF, 377 μ l (354 mg, 2.92 mmol, 1.00 eq) of *N*-benzylmethylamine was added dropwise. The reaction mixture was stirred for 16 h at room temperature. The suspension was diluted in 10 mL EtOAc and treated with saturated NaHCO₃ solution (10 ml). The aqueous phase was extracted with EtOAc (3 x 10 ml), the combined organic phases were dried over Na₂SO₄ and the solvent was removed under reduced pressure. Purification by column chromatography (P/EtOAc 10/1 – 4/1) afforded the product. 512 mg (83%, 2.42 mmol) of the product was obtained as a yellow oil.

TLC: R_f (EtOAc/Pentane 1:4) 0.54 [UV]

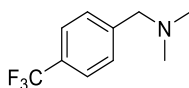
¹H NMR (400 MHz, CDCl₃, 300K): δ (ppm) = 7.44 – 7.18 (m, 10H), 3.53 (s, 4H), 2.19 (s, 3H).

¹³C NMR (101 MHz, CDCl₃, 300K): δ (ppm) = 139.5, 129.1, 128.4, 127.1, 62.0, 42.4.

The NMR data matched reported literature values.^[25]

HRMS (ESI): [M+H]⁺ calculated for C₁₅H₁₇N: 212.1434; found: 212.1434.

***N,N*-dimethyl-(4-trifluoromethyl)benzylamine (6i)**



C₁₀H₁₂F₃N
Mw: 203,21 g/mol

To a solution of 1.00 g (4.18 mmol, 1.00 eq.) of 4-(Trifluoromethyl)benzylbromide in 4.00 ml anhydrous Et₂O, 4.14 ml (3.14 g, 20.9 mmol, 5.00 eq.) of a 30 wt% Diethylamine solution was added in one portion. The reaction mixture was stirred for 12 h at room temperature. The suspension was diluted in 10 ml Et₂O and extracted with 1 M HCl solution. The combined aqueous phases were neutralized with 2 M NaOH solution until a precipitate formed. The aqueous phase was then extracted with 20 ml Et₂O. The combined organic phases were dried over Na₂SO₄ and the solvent was removed under reduced pressure. 838 mg (98%, 4.12 mmol) of the **6h** was obtained as a clear oil.

TLC: R_f (EtOAc/Pentane 1:4) 0.41 [UV]

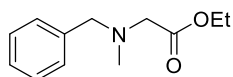
¹H NMR (400 MHz, CDCl₃, 300K): δ (ppm) = 7.57 (d, ³J = 8.0 Hz, 2H), 7.43 (d, ³J = 8.0 Hz, 2H), 3.47 (s, 2H), 2.25 (s, 6H).

¹³C NMR (101 MHz, CDCl₃, 300K): δ (ppm) = 143.2, 129.14, 125.2 (q, ¹J = 3.8 Hz), 63.8, 45.4.

The NMR data matched reported literature values.^[26]

HRMS (ESI): [M+H]⁺ calculated for C₁₀H₁₂F₃N: 204.0995; found: 204.0995

Ethyl *N*-benzyl-*N*-methylglycinate (6j)



C₁₂H₁₇NO₂
Mw: 207,27 g/mol

To a solution of 1.93 ml (1.81 g, 15.0 mmol, 1.25 eq.) *N*-benzylmethylamine in 20.0 ml anhydrous MeCN, 1.33 mL (2.00 g, 12.0 mmol, 1.00 eq) of ethylbromoacetate was added dropwise at 0°C. The reaction mixture was stirred for 16 h at room temperature. The suspension was diluted in 20 mL Et₂O and treated with NaHCO₃ solution (40 ml). The aqueous phase was extracted with Et₂O (3 x 30 ml), the combined organic phases were dried over Na₂SO₄ and the solvent was removed under reduced pressure. Purification by column chromatography (P/EtOAc 10/1 – 4/1) afforded the product. 1.26 g (51%, 6.08 mmol) of the product was obtained as a yellow oil.

TLC: R_f (EtOAc/Pentane 1:4) 0.58 [UV]

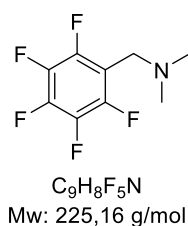
¹H NMR (400 MHz, CDCl₃, 300K): δ (ppm) = 7.38 – 7.21 (m, 5H), 4.18 (q, ³J = 7.1 Hz, 2H), 3.68 (s, 2H), 3.25 (s, 2H), 2.39 (s, 3H), 1.27 (t, ³J = 7.1 Hz, 3H).

¹³C NMR (101 MHz, CDCl₃, 300K): δ (ppm) = 171.1, 138.3, 129.3, 128.4, 127.3, 61.3, 60.5, 57.7, 42.4, 14.4.

The NMR data matched reported literature values.^[27]

HRMS (ESI): [M+H]⁺ calculated for C₁₂H₁₇NO₂: 208.1332; found: 208.1332.

***N,N*-dimethyl-2,3,4,5,6-pentafluorobenzylamine (6k)**



To a solution of 1.00 g (3.83 mmol, 1.00 eq.) of 2,3,4,5,6-Pentafluorobenzylbromide in 4.00 ml anhydrous Et₂O, 3.79 ml (2.88 g, 19.2 mmol, 5.00 eq.) of a 30 w% diethylamine solution was added in one portion. The reaction mixture was stirred for 12 h at room temperature. The suspension was diluted in 10 ml Et₂O and extracted with 1 M HCl solution. The combined water phases were neutralized with 2 M NaOH solution until a precipitate formed. The aqueous phase was extracted with 20 ml Et₂O. The combined organic phases were dried over Na₂SO₄ and solvent removed under reduced pressure. 830 mg (96%, 3,69 mmol) of the product was obtained as a clear oil.

TLC: R_f (EtOAc/Pentane 1:4) 0.41 [UV]

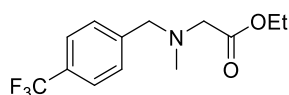
¹H NMR (400 MHz, CDCl₃, 300K): δ (ppm) = 7.57 (d, ³J = 8.0 Hz, 1H), 7.43 (d, ³J = 8.0 Hz, 1H), 3.47 (s, 1H), 2.25 (s, 3H).

¹³C NMR (126 MHz, CDCl₃, 300K): δ (ppm) = 145.5 (dddd, ¹J = 247.4, ²J = 13.8, ²J = 8.6, ⁴J = 4.0 Hz), 140.5 (dddd, ¹J = 253.4, ²J = 18.9, ³J = 12.7, ⁴J = 5.4 Hz), 137.3 (dddd, ¹J = 251.1, ²J = 17.6, ³J = 12.5, ⁴J = 4.8 Hz), 110.8 (td, ²J = 18.7, ³J = 3.7 Hz), 49.4, 44.5.

The NMR data matched reported literature values.^[28]

HRMS (ESI): [M+H]⁺ calculated for C₁₀H₁₂F₅N: 204.0995; found: 204.0995.

Ethyl *N*-(4-trifluoromethyl)benzyl-*N*-methylglycinate (6l)



C₁₃H₁₆F₃NO₂
Mw: 275,27 g/mol

To a solution of 856 mg (3.58 mmol, 1.10 eq.) 4-(Trifluoromethyl)-benzylbromide and 288 μ l (282 mg, 3.58 mmol, 1.10 eq.) pyridin in 10 ml anhydrous CH₂Cl₂, 500 mg (3.26 mmol, 1.00 eq) of sarcosineethylester hydrochloride in 10 ml anhydrous CH₂Cl₂ was added dropwise at 0°C. The reaction mixture was stirred for 16 h at room temperature. The suspension was diluted in 25 mL CH₂Cl₂ and treated with saturated NaHCO₃ solution (25 ml). The aqueous phase was extracted with CH₂Cl₂ (3 x 20 ml), the combined organic phases were dried over Na₂SO₄ and the solvent was removed under reduced pressure. Purification by column chromatography (P/EtOAc 10/1 – 4/1) afforded the product. 312 mg (35%, 1.13 mmol) of the product could be obtained as a yellow oil.

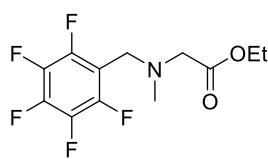
TLC: R_f (EtOAc/Pentane 1:4) 0.58 [UV]

¹H NMR (400 MHz, CDCl₃, 300K): δ (ppm) = 7.57 (d, ³J = 8.0 Hz, 2H), 7.47 (d, ³J = 8.0 Hz, 2H), 4.18 (q, ³J = 7.1 Hz, 2H), 3.74 (s, 2H), 3.27 (s, 2H), 2.38 (s, 3H), 1.28 (t, ³J = 7.1 Hz, 3H).

¹³C NMR (101 MHz, CDCl₃, 300K): δ (ppm) = 171.0, 142.9, 129.3, 125.4 (q, ¹J = 3.8 Hz), 60.7, 60.6, 57.9, 42.4, 14.4.

HRMS (ESI): [M+H]⁺ calculated for C₁₃H₁₆F₃NO₂: 276.1206; found: 276.1206.

Ethyl *N*-methyl-*N*-(2,3,4,5,6-pentafluoro)benzylglycinate (6m)



C₁₂H₁₂F₅NO₂
Mw: 297,23 g/mol

To a solution of 934 mg (3.58 mmol, 1.10 eq.) 2,3,4,5,6-pentafluorobenzoylbromide and 288 μ l (283 mg, 3.58 mmol, 1.10 eq.) pyridin in 10 ml anhydrous CH₂Cl₂, 500 mg (3.26 mmol, 1.00 eq) of sarcosineethylester hydrochloride in 10 ml anhydrous CH₂Cl₂ was added dropwise at 0°C. The reaction mixture was stirred for 16 h at room temperature. The suspension was diluted in 25 mL CH₂Cl₂ and treated with saturated NaHCO₃ solution (25 ml). The aqueous phase was extracted with CH₂Cl₂ (3 x 20 ml), the combined organic phases were dried over Na₂SO₄ and the solvent was removed under reduced pressure. Purification by column chromatography (P/EtOAc 10/1 – 4/1) afforded the product. 161 mg (17%, 542 μ mol) of the product was obtained as a yellow oil.

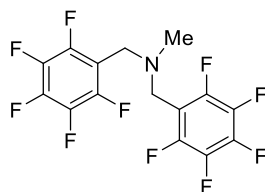
TLC: R_f (EtOAc/Pentane 1:4) 0.54 [UV]

¹H NMR (400 MHz, CDCl₃, 300K): δ (ppm) = 4.19 (q, ³J = 7.1 Hz, 2H), 3.93 (s, 2H), 3.30 (s, 2H), 2.40 (s, 3H), 1.28 (t, ³J = 7.1 Hz, 3H).

¹³C NMR (101 MHz, CDCl₃, 300K): δ (ppm) = 170.6, 145.8 (dddd, ¹J = 247.5, ²J = 15.0, ³J = 8.5, ⁴J = 4.1 Hz), 140.8 (ddd, ¹J = 253.5, ²J = 13.3, ³J = 2.5 Hz), 137.5 (ddd, ¹J = 251.1, ²J = 17.6, ³J = 12.5 Hz), 110.3 (td, ²J = 18.7, ³J = 3.7 Hz), 60.8, 57.5, 47.0, 41.7, 14.4.

HRMS (ESI): [M+H]⁺ calculated for C₁₂H₁₂F₅NO₂: 298.0861; found: 298.0861.

***N,N*-bis-(2,3,4,5,6-pentafluorobenzyl)methylamine (6n)**



C₁₅H₇F₁₀N
Mw: 391,04 g/mol

To a flame dried 25 mL round-bottom flask containing 773 mg (5.6 mmol, 2.1 equiv.) of K₂CO₃ were added 5 mL of THF followed by 850 μL (5.6 mmol, 2.1 equiv.) of 2,3,4,5,6-pentafluorobenzyl bromide. The mixture was stirred at room temperature for 10 min. 1.34 mL of a 2M solution of methylamine in THF (2.7 mmol, 1 equiv.) were added and the reaction mixture was stirred at room temperature for 72 h. The heterogeneous mixture was filtered and the filtrate was concentrated. The crude product was purified by column chromatography (98:2 to 95:5 hexane:EtOAc) to give 942 mg of product (89% yield) as a colorless oil.

TLC: R_f (EtOAc/Pentane 1:9) 0.62 [UV]

¹H NMR (400 MHz, CDCl₃, 300K): δ (ppm) = 3.77 (s, 4H), 2.24 (s, 3H)

¹³C NMR (101 MHz, CDCl₃, 300K): δ (ppm) = 145.8 (dddd, ¹J = 247.8, ²J = 14.9, ³J = 8.3, ⁴J = 4.0 Hz), 141.0 (dddd, ¹J = 253.7, ²J = 18.7, ³J = 13.3, ⁴J = 5.3 Hz), 138.6 (ddd, ¹J = 251.1, ²J = 17.6, ³J = 12.5 Hz), 111.2 (t, ²J = 17.9 Hz), 48.0, 40.7.

HRMS (ESI): [M+H]⁺ calculated for C₁₅H₇F₁₀N: 392.0492; found: 392.0492.

Molecular Structures

Molecular Structure of Ni(Mabiq)OTf (1)

A clear yellow fragment-like specimen of $C_{35}H_{35}Cl_2F_3N_8NiO_3S$, approximate dimensions 0.110 mm x 0.126 mm x 0.245 mm, was used for the X-ray crystallographic analysis. The X-ray intensity data were measured on a Bruker D8 Venture Duo IMS system equipped with a Helios optic monochromator and a Mo IMS microsource ($\lambda = 0.71073 \text{ \AA}$).

A total of 1843 frames were collected. The total exposure time was 15.36 hours. The frames were integrated with the Bruker SAINT software package using a narrow-frame algorithm. The integration of the data using a triclinic unit cell yielded a total of 39797 reflections to a maximum θ angle of 25.68° (0.82 \AA resolution), of which 6667 were independent (average redundancy 5.969, completeness = 99.80, $R_{int} = 3.990$, $R_{sig} = 2.510$) and 5772 (86.580) were greater than $2\sigma(F_2)$. The final cell constants of $a = 10.0222(8) \text{ \AA}$, $b = 12.1506(11) \text{ \AA}$, $c = 16.0254(14) \text{ \AA}$, $\alpha = 69.063(4)^\circ$, $\beta = 75.075(4)^\circ$, $\gamma = 81.389(4)^\circ$, volume = $1757.6(3) \text{ \AA}^3$, are based upon the refinement of the XYZ-centroids of 125 reflections above $2\sigma(I)$ with $4.544^\circ < 2\theta < 43.92^\circ$. Data were corrected for absorption effects using the Multi-Scan method (SADABS). The ratio of minimum to maximum apparent transmission was 0.933. The calculated minimum and maximum transmission coefficients (based on crystal size) are 0.8230 and 0.9140.

The structure was solved and refined using the Bruker SHELXTL Software Package in conjunction with SHELXLE, using the space group $P -1$, with $Z = 2$ for the formula unit, $C_{35}H_{35}Cl_2F_3N_8NiO_3S$. The final anisotropic full-matrix least-squares refinement on F_2 with 725 variables converged at $R_1 = 2.880$, for the observed data and $wR_2 = 7.550$ for all data. The goodness-of-fit was 1.032. The largest peak in the final difference electron density synthesis was $0.451 \text{ e}/\text{\AA}^3$ and the largest hole was $-0.438 \text{ e}/\text{\AA}^3$ with an RMS deviation of $0.053 \text{ e}/\text{\AA}^3$. On the basis of the final model, the calculated density was $1.577 \text{ g}/\text{cm}^3$ and $F(000)$, 860 e $^-$.

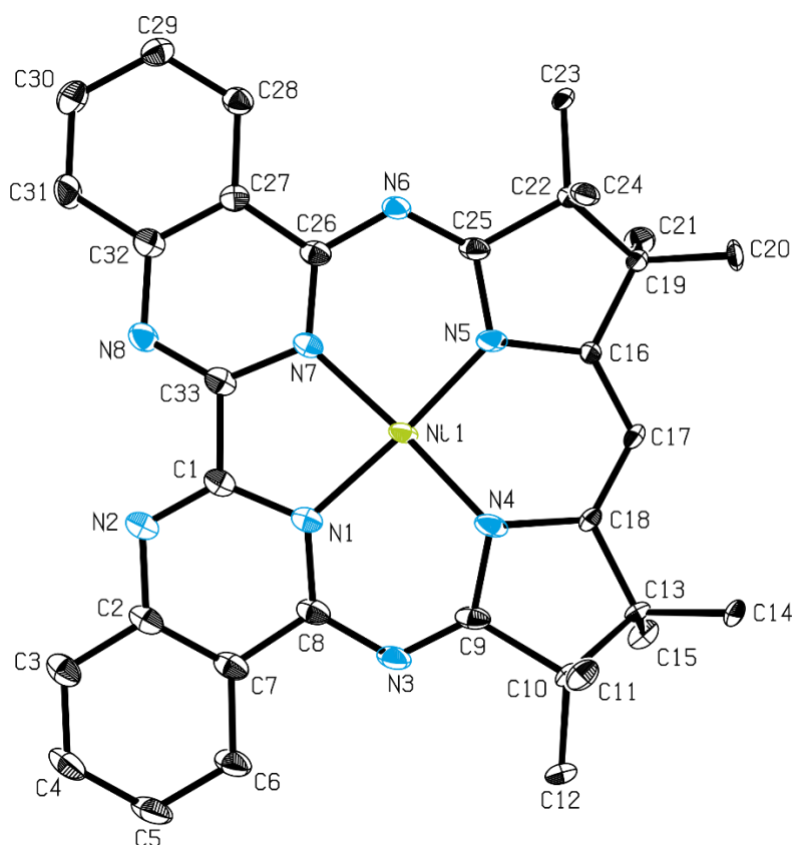


Figure S1: ORTEP style representation of **1**. Ellipsoids are shown at the 50% probability level. Hydrogen atoms, dichloromethane molecule and triflate counterion are omitted for clarity.

Table S2: Sample and crystal data for **1**.

Identification code	GruMi1 AP8017-100	
Chemical formula	$C_{35}H_{35}Cl_2F_3N_8NiO_3S$	
Formula weight	834.38	
Temperature	100 (2) K	
Wavelength	0.71073 Å	
Crystal size	0.110 x 0.126 x 0.245 mm	
Crystal habit	Clear yellow fragment	
Crystal system	Triclinic	
Space group	P -1	
Unit cell dimensions	a = 10.0222 (8) Å	$\alpha = 69.063 (4)$
	b = 12.1506 (11) Å	$\beta = 75.075 (4)$
	c = 16.0254 (14) Å	$\gamma = 81.389 (4)$
Volume	1757.6 (3) Å ³	
Z	2	
Density	1.577 g/cm ³	
Absorption	0.839 mm ⁻¹	
F (000)	860	

Table S3: Data collection and structure refinement of **1**.

Diffractometer	Bruker D8 Venturo Duo IMS		
Radiation source	IMS microsource, Mo		
Theta range for data collection	2.48 to 25.68°		
Index ranges	-12<=h<=12, -14<=k<=14, -19<=l<=19		
Reflections collected	39797		
Independent reflections	667 [R(int) = 0.0399]		
Coverage of independent reflections	99.8 %		
Absorption correction	Multi-Scan		
Max. and. Min. transmission	0.9149 and 0.8230		
Structure solution technique	Direct methods		
Structure solution program	XT, VERSION 2014/4		
Refinement method	Full-matrix least-squares on F ²		
Refinement program	SHELXL-2014/7 (Sheldrick, 2014)		
Function minimized	$\sum w (F_o^2 - F_c^2)^2$		
Data/ restraints / parameters	6667 / 381 / 725		
Goodness-of-fit on F²	1.032		
Δ / σ_{\max}	0.001		
Final R indices	5772 data; I>2 σ	R1 = 0.0288,	wR2 = 0.0711
	All data	R1 = 0.0375	wR2 = 0.0755
Weighting scheme	$w = 1/[\sigma^2/(F_o^2) + (0.0390P)^2 + 0.9346P]$		
	Where P = (F _o ² + 2F _c ²)/3		
Largest diff. peak and hole	0.451 and -0.438 eÅ ⁻³		
R.M.S. deviation from mean	0.053 eÅ ⁻³		

Molecular structure of Ni(Mabiq) (2)

A green needle-like specimen of $C_{33}H_{33}N_8Ni$, approximate dimensions 0.040 mm x 0.055 mm x 0.417 mm, was used for the X-ray crystallographic analysis. The X-ray intensity data were measured on a Bruker D8 Venture Duo IMS system equipped with a Helios optic monochromator and a Mo IMS microsource ($\lambda = 0.71073 \text{ \AA}$).

A total of 2322 frames were collected. The total exposure time was 58.05 hours. The frames were integrated with the Bruker SAINT software package using a narrow-frame algorithm. The integration of the data using an orthorhombic unit cell yielded a total of 192057 reflections to a maximum θ angle of 25.03° (0.84 \AA resolution), of which 9767 were independent (average redundancy 19.664, completeness = 99.9%, $R_{int} = 8.57\%$, $R_{sig} = 3.29\%$) and 8669 (88.76%) were greater than $2\sigma(F_2)$. The final cell constants of $a = 10.1802(7) \text{ \AA}$, $b = 20.4136(17) \text{ \AA}$, $c = 26.689(2) \text{ \AA}$, volume = $5546.4(7) \text{ \AA}^3$, are based upon the refinement of the XYZ-centroids of 9623 reflections above $2\sigma(I)$ with $4.471^\circ < 2\theta < 50.39^\circ$. Data were corrected for absorption effects using the Multi-Scan method (SADABS). The ratio of minimum to maximum apparent transmission was 0.875. The calculated minimum and maximum transmission coefficients (based on crystal size) are 0.7480 and 0.9710.

The structure was solved and refined using the Bruker SHELXTL Software Package in conjunction with SHELXLE, using the space group P 21 21 21, with $Z = 8$ for the formula unit, $C_{33}H_{33}N_8Ni$. The final anisotropic full-matrix least-squares refinement on F_2 with 773 variables converged at $R_1 = 3.08\%$, for the observed data and $wR_2 = 6.73\%$ for all data. The goodness-of-fit was 0.946. The largest peak in the final difference electron density synthesis was $0.221 \text{ e}/\text{\AA}^3$ and the largest hole was $-0.312 \text{ e}/\text{\AA}^3$ with an RMS deviation of $0.052 \text{ e}/\text{\AA}^3$. On the basis of the final model, the calculated density was $1.438 \text{ g}/\text{cm}^3$ and $F(000)$, 2520 e $^-$.

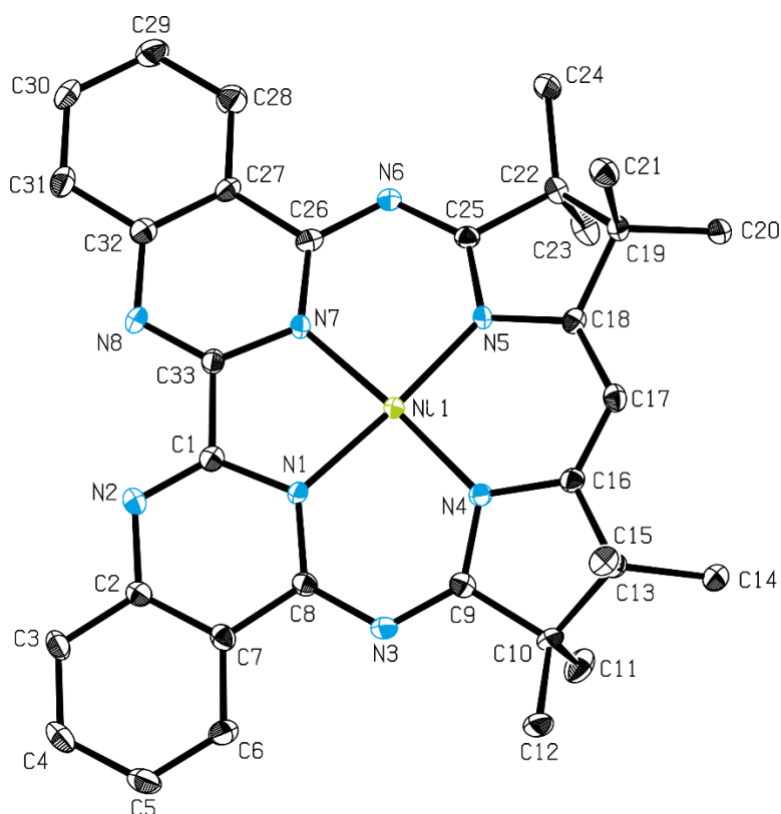


Figure S2: ORTEP style representation of **2**. Ellipsoids are shown at the 50% probability level. Hydrogen atoms are omitted for clarity.

Table S4: Sample and Crystal data for **2**.

Identification code	GruMi1 AP8030-100	
Chemical formula	$C_{33}H_{33}N_8Ni$	
Formula weight	600.38	
Temperature	100 (2) K	
Wavelength	0.71073 Å	
Crystal size	0.040 x 0.055 x 0.417 mm	
Crystal habit	Green needle	
Crystal system	Orthorhombic	
Space group	P 21 21 21	
Unit cell dimensions	$a = 10.1802 (7) \text{ \AA}$	$\alpha = 90^\circ$
	$b = 20.4136 (17) \text{ \AA}$	$\beta = 90^\circ$
	$c = 26.689 (2) \text{ \AA}$	$\gamma = 90^\circ$
Volume	$5546.4 (7) \text{ \AA}^3$	
Z	8	
Density	1.438 g/cm^3	
Absorption	0.740 mm^{-1}	
F (000)	2520	

Table S5: Data collection and structure refinement for **2**.

Diffractometer	Bruker D8 Venturo Duo IMS		
Radiation source	IMS microsource, Mo		
Theta range for data collection	2.24 to 25.03°		
Index ranges	-12<=h<=12, -24<=k<=24, -31<=l<=31		
Reflections collected	192057		
Independent reflections	9767 [R(int) = 0.0857]		
Coverage of independent reflections	99.9 %		
Absorption correction	Multi-Scan		
Max. and. Min. transmission	0.9710 and 0.7480		
Structure solution technique	Direct methods		
Structure solution program	XT, VERSION 2014/4		
Refinement method	Full-matrix least-squares on F ²		
Refinement program	SHELXL-2014/7 (Sheldrick, 2014)		
Function minimized	$\Sigma w (F_o^2 - F_c^2)^2$		
Data/ restraints / parameters	9767 / 0 / 773		
Goodness-of-fit on F²	0.946		
Δ / σ_{\max}	0.001		
Final R indices	8669 data; $l > 2\sigma$	R1 = 0.0308,	wR2 = 0.0632
	All data	R1 = 0.0410	wR2 = 0.0673
Weighting scheme	$w = 1/[\sigma^2/(F_o^2) + (0.0248P)^2 + 6.2581P]$		
	Where $P = (F_o^2 + 2F_c^2)/3$		
Absolute structure parameter	0.5 (0)		
Largest diff. peak and hole	0.221 and -0.312 eÅ ⁻³		
R.M.S. deviation from mean	0.052 eÅ ⁻³		

Molecular structure of $\text{Cy}_2\text{NCH}_2\text{Mes}$ (6f)

A clear colourless fragment-like specimen of $\text{C}_{22}\text{H}_{35}\text{N}$, approximate dimensions 0.136 mm x 0.139 mm x 0.174 mm, was used for the X-ray crystallographic analysis. The X-ray intensity data were measured on a Bruker D8 Venture system equipped with a Helios optic monochromator and a Mo TXS rotating anode ($\lambda = 0.71073 \text{ \AA}$).

A total of 1272 frames were collected. The total exposure time was 1.57 hours. The frames were integrated with the Bruker SAINT software package using a narrow-frame algorithm. The integration of the data using a monoclinic unit cell yielded a total of 33127 reflections to a maximum θ angle of 25.03° (0.84 \AA resolution), of which 3359 were independent (average redundancy 9.862, completeness = 99.9%, $R_{\text{int}} = 3.67\%$, $R_{\text{sig}} = 1.81\%$) and 2978 (88.66%) were greater than $2\sigma(F_2)$. The final cell constants of $a = 17.6983(15) \text{ \AA}$, $b = 6.2954(6) \text{ \AA}$, $c = 17.4420(15) \text{ \AA}$, $\beta = 102.677(3)^\circ$, volume = $1896.0(3) \text{ \AA}^3$, are based upon the refinement of the XYZ-centroids of 117 reflections above $20 \sigma(I)$ with $7.564^\circ < 2\theta < 48.35^\circ$. Data were corrected for absorption effects using the Multi-Scan method (SADABS). The ratio of minimum to maximum apparent transmission was 0.905. The calculated minimum and maximum transmission coefficients (based on crystal size) are 0.9890 and 0.9920.

The final anisotropic full-matrix least-squares refinement on F^2 with 211 variables converged at $R_1 = 3.92\%$, for the observed data and $wR_2 = 10.02\%$ for all data. The goodness-of-fit was 1.061. The largest peak in the final difference electron density synthesis was $0.180 \text{ e}/\text{\AA}^3$ and the largest hole was $-0.202 \text{ e}/\text{\AA}^3$ with an RMS deviation of $0.038 \text{ e}/\text{\AA}^3$. On the basis of the final model, the calculated density was $1.098 \text{ g}/\text{cm}^3$ and $F(000)$, 696 e $^-$.

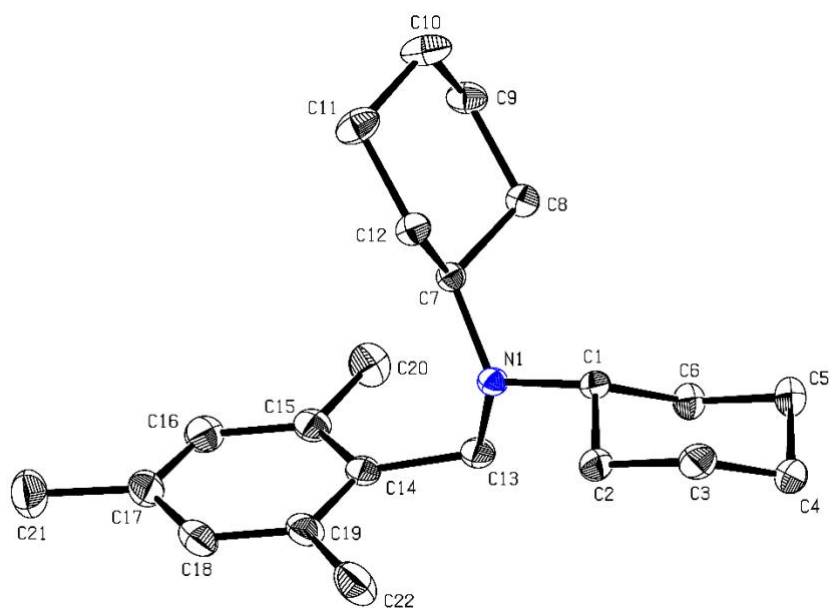


Figure S3: ORTEP style representation of **6f**. Ellipsoids are shown at the 50% probability level. Hydrogen atoms are omitted for clarity.

Table S6: Sample and Crystal data for **6f**.

Identification code	GruMi20 AP9266-135	
Chemical formula	C ₂₂ H ₃₅ N	
Formula weight	313.51	
Temperature	135 (2) K	
Wavelength	0.71073 Å	
Crystal size	0.136 x 0.139 x 0.174 mm	
Crystal habit	Clear colourless fragment	
Crystal system	monoclinic	
Space group	P 1 21/c1	
Unit cell dimensions	a = 17.6983 (15) Å	α = 90°
	b = 6.2954 (6) Å	β = 102.677 (3)°
	c = 17.4420 (15) Å	γ = 90°
Volume	1896.0 (7) Å ³	
Z	4	
Density	1.098 g/cm ³	
Absorption	0.062 mm ⁻¹	
F (000)	696	

Table S7: Data collection and structure refinement for **6f**.

Diffractometer	Bruker D8 Venturo
Radiation source	TXS rotating anode, Mo
Theta range for data collection	2.36 to 25.03°
Index ranges	-21 ≤ h ≤ 21, -7 ≤ k ≤ 7, -20 ≤ l ≤ 20
Reflections collected	33127
Independent reflections	3359 [R(int) = 0.0367]
Coverage of independent reflections	99.9 %
Absorption correction	Multi-Scan
Max. and. Min. transmission	0.9920 and 0.9890

Structure solution technique	Direct method		
Structure solution program	XT, VERSION 2014/4		
Refinement method	Full-matrix least-squares on F^2		
Refinement program	SHELXL-2014/7 (Sheldrick, 2014)		
Function minimized	$\sum w (F_0^2 - F_c^2)^2$		
Data/ restraints / parameters	3359 / 0 / 221		
Goodness-of-fit on F^2	1.061		
Δ / σ_{\max}	0.001		
Final R indices	2978 data; $I > 2\sigma$	R1 = 0.0391,	wR2 = 0.0964
	All data	R1 = 0.0445	wR2 = 0.1002
Weighting scheme	$w = 1/[\sigma^2/(F_0^2) + (0.0455P)^2 + 0.7786P]$		
	Where $P = (F_0^2 + 2F_c^2)/3$		
Absolute structure parameter	0.5 (0)		
Largest diff. peak and hole	0.180 and -0.202 $e\text{\AA}^{-3}$		
R.M.S. deviation from mean	0.038 $e\text{\AA}^{-3}$		

Table S8: Selected bond distances for **1** and **2**.

	1	2
Ni1-N5	1.8599(15)	1.871(3)
Ni1-N4	1.8599(16)	1.873(3)
Ni1-N7	1.8861(15)	1.891(3)
Ni1-N1	1.8885(14)	1.894(3)
N3-C9	1.288(2)	1.313(5)
N4-C9	1.372(2)	1.352(5)
N4-C18	1.481(4)(N4-C18a 1.302(4))	1.390(5)
N6-C25	1.285(2)	1.314(5)
N5-C25	1.363(2)	1.351(5)
N5-C16	1.482(4)(N5-C16a 1.297(4))	1.389(5)
C16-C17	1.381(4)(C16a-C17a 1.386(4))	1.374(5)
C17-C18	1.375(5)(C17a-C18a 1.383(5))	1.370(5)
C16-C19	1.516(4)	1.516(5)
C13-C18	1.519(4)	1.513(5)

EPR Data for Ni(Mabiq) (2)

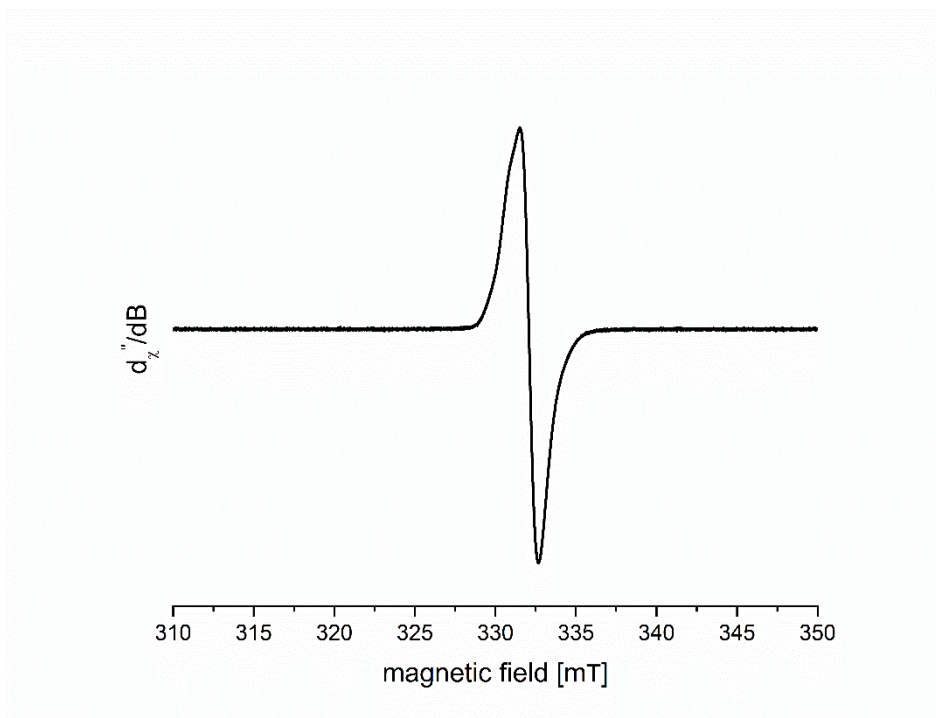


Figure S4: EPR data for **2** in THF at 140 K, frequency = 9.265 GHz, mod. Amp. = 100 G, power = 0.4 mW

DFT Computational Data

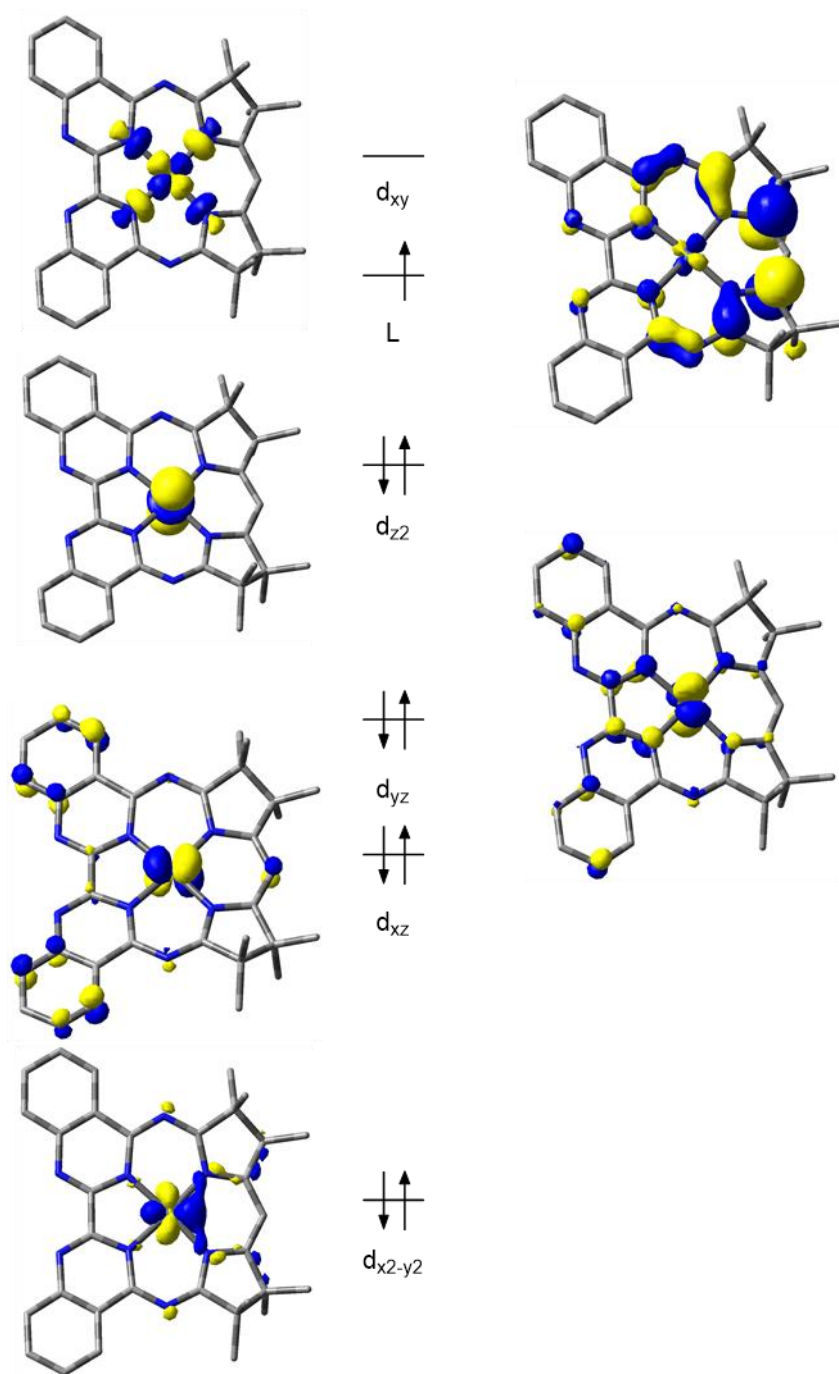


Figure S5: DFT-derived (B3LYP) qualitative MO diagram of **2**.

Table S9: DFT-derived (B3LYP, UKS) Löwdin atomic charges and spin population for **2**.

LOEWDIN ATOMIC CHARGES AND
SPIN POPULATIONS

0 Ni:	-0.062782	0.030413
1 N :	-0.005364	0.034975
2 N :	-0.058331	0.023622
3 N :	-0.135668	0.009777
4 N :	0.021644	-0.038146
5 N :	0.021302	-0.037944
6 N :	-0.135733	0.009957
7 N :	-0.005326	0.034850
8 N :	-0.058293	0.023558
9 C :	0.018471	-0.006404
10 C :	0.004359	0.007854
11 C :	-0.109773	0.000230
12 C :	-0.104640	0.010991
13 C :	-0.117509	-0.000522
14 C :	-0.092874	0.009824
15 C :	-0.052655	-0.002523
16 C :	0.055213	0.044715
17 C :	0.045312	0.117837
18 C :	-0.068280	0.001360
19 C :	-0.295378	0.000496
20 C :	-0.291145	0.007548
21 C :	-0.063440	-0.003515
22 C :	-0.291365	0.016174
23 C :	-0.297371	0.003549
24 C :	0.015015	0.291700
25 C :	-0.188980	-0.095639
26 C :	0.015161	0.291265
27 C :	-0.063407	-0.003503
28 C :	-0.291497	0.016152
29 C :	-0.297485	0.003494
30 C :	-0.068442	0.001399
31 C :	-0.295087	0.000468
32 C :	-0.291214	0.007519
33 C :	0.045397	0.117291
34 C :	0.055405	0.044444
35 C :	-0.052742	-0.002483
36 C :	-0.092709	0.009759
37 C :	-0.117636	-0.000497
38 C :	-0.104721	0.010912
39 C :	-0.109562	0.000256

40 C : 0.004352 0.007791
41 C : 0.018608 -0.006383
42 H : 0.131877 -0.000027
43 H : 0.123530 -0.000365
44 H : 0.122381 0.000011
45 H : 0.131615 -0.000327
46 H : 0.119976 0.000105
47 H : 0.109743 0.000078
48 H : 0.115182 -0.000096
49 H : 0.114554 -0.000215
50 H : 0.112701 0.000584
51 H : 0.119933 -0.000318
52 H : 0.116325 -0.000415
53 H : 0.112800 0.002639
54 H : 0.112918 -0.000088
55 H : 0.115315 0.000231
56 H : 0.112642 -0.000053
57 H : 0.115025 0.000433
58 H : 0.125896 0.003006
59 H : 0.116243 -0.000423
60 H : 0.112938 -0.000077
61 H : 0.113011 0.002625
62 H : 0.115358 0.000236
63 H : 0.115043 0.000434
64 H : 0.112683 -0.000047
65 H : 0.115095 -0.000092
66 H : 0.109637 0.000073
67 H : 0.120005 0.000112
68 H : 0.120002 -0.000315
69 H : 0.112715 0.000579
70 H : 0.114561 -0.000208
71 H : 0.131632 -0.000324
72 H : 0.122414 0.000011
73 H : 0.123566 -0.000362
74 H : 0.131855 -0.000028

Table S10: DFT-optimized (B3LYP, UKS) geometry (.XYZ format) for the monomeric unit of **2**.

CARTESIAN COORDINATES (ANGSTROEM)

Ni	-0.014436	0.018188	0.106099
N	-1.447801	-1.266475	0.141766
N	-3.821927	-1.377673	-0.149570
N	-0.203437	-3.228146	0.661655
N	1.283214	-1.363237	0.330066
N	1.300647	1.400895	0.045893
N	-0.161928	3.312350	-0.014034
N	-1.430928	1.301267	-0.124729
N	-3.802968	1.380152	-0.443471
C	-2.696839	-0.731329	-0.090584
C	-3.784193	-2.730325	0.068556
C	-4.988805	-3.472077	0.006782
C	-4.973870	-4.836951	0.241535
C	-3.761365	-5.497417	0.545281
C	-2.571821	-4.787702	0.608384
C	-2.565719	-3.395433	0.367589
C	-1.350378	-2.598393	0.394406
C	0.976904	-2.644633	0.629048
C	2.233236	-3.434380	1.000757
C	2.157433	-4.914772	0.608234
C	2.377629	-3.332557	2.540385
C	3.329076	-2.592030	0.247611
C	3.486730	-3.053545	-1.224820
C	4.713335	-2.601925	0.913813
C	2.652656	-1.224171	0.235792
C	3.295060	-0.005429	0.072843
C	2.668448	1.228913	-0.014984
C	3.361263	2.563081	-0.277869
C	3.519648	2.717300	-1.813200
C	4.746931	2.688852	0.372734
C	2.276534	3.552233	0.291107
C	2.219466	4.927061	-0.385505
C	2.420268	3.756167	1.820688
C	1.010630	2.719962	0.079303
C	-1.316350	2.655176	-0.152789
C	-2.520482	3.444815	-0.351045
C	-2.507925	4.856681	-0.405029
C	-3.687637	5.553132	-0.619166
C	-4.908587	4.859758	-0.784111
C	-4.941741	3.476221	-0.730565
C	-3.747378	2.747980	-0.510904

C	-2.686910	0.745749	-0.246080
H	-5.911013	-2.933962	-0.225477
H	-5.905607	-5.409616	0.193992
H	-3.763138	-6.576027	0.730639
H	-1.627132	-5.282607	0.838853
H	1.399470	-5.429369	1.221038
H	3.130954	-5.410324	0.780457
H	1.875422	-5.057910	-0.446605
H	2.476993	-2.285364	2.875676
H	3.260299	-3.894138	2.893308
H	1.483781	-3.763219	3.023463
H	2.514998	-3.095575	-1.746596
H	3.952734	-4.052988	-1.282906
H	4.132266	-2.344901	-1.772253
H	4.708290	-2.127237	1.908184
H	5.452920	-2.067613	0.291304
H	5.078631	-3.638845	1.027539
H	4.383542	-0.021912	-0.007417
H	2.545447	2.672858	-2.330368
H	4.148106	1.900823	-2.209562
H	4.003744	3.675591	-2.071437
H	4.737620	2.423555	1.442013
H	5.126472	3.722376	0.276014
H	5.478044	2.030670	-0.129553
H	1.947500	4.862070	-1.450428
H	3.196480	5.438238	-0.302893
H	1.461247	5.558230	0.106057
H	1.531321	4.283130	2.207776
H	3.308192	4.369007	2.055243
H	2.510470	2.796684	2.359345
H	-1.556764	5.376143	-0.278812
H	-3.675069	6.646657	-0.661974
H	-5.832424	5.422205	-0.953012
H	-5.870756	2.913636	-0.850400

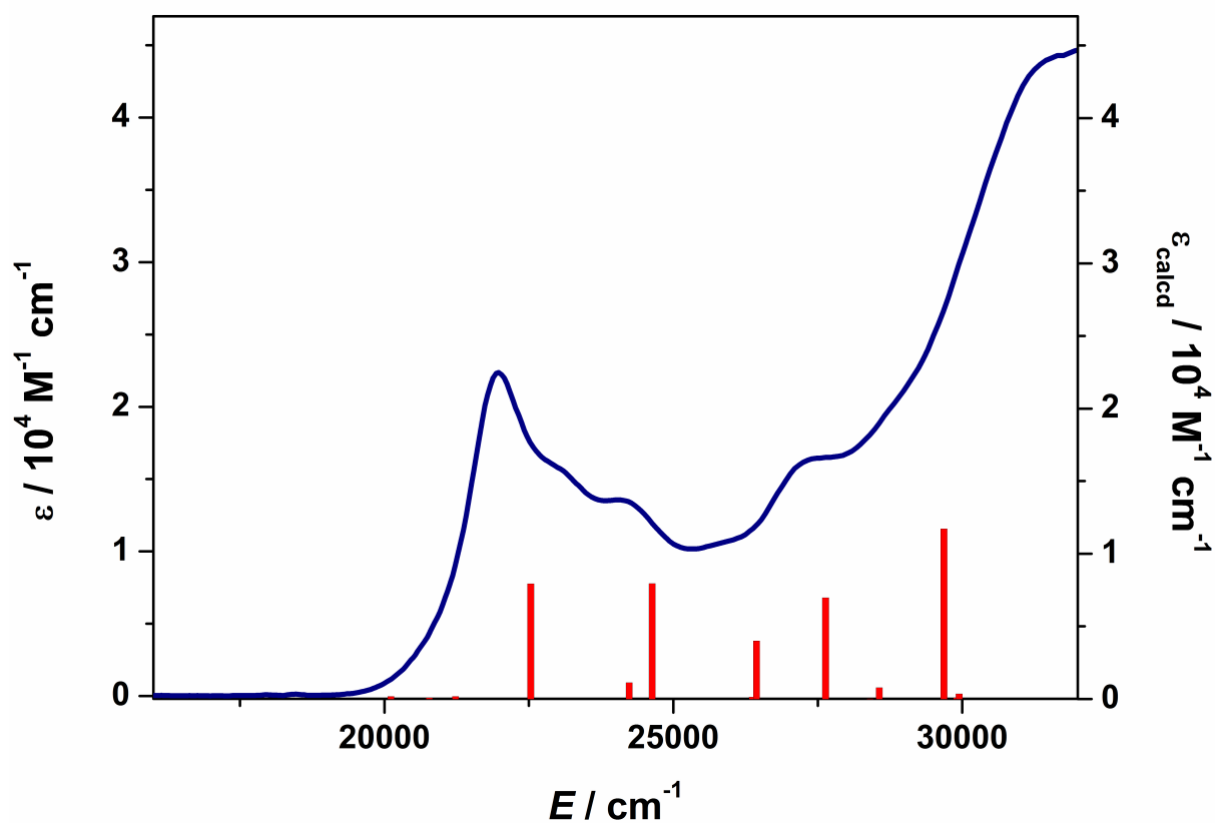


Figure S6: Calculated (B3LYP) electronic absorption spectrum for **1**.

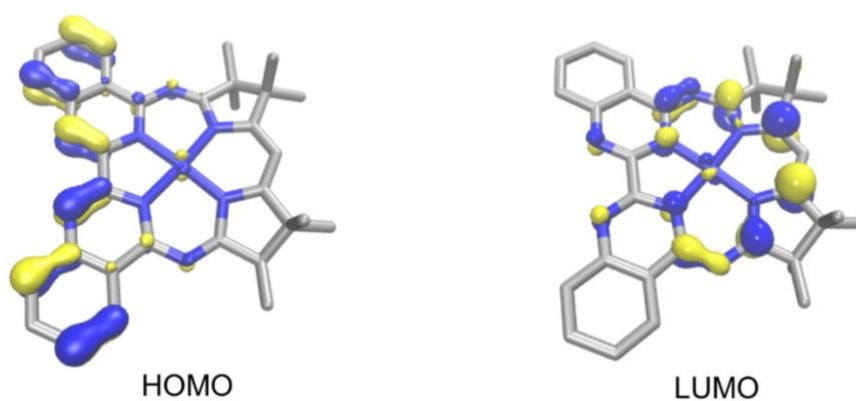


Figure S7: Orbitals involved in the electronic transition calculated at 22,532 cm^{-1} of **1**.

Table S11: DFT-optimized (BP86) coordinates for **1**.

Ni	0.05896768067087	0.01125961724558	0.07875142176482
N	-1.30389672401400	1.34211427903215	0.20670282654254
N	-3.64860743173783	1.54197828550295	0.71659820275700
N	0.00297864949814	3.29821002671260	-0.22445283849090
N	1.39803509496731	1.32966071862351	-0.06393807329299

N	1.30878107950911	-1.39633496309796	0.00515063342351
N	-0.21067012916504	-3.27550740113458	-0.09535505622629
N	-1.38953805317275	-1.22177025097025	0.24524864435922
N	-3.74759924319598	-1.24805181766321	0.73290787328206
C	-2.56812561033255	0.84183918037599	0.49386776530804
C	-3.55585188299511	2.90382561343707	0.65857200738819
C	-4.70964950973742	3.69505153716963	0.91346308822739
C	-4.61907416443092	5.08169178389264	0.84151337947031
C	-3.38729625550859	5.71189793622875	0.51125429392084
C	-2.24504404374482	4.95623741531668	0.25688826217288
C	-2.31201494046510	3.53997954424162	0.33197644664654
C	-1.16795509699796	2.68579624208167	0.10145350259182
C	1.13826317107800	2.67654064156293	-0.30261727896173
C	2.41431431358134	3.40268973827658	-0.71712401450544
C	2.48660268327061	3.31416154985387	-2.26875850249557
C	2.43492067479703	4.87843386435410	-0.29467310931339
C	3.49601975997316	2.48086817347099	-0.03112580211743
C	4.85399556029897	2.42969553412413	-0.75228556358605
C	3.72679347126024	2.88460598892188	1.45350093741749
C	2.66632740955362	-1.30200493420988	0.06534217864482
C	3.36334556763726	-0.09533449009169	0.08110192557043
C	2.74673953360994	1.15120199435507	-0.01494551748608
C	3.32308219851971	-2.67644451608637	0.15625352946870
C	4.70323915609521	-2.76637372516377	-0.51614638634592
C	3.47428274548920	-2.99602865416013	1.67172791724580
C	2.20058083246131	-3.56398841710626	-0.50839910903367
C	2.11369656063704	-5.01191834947483	-0.00652140955541
C	2.31795418145902	-3.56918358846114	-2.05942985361628
C	0.96545933378259	-2.73397816977749	-0.16965804996342
C	-1.34425600896421	-2.57410701970874	0.17877217273932
C	-2.54985165730238	-3.34145761660585	0.40268524226114
C	-2.58218913789837	-4.75999575223473	0.35171330342337
C	-3.77978921023864	-5.42857329562497	0.59524995503897
C	-4.96912444250755	-4.70755846287938	0.89371199993503
C	-4.96182329046575	-3.31702777873359	0.94411736929682
C	-3.75080984297161	-2.61379077435573	0.69703991229491
C	-2.61897343025502	-0.62949509688736	0.50801702963150
H	-5.65065744468287	3.18070106571700	1.16154960125318
H	-5.50950925863144	5.70108122652264	1.03827301379494
H	-3.33894400962932	6.81160695349657	0.45500126768881
H	-1.28842524447009	5.43356737281825	-0.00027759030390
H	2.51587674771707	2.26346413411684	-2.63222240680277
H	3.39093867511252	3.83889845519275	-2.64478624148801
H	1.59673925157257	3.80807238051132	-2.71491438467204
H	1.67189295108304	5.44893758848649	-0.86465939546418
H	3.42872771576815	5.32805795059953	-0.51386220153110
H	2.21511739956222	5.01811115837704	0.78354212640951
H	4.79166665702188	1.97062924899172	-1.76086366836135
H	5.60187053165034	1.85789866473239	-0.16039498694457
H	5.26023558950087	3.45865689064105	-0.86650128481355
H	4.26701455215161	3.85412386382915	1.50819824354855
H	4.34875298576362	2.12120075242665	1.96915378995574

H	2.77286845506659	2.98412967759782	2.01598590792728
H	4.45932264256710	-0.13091099135950	0.13516833928771
H	5.03732480267650	-3.82666201215492	-0.55384719503742
H	5.47106344471426	-2.21381572932219	0.06843865748924
H	4.70569317476917	-2.36726770717078	-1.55165236990510
H	2.49550101609677	-2.99175615047448	2.19916697796041
H	4.12943166488923	-2.24341159268438	2.16156410395831
H	3.94170993296146	-3.99451484801323	1.81046836560864
H	1.86235399435147	-5.07853223952969	1.07185864326761
H	3.07941531593206	-5.53797564070429	-0.17638515654436
H	1.32692531515803	-5.56213678756451	-0.56408596912348
H	1.41293054328283	-4.03741989821398	-2.50274402533799
H	3.19968130772788	-4.16478164630662	-2.37939748518194
H	2.41716445866612	-2.54514167292084	-2.48203194638303
H	-1.65763769448834	-5.30806077812238	0.11987087919857
H	-3.80877078566006	-6.52969055882942	0.55563195024876
H	-5.90456983514263	-5.25909226948151	1.08328927983791
H	-5.86776054410666	-2.73328279555698	1.16794395362672

ESI-MS of Ni(Mabiq)OTf (1) after the photocatalytic reaction

D:\Desktop\Masse\mg49435

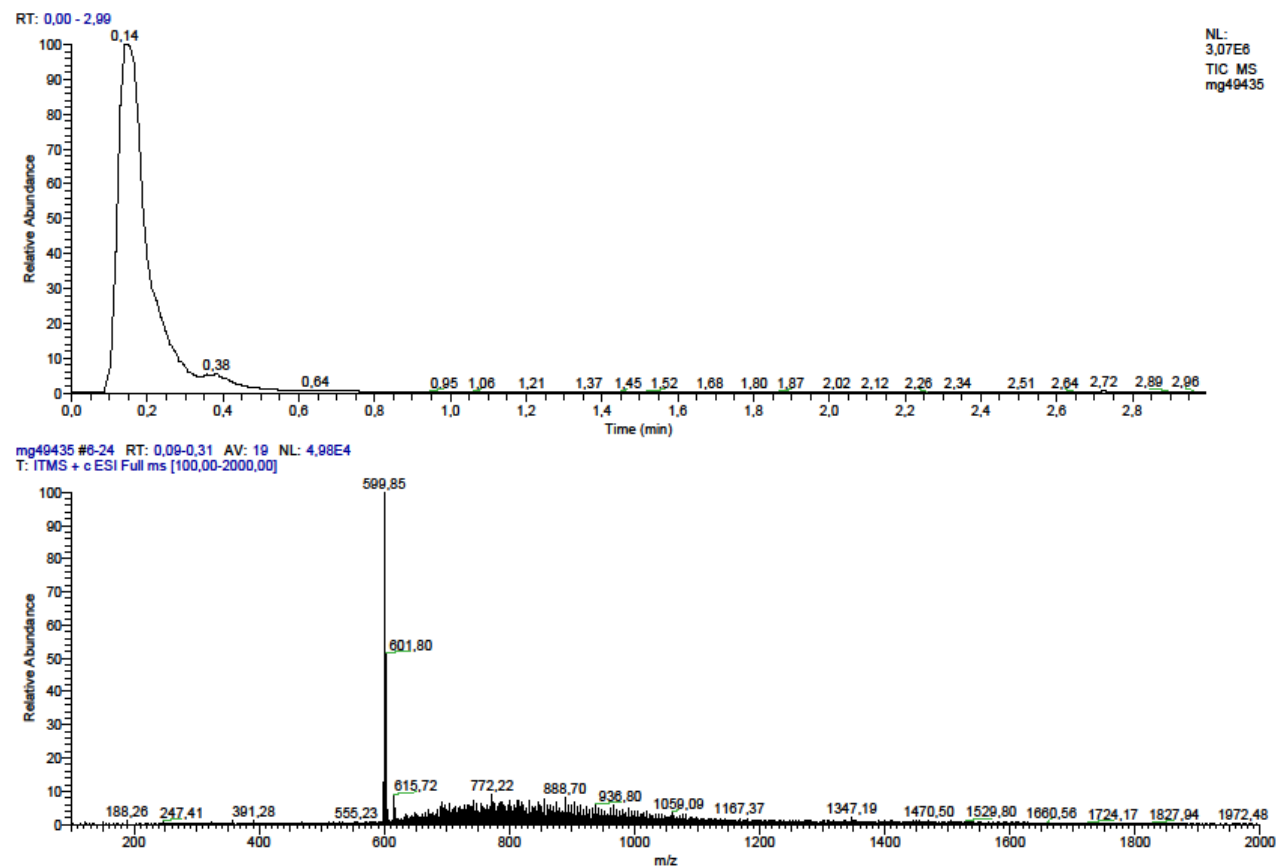


Figure S8: GC-MS of product mixture (after photoredox catalysis with **1** and **3**).

Cyclic Voltammetry (CV) experiments

Cyclic Voltammogram of Ni(Mabiq)OTf (1)

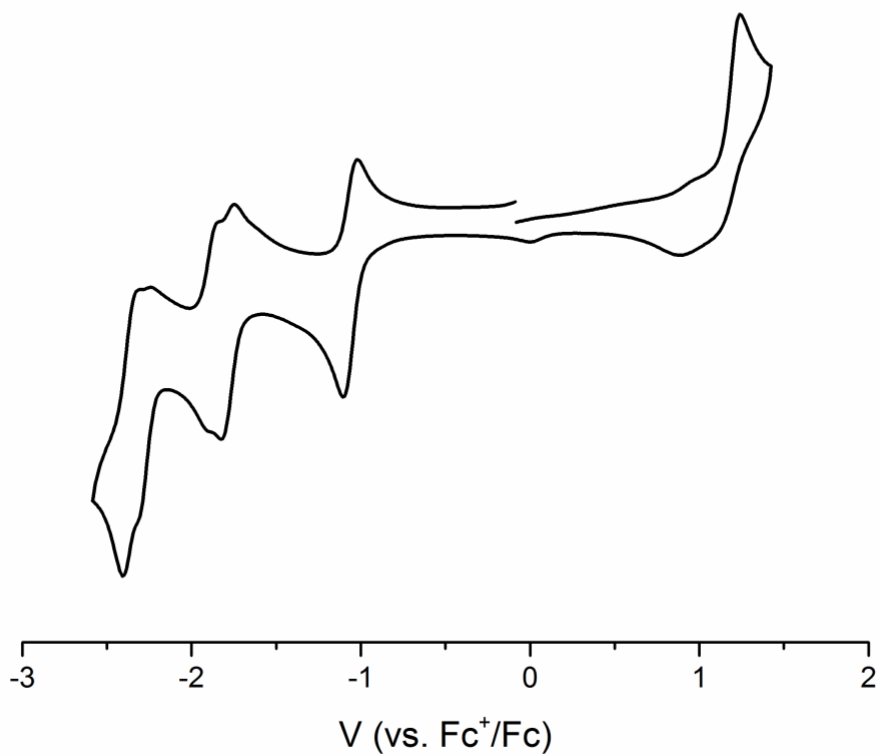


Figure S9: Cyclic voltammogram of **1** (1 mM) in MeCN; 0.1 M [N(*n*-Bu)₄]PF₆; scan rate: 0.1 V/s.

Cyclic Voltammograms for Amines 6a to 6n

The CV measurements were performed with the corresponding amine **6** (1 mM) in 0.1 M of $[N(n\text{-Bu})_4]PF_6$ in MeCN. Glassy carbon electrode was used as working electrode, a platinum wire as counter electrode, $Ag/AgNO_3$ (0.01 M in MeCN) as reference electrode, and a scan rate of 100 mV/s. The value of the potential at the inflexion point of each oxidation curve was selected as the oxidation potential of the given amine **6**. 300 mV were added to this value to give the corresponding oxidation potentials (E^{ox}) vs. the Saturated Calomel Electrode (SCE).

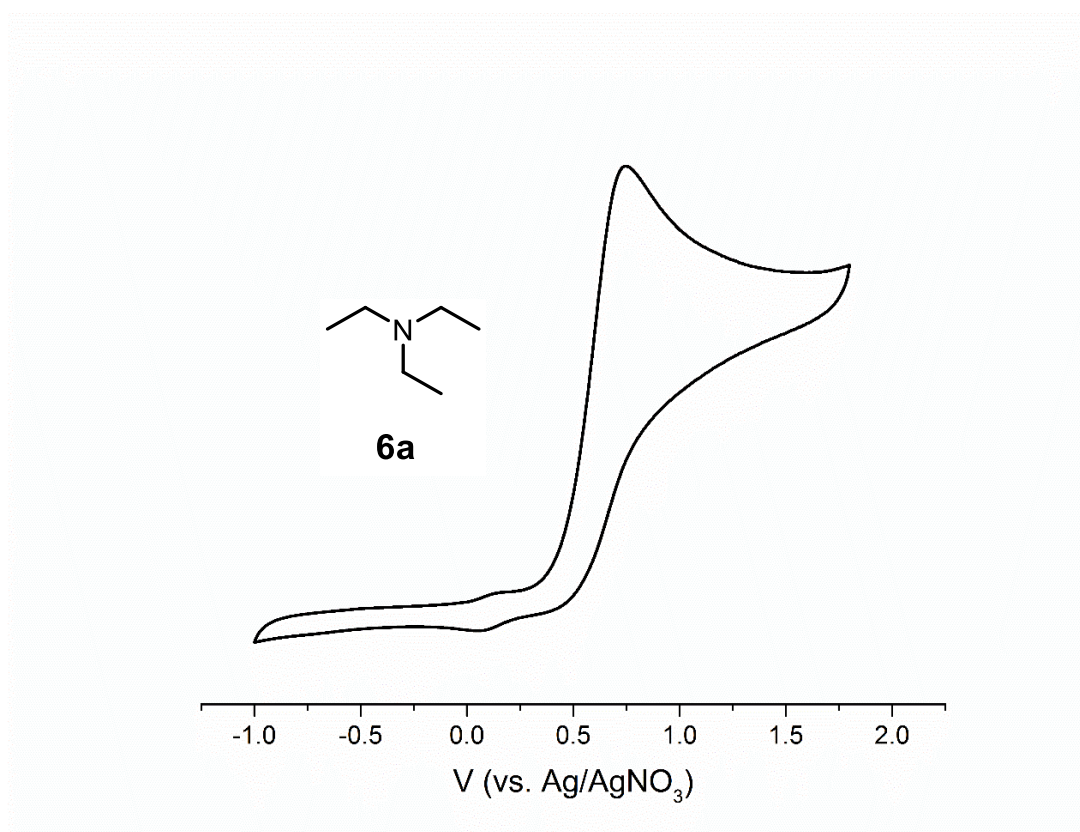


Figure S10: Cyclic voltammogram of **6a**.

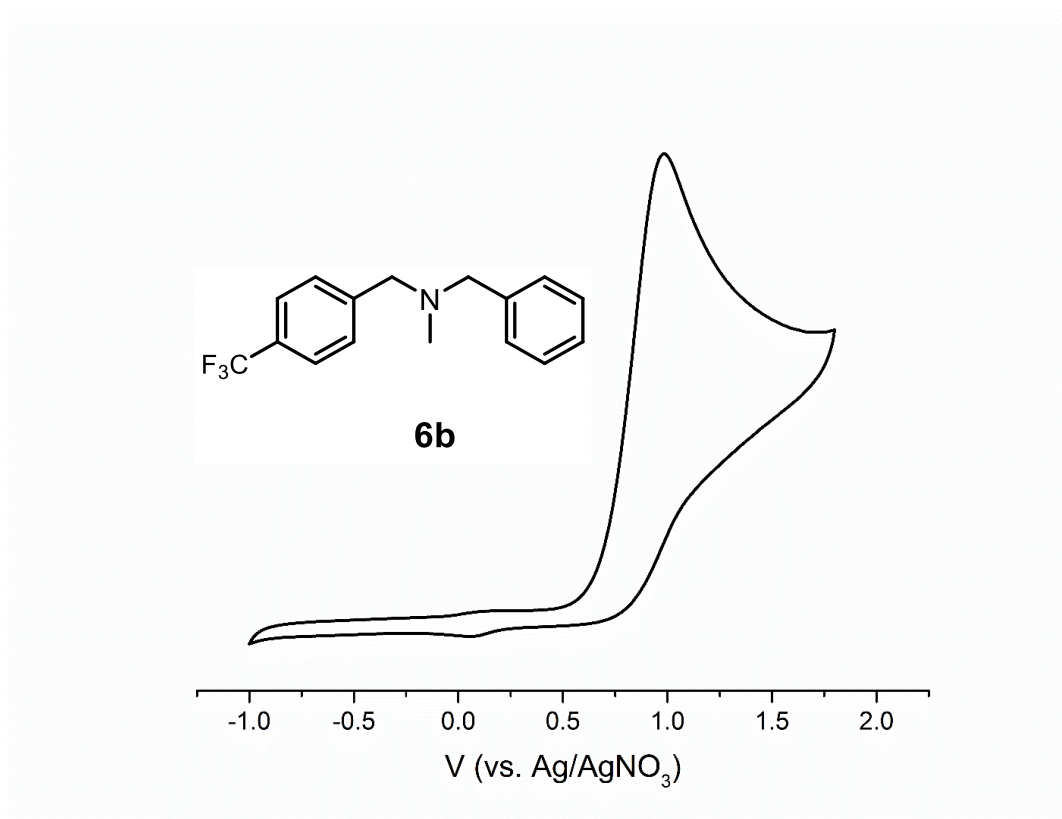


Figure S11: Cyclic voltammogram of **6b**.

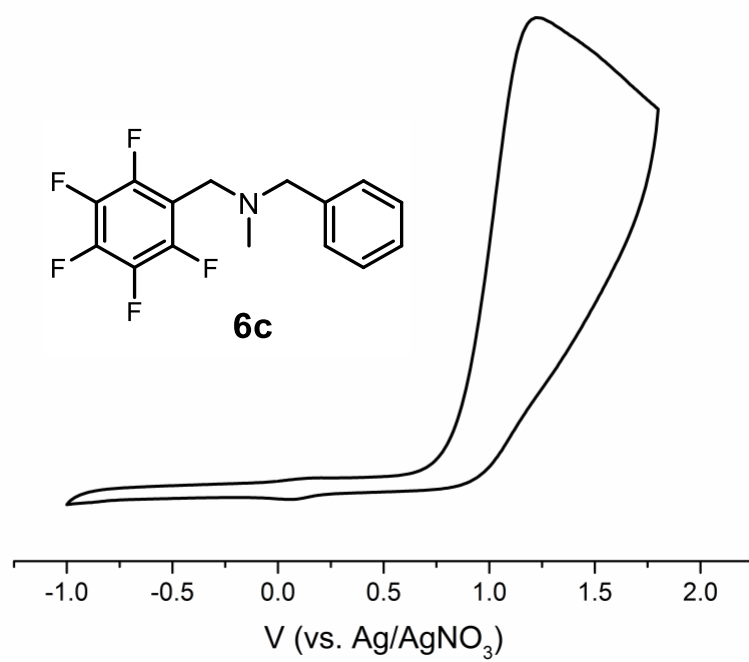


Figure S12: Cyclic voltammogram of **6c**.

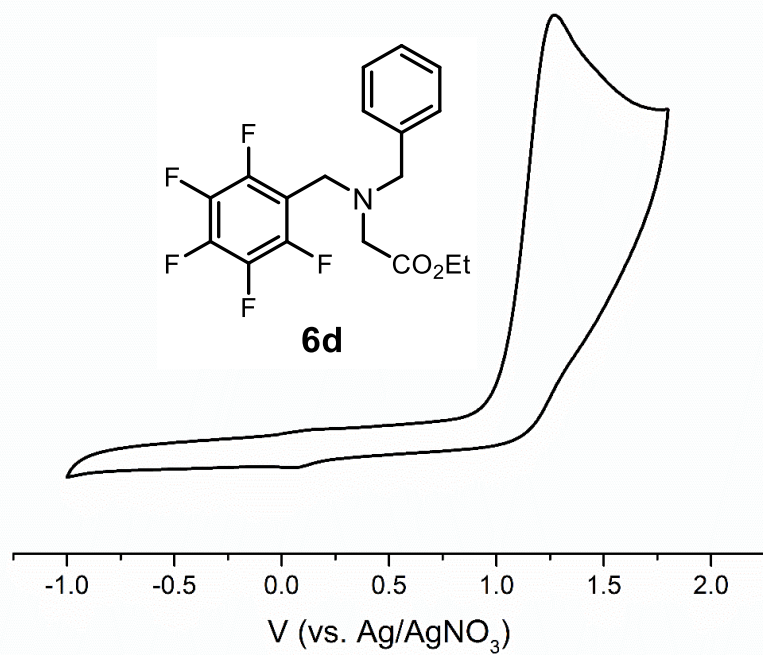


Figure S13: Cyclic voltammogram of **6d**.

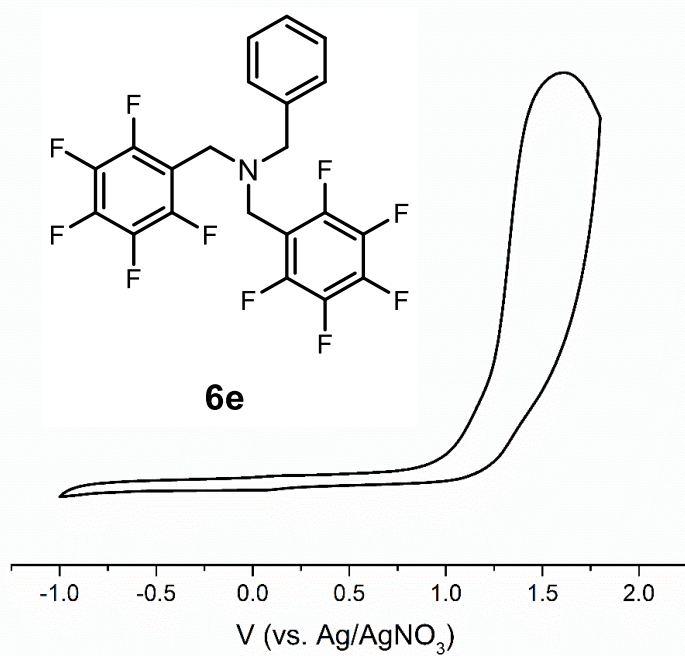


Figure S14: Cyclic voltammogram of **6e**.

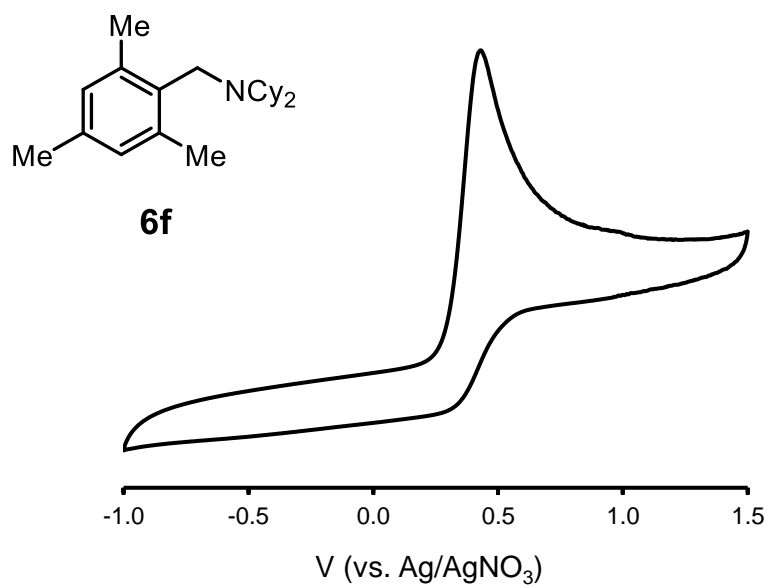


Figure S15: Cyclic voltammogram of **6f**.

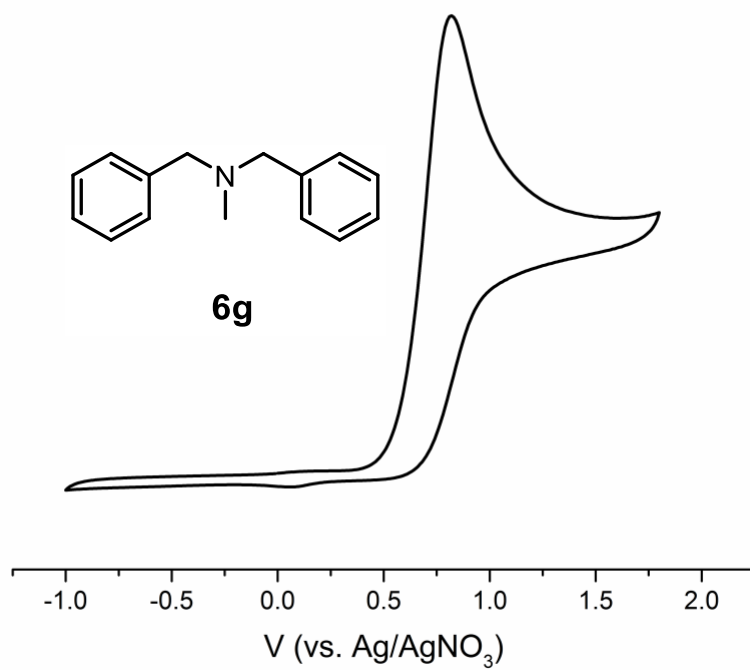


Figure S16: Cyclic voltammogram of **6g**.

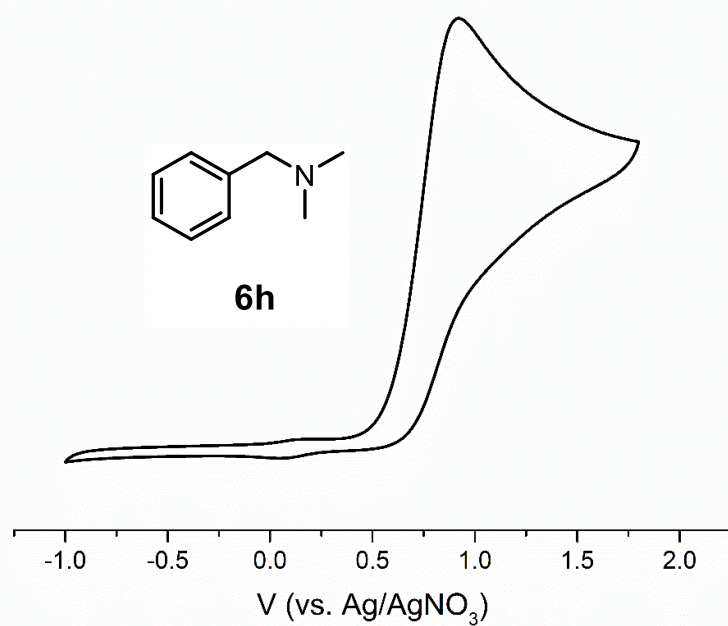


Figure S17: Cyclic voltammogram of **6h**.

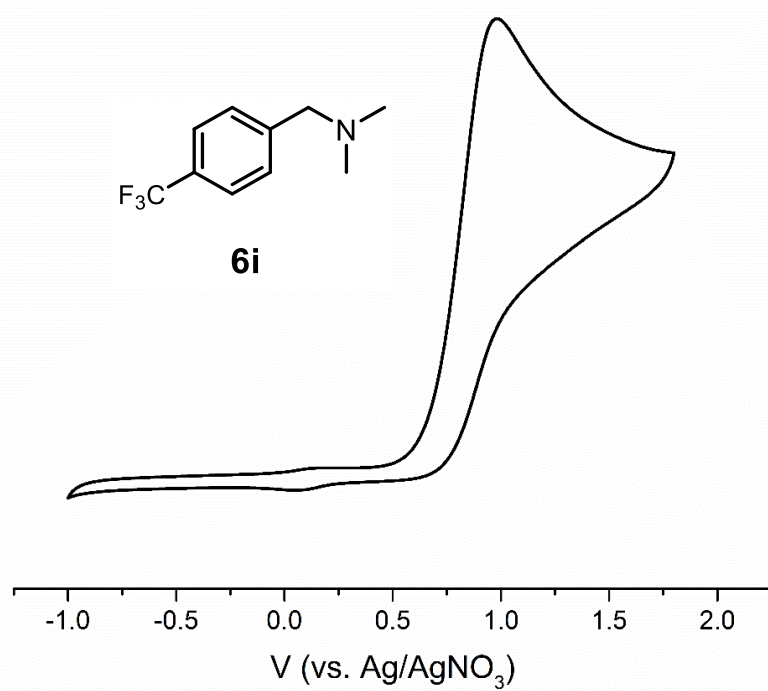


Figure S18: Cyclic voltammogram of **6i**.

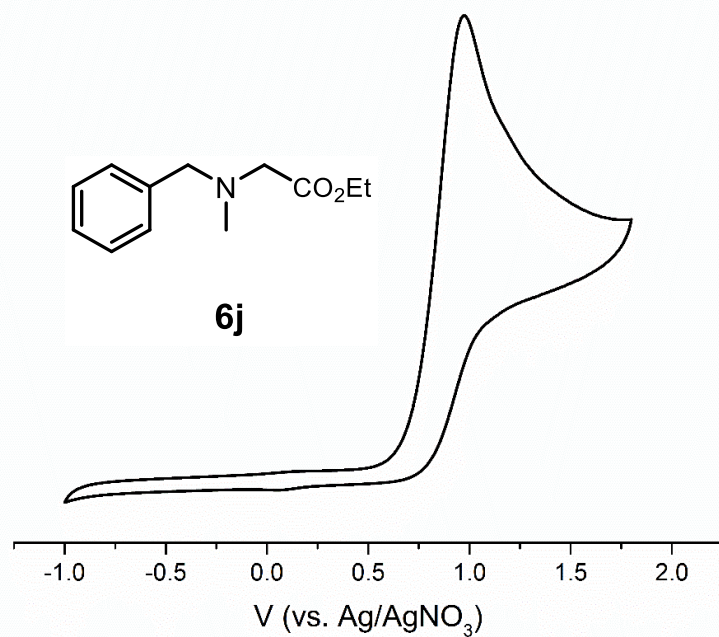


Figure S19: Cyclic voltammogram of **6j**.

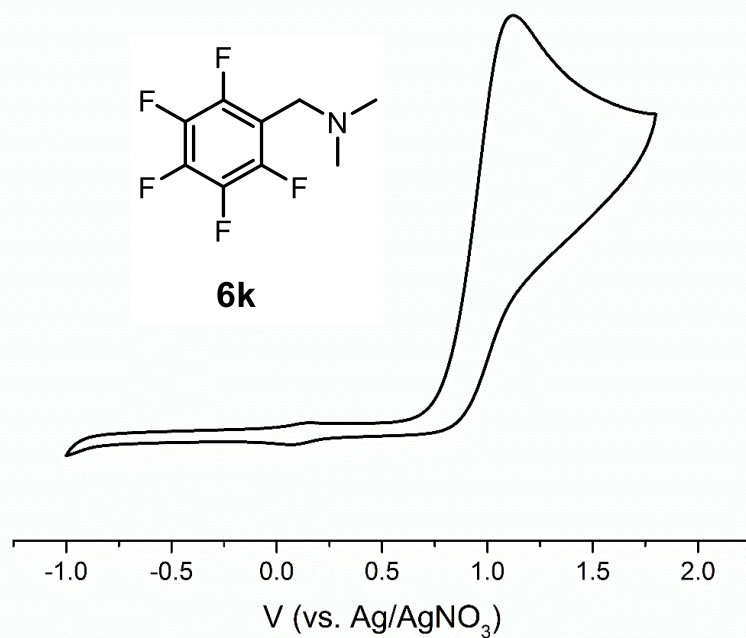


Figure 20 Cyclic voltammogram of **6k**.

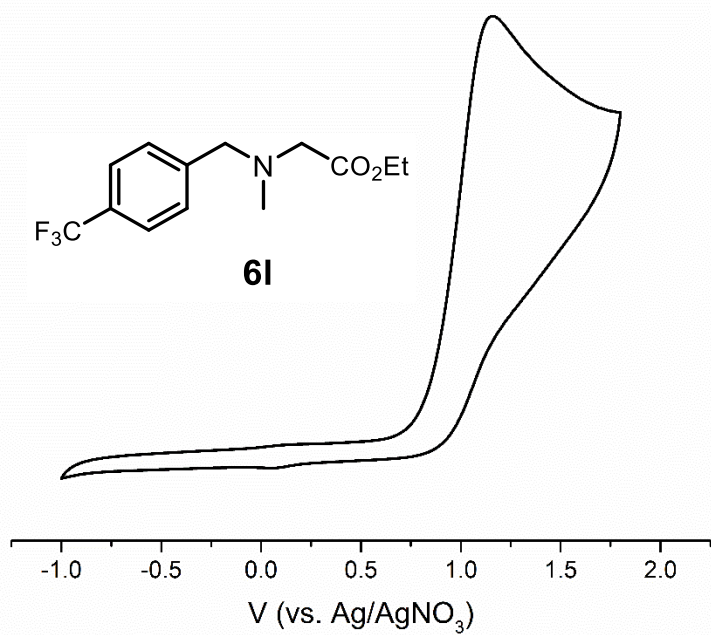


Figure S21: Cyclic voltammogram of **6l**.

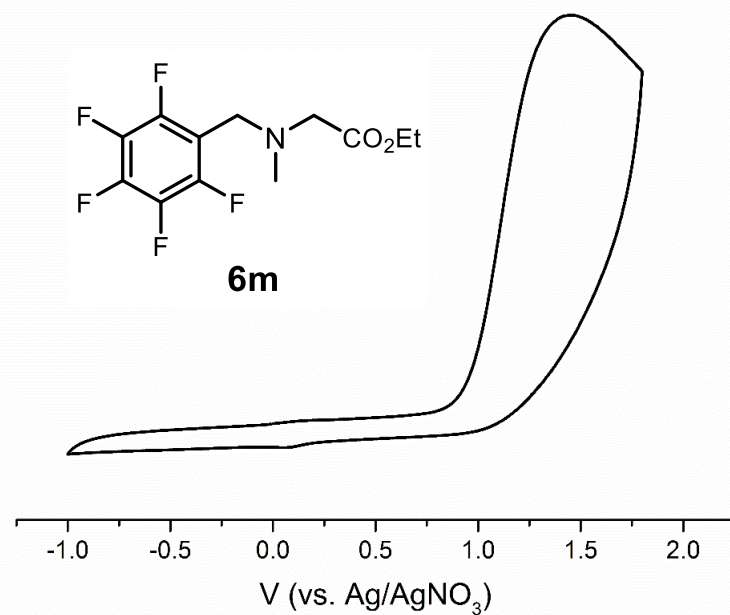


Figure S22: Cyclic voltammogram of **6m**.

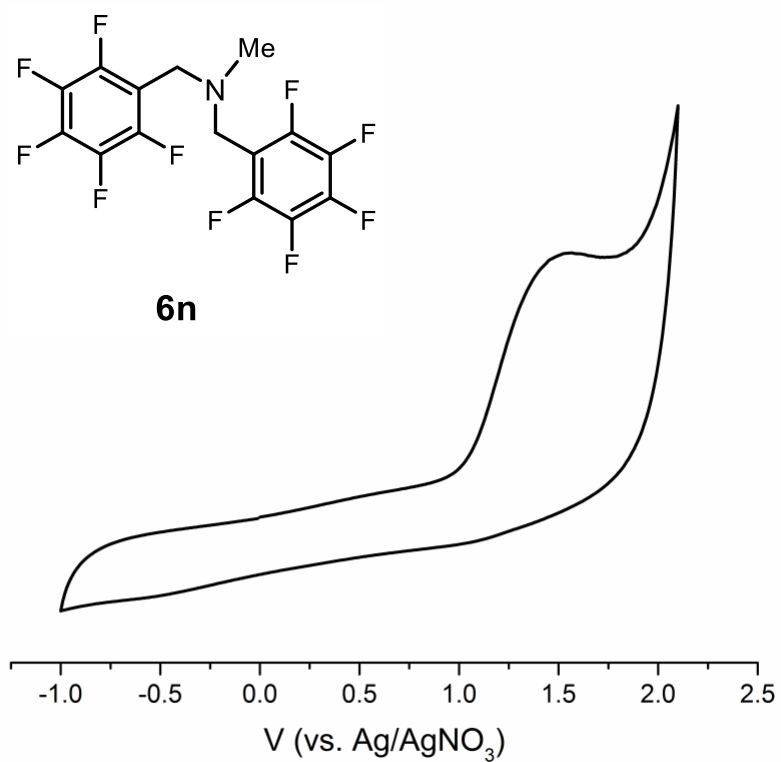


Figure S23: Cyclic voltammogram of **6n**.

Chemical actinometry: Determination of the photon-flux

The set up used for the chemical actinometry consisted of a LED (455 ± 10 nm) mounted on a heat sink and a set of focusing lenses ($f = 25$, $f = 150$) to direct the light into the cuvette, which was placed in a cuvette holder situated at 21 cm distance from the LED (Figure S24). A magnetic stirbar drive (2mag, cuvetteMixdrive1) was installed under the cuvette holder.

The photon flux in the cuvette after thermal equilibration of the LED (working at a constant current of 0.7 V) was measured using a radiometrically calibrated setup (USB-4000, Ocean Optics) connected by a fiber and a cosine corrector^[29] which gave 104 mW/cm^2 on an irradiated area of $9.5 \text{ mm} \times 9.5 \text{ mm}$. These values correspond to 94 mW or $3.56 \times 10^{-7} \text{ Einstein}\cdot\text{s}^{-1}$.

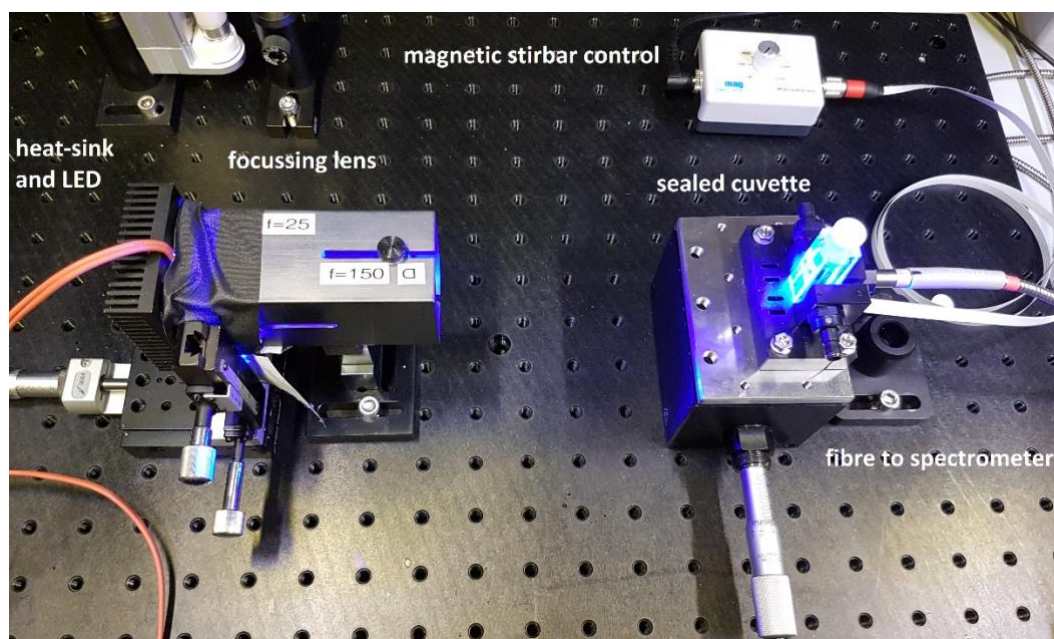


Figure S24: Set up used for the actinometry and quantum yield experiments.

Chemical actinometry was used to verify this value:^{[30]-[31]} A potassium ferrioxalate solution (150 mM) was prepared under strict exclusion of light (dark room under red light conditions) by dissolving 1.639 g of $\text{K}_3[\text{Fe}(\text{C}_2\text{O}_4)_3]$ in 2.5 mL of a 0.5 M H_2SO_4 aqueous solution, and water

was added to a final sample volume of 25 mL. The solution was stored in a dark 10 mL volumetric flask, and used on the same day as prepared.

The 1,10-phenanthroline solution (10 mM) was prepared by dissolving 45.1 mg of 1,10-phenanthroline and 2.05 g of NaOAc in 10 mL of water and 9.7 mL of 0.5 M H₂SO₄ aqueous solution, and water was added to a final volume of 25 mL. The solution was stored in a dark 10 mL volumetric flask, and used on the same day as prepared.



Figure S25: Black box with a red window used for the actinometry and quantum yield experiments.

In a black box under red-light conditions (Figure S25), 3 mL samples of the ferrioxalate solution were irradiated in a 10 x 10 mm cuvette for 5, 10, 20 and 30 seconds. After irradiation, 100 μ L aliquots of each sample and a non-irradiated blank were transferred into brown GC-vials. 900 μ L of the 1,10-phenanthroline solution were added to each GC-vial and the cuvettes were left for 60 min in the black box, after which time the UV-visible spectra were measured (Figure S26). The fit of the $\Delta A/t$ plot (Figure S26) yields a slope of = 0.0696 s⁻¹.

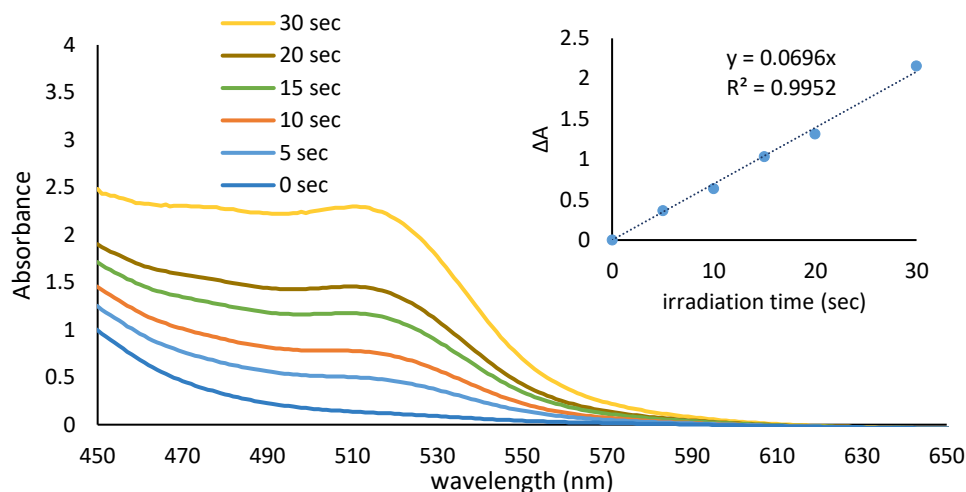


Figure S26: UV-visible spectra for the potassium ferrioxalate solutions after 0, 5, 10, 15, 20 and 30 s of irradiation at 455 nm. Inset: change in absorbance (510 nm) vs irradiation time plot.

The experimental photon flux was calculated according to the following equation:

$$photon\ flux = \frac{mol\ Fe^{2+}}{\Phi \times t \times f}$$

Where Φ is the reference quantum yield for the ferrioxalate actinometer (0.845 for a 0.15 M solution at $\lambda = 457\ nm$)^[32], t is the irradiation time (in s) and f is the fraction of light absorbed at $\lambda = 457\ nm$ ($f = 1$, as the optical density of the ferrioxalate solution at 457 nm is > 3).

Given the following equation for the calculation of the mols of Fe^{2+} generated:

$$mol\ Fe^{2+} = \frac{V \times d \times \Delta A}{l \times \varepsilon}$$

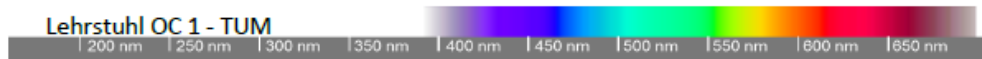
where V is the total volume in the cuvette of the analysis (0.001 L), d is the dilution factor (30, as 0.1 mL out of 3 mL of initial solution were taken for the analysis), ΔA is the increment of absorbance after certain irradiation time, l is the path length of the cuvette (1 cm) and ε is the molar absorption coefficient at 510 nm ($11,100\ M^{-1}\ cm^{-1}$)^[36], the photon flux can be determined by:

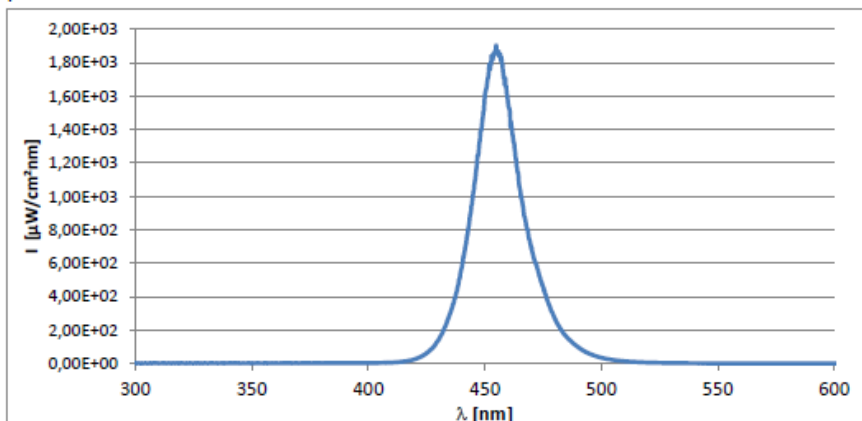
$$photon\ flux = \frac{V \times d}{\Phi \times f \times l \times \varepsilon} \times \frac{\Delta A}{t}$$

where $\Delta A/t$ is the slope of the absorbance vs time (0.0696 s^{-1} , vide supra). The photon flux calculated accordingly was found to be:

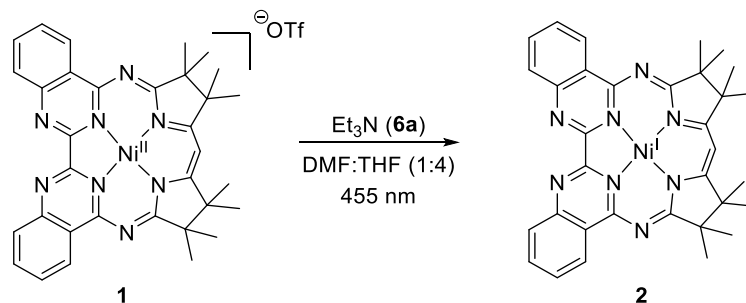
$$\text{photon flux} = \frac{0.001 \text{ L} \times 30 \times 0.0696 \text{ s}^{-1}}{0.845 \times 1 \times 1.00 \text{ cm} \times 11100 \text{ L} \cdot \text{mol}^{-1} \cdot \text{cm}^{-1}} = 2.226 \cdot 10^{-7} \text{ Einstein s}^{-1}$$

Emission spectra of the LED (455 nm)

Lehrstuhl OC 1 - TUM		Av-455-3W	
			
Datasheet LED028			
Basic Information			
Type	High-Power-LED		
Description	Avonec 455-460 nm / 3 W		
Manufacturer / Supplier	n/a / Avonec		
Order number / Date of purch.	n/a / 01/2016		
Internal lot / serial number	2016-01 / LED028		
Specification Manufacturer			
Type / size	single emitter / ca. 1 x 1 mm		
Mechanical specification			
Electrical specification	700 mA, UF 3.7 V		
Wavelength (range, typ.)	455-460 nm, typ. n/a		
Spectral width (FWHM)	n/a		
Datasheet	n/a		
Characterization			
Description of measurement	Measured with Ocean-optics USB4000 spectrometer using a calibrated setup (cosine corrector/fibre). The distance between the emitting surface and the surface of the cosine corrector was 20 mm. The LED was operated at 700 mA on a passive heat-sink at approx. 20 °C		
Measured wavelength	455 nm		
Measured spectral width	22 nm		
Integral Reference intensity	50200 $\mu\text{W}/\text{cm}^2$ (400-550 nm @ 20 mm distance, 4 mm cosine corr.)		
Spectrum			



Determination of the quantum yield for the photoconversion of **1** to **2**



The reaction mixture was prepared in a glove box equipped with a red LED in a dark room, using a cuvette fitted with a J-Young tap and equipped with a stir bar inside.

Two stock solutions were prepared: A stock solution of **1** was prepared by dissolving 4 mg of **1** in 25 mL of THF:DMF (4:1) ($[1] = 2.13 \cdot 10^{-4}$ M). A stock solution of Et₃N (**6a**) was prepared by diluting 118.8 μ L of Et₃N (**6a**) in 10 mL of THF:DMF (4:1) ($[6a] = 8.50 \cdot 10^{-2}$ M).

For each measurement, 1 mL of the stock solution of **1** was added to a cuvette, followed by 0.5 mL of the stock solution of **6a** (200 equiv. of **6a**). 1.5 mL of a THF:DMF (4:1) solution was subsequently added to a total volume of 3 mL. Therefore, the final reaction solution contained $2.13 \cdot 10^{-4}$ mmol of **1** ($7.13 \cdot 10^{-5}$ M) and $4.27 \cdot 10^{-2}$ mmol of Et₃N (**6a**) ($1.43 \cdot 10^{-2}$ M).

The cuvette was sealed, covered with aluminum foil to avoid any light exposure, and transferred to a dark room equipped with a UV-visible spectrometer and a dark box. A UV-visible spectrum of the reaction mixture was recorded for $t = 0$ min. The reaction mixture was subsequently irradiated at 455 nm for three 10 min periods (10, 20 and 30 min total). After each of these periods, the absorption spectra were recorded.

The same procedure was followed using 300, 400, 600 or 800 equivalents of Et₃N.

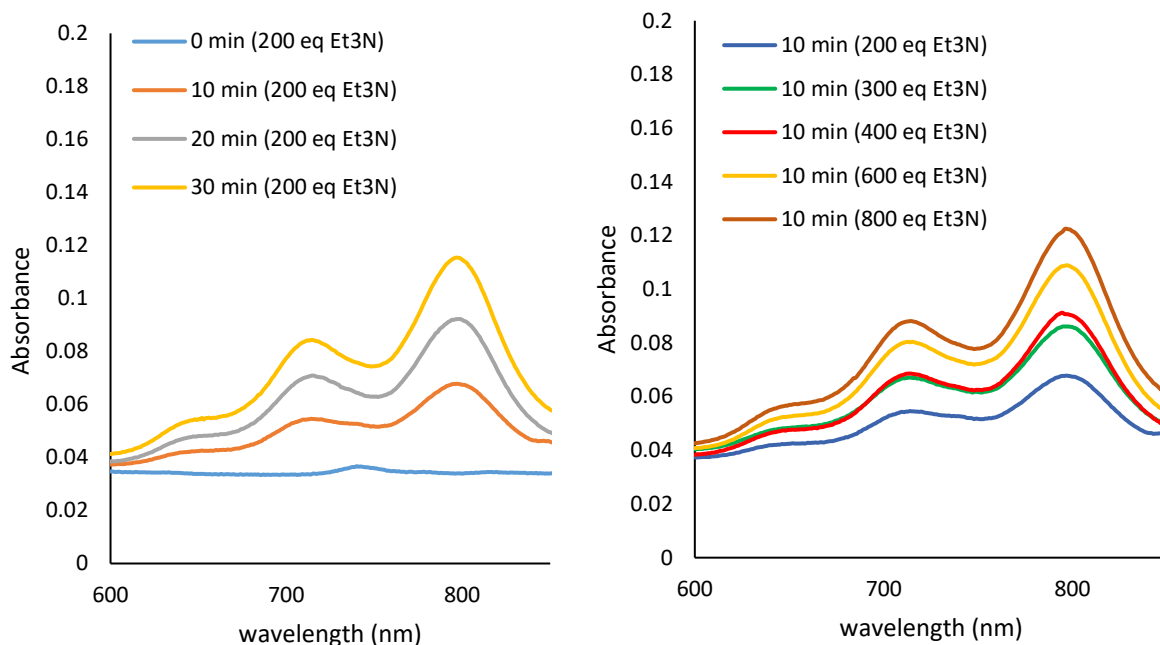


Figure S27: Left: UV-visible spectra for mixtures of **1** in the presence of 200 equiv. of Et₃N in THF:DMF (4:1) after 0, 10, 20 or 30 min irradiation at 455 nm; Right: UV-visible spectra for mixtures of **1** in the presence of different concentrations of Et₃N in THF:DMF (4:1) after 10 min irradiation at 455 nm.

We note that in the region from 600 – 850 nm the absorption observed in the UV-visible spectra is only due to Ni(Mabiq) (**2**), whereas in the region from 400 – 500 nm both Ni(Mabiq)OTf (**1**) and Ni(Mabiq) (**2**) absorb (see Figure 2 in the manuscript). The concentration of **1** was chosen to avoid saturation of the signal at 455 nm, allowing us to determine the photons absorbed exclusively by **1**.

The absorbance due to **1** was corrected using the molar absorption coefficient of **2** at 455 nm ($\epsilon_{455} = 5493 \text{ M}^{-1} \text{ cm}^{-1}$) and the known concentration of **2** as determined at 796 nm ($\epsilon_{796} = 5551 \text{ M}^{-1} \text{ cm}^{-1}$) at 10 min. Although this is a slight overcorrection, the data treatment revealed that (e.g. for the 200 equiv. Et₃N, 10 min data) a maximum of 5% of the light is absorbed by Ni(Mabiq) (**2**) while 95% is absorbed by Ni(Mabiq)OTf (**1**). The correction provides a value of $f = 0.95$ used in the quantum yield calculations.

From the absorbance at 796 nm (Figure S27, left), the concentration of Ni(Mabiq) (**2**) generated after irradiation was calculated. The slope of the plot of [**2**] vs the irradiation time (Figure S28), gives the observed rate of product formation ($k_p = [\mathbf{2}]/_t = 7.13 \cdot 10^{-9} M \cdot s^{-1}$), from which the quantum yield was determined according to the following equation:

$$\phi_{pc} = \frac{k_p \cdot V}{\text{photon flux} \cdot f} = \frac{7.13 \cdot 10^{-9} M \cdot s^{-1} \cdot 0.003 L}{2.226 \cdot 10^{-7} \text{Einstein} \cdot s^{-1} \cdot 0.95} = 1.011 \cdot 10^{-4}$$

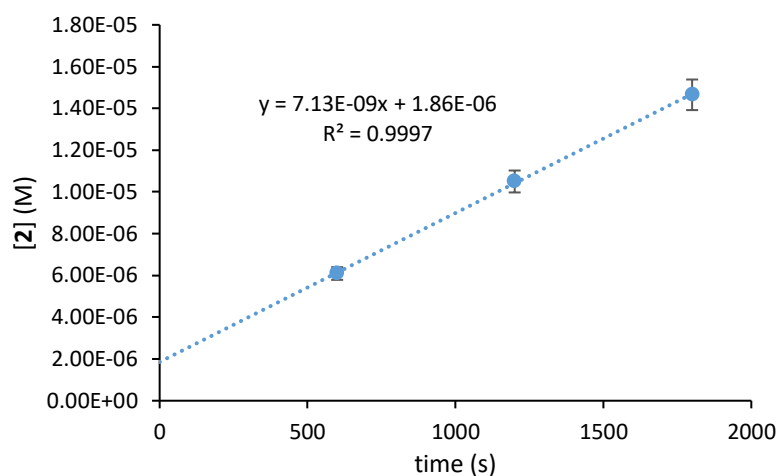


Figure S28: Concentration of Ni(Mabiq) (**2**) generated in solution vs irradiation time, in a reaction mixture with 200 equiv. Et₃N, measured at 796 nm.

In this manner, the quantum yield of the photoconversion at various concentrations of Et₃N was calculated (Table S3).

Table S3: Quantum yields calculated for the different concentrations of Et₃N.

[Et ₃ N] (M)	0.0142	0.0214	0.0285	0.0428	0.0570
k_p (M · s ⁻¹)	7.13 · 10 ⁻⁹	1.07 · 10 ⁻⁸	1.24 · 10 ⁻⁸	1.72 · 10 ⁻⁸	2.30 · 10 ⁻⁸
$\phi_{pc,[Et_3N]}$	1.01 · 10 ⁻⁴	1.52 · 10 ⁻⁴	1.76 · 10 ⁻⁴	2.44 · 10 ⁻⁴	3.26 · 10 ⁻⁴
1/[Et ₃ N] (M ⁻¹)	70.12	46.75	35.06	23.37	17.53
1/ $\phi_{pc,[Et_3N]}$	9886.4	6587.8	5684.7	4098.3	3064.8

As described by Kaneko *et al.*^[33] a relationship between the excited state lifetime and the reciprocal of the quantum yield can be described as:

$$\frac{1}{\phi_{pc}} = \frac{1}{f_{CS} \phi^*} \left(1 + \frac{1}{k_d \tau^* [Et_3N]} \right)$$

Where ϕ_{pc} is the quantum yield of the photoconversion, f_{CS} is a factor that takes into account the efficiency for charge separation and the rate for reverse electron transfer, ϕ^* is the quantum yield for the production of the reactive excited state specie, k_d is the diffusion rate constant and τ^* is the lifetime of the excited state of the photocatalyst.

Consequently, the life time of the excited state of Ni(Mabiq)OTf (**1***) can be estimated from the plot of the reciprocal of the calculated quantum yields vs the reciprocal of the various Et₃N concentrations (Figure S29). The reciprocal of the intercept affords $\phi^* f_{CS} = 9.72 \cdot 10^{-4}$ and division of the intercept by the slope gives $1/k_d \tau^* = 0.12 M$.

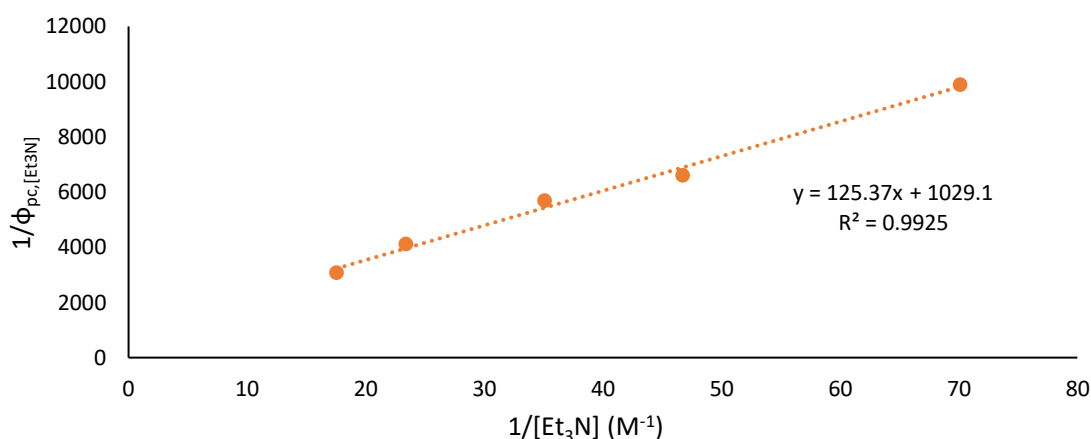


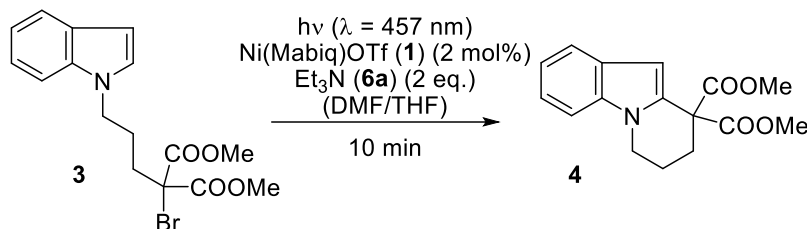
Figure S29: Representation of the reciprocal of the quantum yield of Ni(Mabiq) (**2**) generated after 10 min irradiation at 455 nm vs the reciprocal of the concentration of the Et₃N for individual samples.

The diffusion rate constant (k_d) can be calculated from the dynamic viscosity of the solvent according to the following equation:

$$k_d = \frac{8 \cdot N_A \cdot kT}{3 \cdot \eta}$$

Where N_A is the Avogadro number ($6.022 \cdot 10^{23} \text{ mol}^{-1}$), k is the Boltzmann constant ($1.38 \cdot 10^{-23} \text{ m}^2 \text{ Kg s}^{-2} \text{ K}^{-1}$), T is the temperature (298 K) and η is the viscosity of the solvent. Since a 4:1 THF:DMF mixture was used for the experiments, the diffusion rate constant was calculated for both solvents from their corresponding viscosities ($\eta_{THF} = 0.0047 \text{ Pa s}$; ^[34] $\eta_{DMF} = 0.00724 \text{ Pa s}$ ^[35]), yielding $k_{d,THF} = 1.41 \cdot 10^9 \text{ s}^{-1} \text{ M}^{-1}$ and $k_{d,DMF} = 9.12 \cdot 10^8 \text{ s}^{-1} \text{ M}^{-1}$, which gives a lifetime range of $5.82 \cdot 10^{-9} \text{ s} - 9 \cdot 10^{-9} \text{ s}$.

Determination of the quantum yield for the photocatalytic conversion of **3** to **4**



The reaction mixture was prepared in a glove box equipped with a red LED in a dark room, using a cuvette (equipped with a stir bar) fitted with a J-Young tap.

For these experiments, three stock solutions were prepared: A stock solution of **3** was prepared by dissolving 216 mg of **3** in 14.4 mL of THF. A stock solution of NEt₃ (**6a**) was prepared by dissolving 164 μ L of NEt₃ in 4.8 mL of THF. A stock solution of Ni(Mabiq)OTf (**1**) was prepared by dissolving 4.4 mg of Ni(Mabiq)OTf in 2.4 mL of DMF.

1.8 mL of the stock solution of **3** were added to a cuvette, after which 0.6 mL of the stock solution of NEt₃ (**6a**) were added, followed by 0.6 mL of the Ni(Mabiq)OTf (**1**) stock solution. The final reaction mixture contained $7.34 \cdot 10^{-2}$ mmol of **3**, 0.148 mmol of NEt₃ (**6a**) (2 equiv.) and $1.47 \cdot 10^{-3}$ mmol of Ni(Mabiq)OTf (**1**) (2 mol%) in 3 mL of a 4:1 THF:DMF mixture.

The cuvette was sealed, covered with aluminum foil, removed from the glove box and introduced into a black box equipped with a red LED and a red window. The reaction mixture was irradiated at 455 nm for 60 min (with stirring at 400 rpm).

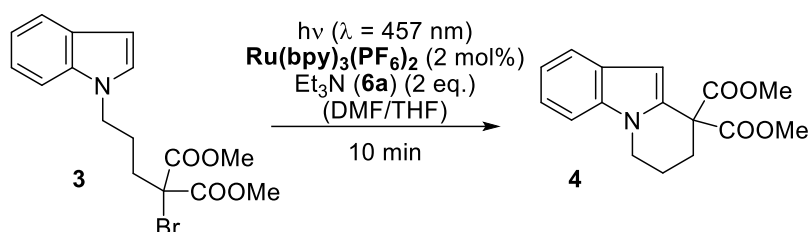
During the irradiation time a dibromomethane stock solution was prepared. 128 mg of dibromomethane were added to a 10 mL volumetric flask and diluted with CDCl₃ to a final volume of 10 mL. With 0.5 mL aliquots of this solution the NMR sample was prepared.

After the irradiation time the reaction was stopped by addition of 5 mL water. The mixture was poured into a separation funnel and extracted with ether (3 x 10 mL). The combined organic phases were washed with 20 mL brine solution, dried over 3.00 g of Na₂SO₄ and filtered. After removing the solvents under vacuum a NMR sample was prepared by adding 0.5 mL aliquots of the dibromomethane stock solution.

The product yield, based on the NMR analysis, was determined as 6%, which yields a quantum yield of 0.006:

$$\Phi (1, 1 \text{ h}) = \frac{\text{mol of } \mathbf{4}}{\text{photon flux} \times t \times f} = \frac{4.41 \cdot 10^{-6}}{2.226 \cdot 10^{-7} \times 3600 \times 1} = 0.006$$

An analogous reaction was carried out using $\text{Ru}(\text{bpy})_3(\text{PF}_6)_2$ as the catalyst.



Stock solutions of **3** and Et_3N (**6a**) were as previously described. A stock solution of $\text{Ru}(\text{bpy})_3(\text{PF}_6)_2$ was prepared by dissolving 5.0 mg of $\text{Ru}(\text{bpy})_3(\text{PF}_6)_2$ in 2.4 mL of DMF.

Samples were prepared as described above, such that the final reaction mixture contained $7.34 \cdot 10^{-2}$ mols of **3**, 0.148 mmol of NEt_3 (**6a**) (2 equiv.) and $1.47 \cdot 10^{-3}$ mmol of $\text{Ru}(\text{bpy})_3(\text{PF}_6)_2$ (2 mol%) in 3 mL of a 4:1 THF:DMF mixture.

The analogous procedure to the one described for **1** was followed to determine the quantum yield for the $\text{Ru}(\text{bpy})_3(\text{PF}_6)_2$ catalyzed reaction.

The product yield was determined to be 36%, from which the quantum yield was calculated to be 0.033.

$$\Phi ([\text{Ru cat}], 1 \text{ h}) = \frac{\text{mols of } \mathbf{4}}{\text{photon flux} \times t \times f} = \frac{2.65 \cdot 10^{-5}}{2.226 \cdot 10^{-7} \times 3600 \times 1} = 0.033$$

We note that we observe decomposition of the $[\text{Ru}(\text{bpy})_3]^{2+}$ catalyst during the 1 h reaction period (as analyzed by mass spectrometry, where peaks corresponding to brominated complex can be observed). Thus, the decomposition of the Ru catalysts presents a limitation to any direct comparison of quantum yields.

Absorption spectra of Ni(Mabiq)OTf (1) in the presence of Et₃N (6a) or Cy₂NCH₂Mes (6f)

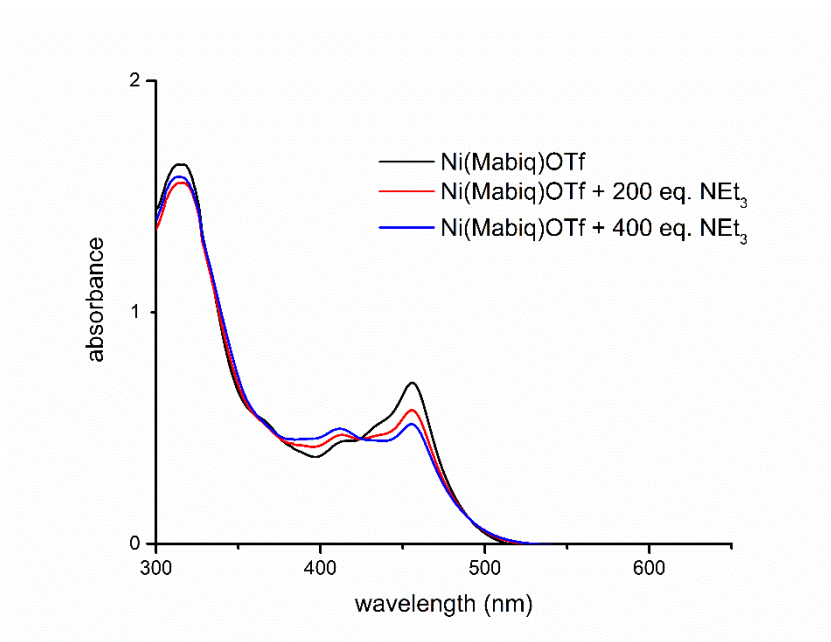


Figure S30: Absorption spectra of a 10⁻⁴ M solution of Ni(Mabiq)OTf in DMF:THF (1:4), and after addition of 200 or 400 equivalents of Et₃N (6a).

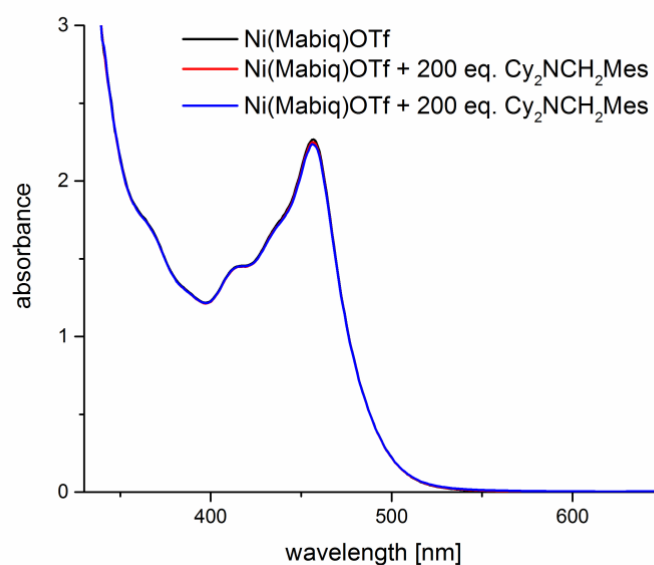


Figure S31: Absorption spectra of a 10⁻⁴ M solution of Ni(Mabiq)OTf in DMF:THF (1:4), and after addition of 200 or 400 equivalents of Cy₂NCH₂Mes (6f).

NMR Spectra

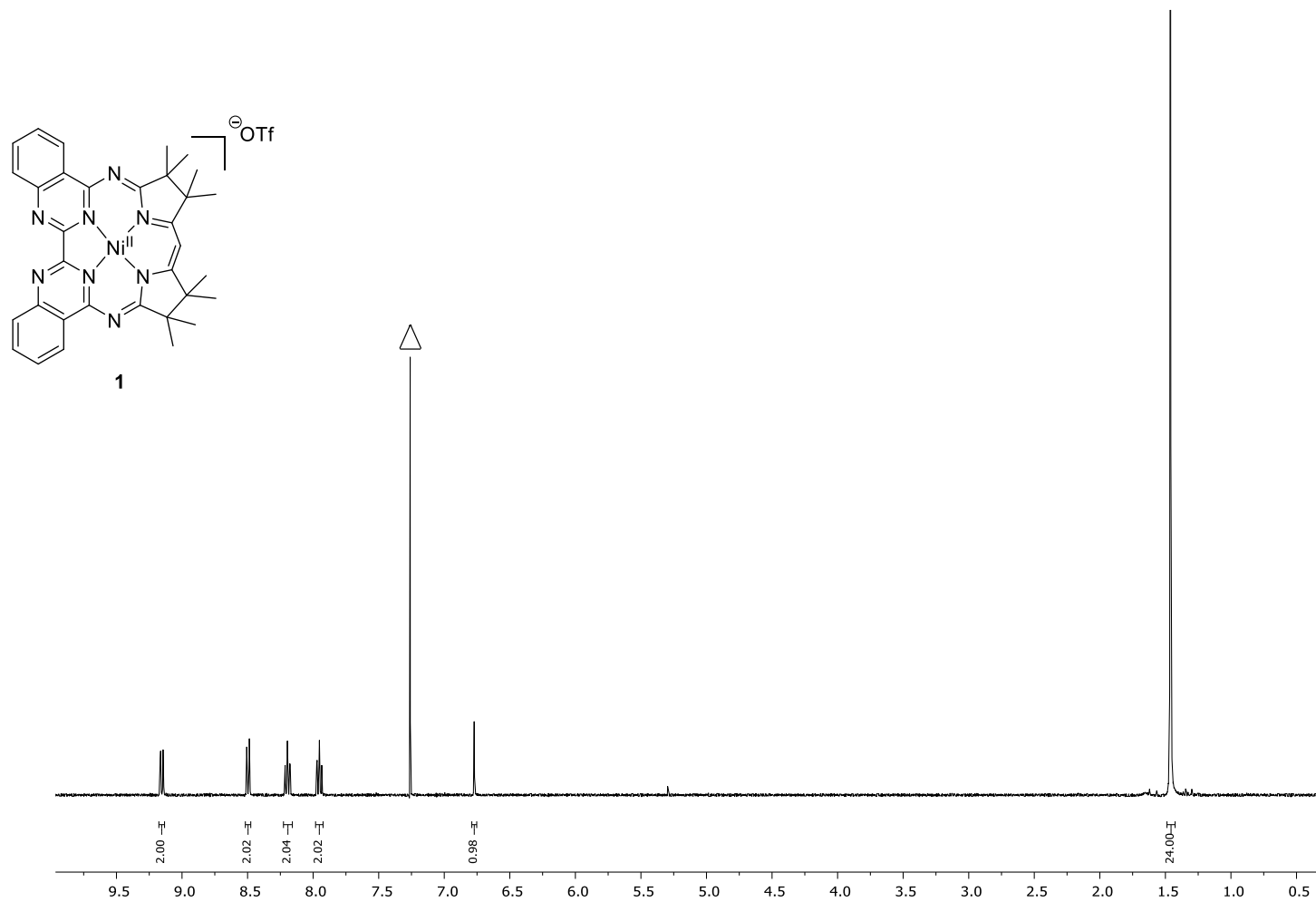


Figure S32: ¹H NMR (400 MHz, CDCl₃) of **1**; (Δ= CDCl₃ solvent residual signal in all NMR spectra throughout).

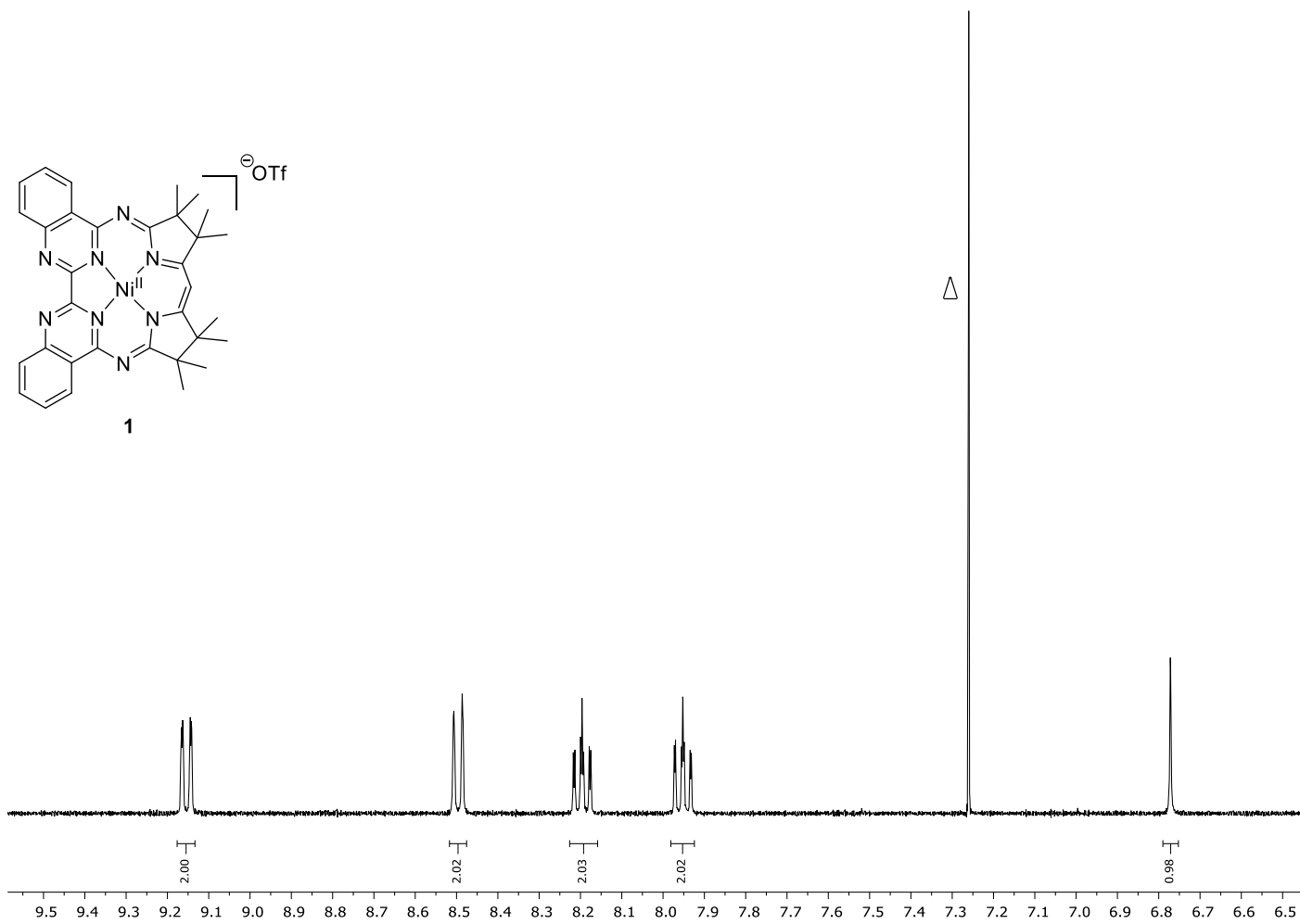


Figure S33: ¹H NMR (400 MHz, CDCl₃) of **1** in the range 6.5 ppm and 9.5 ppm.

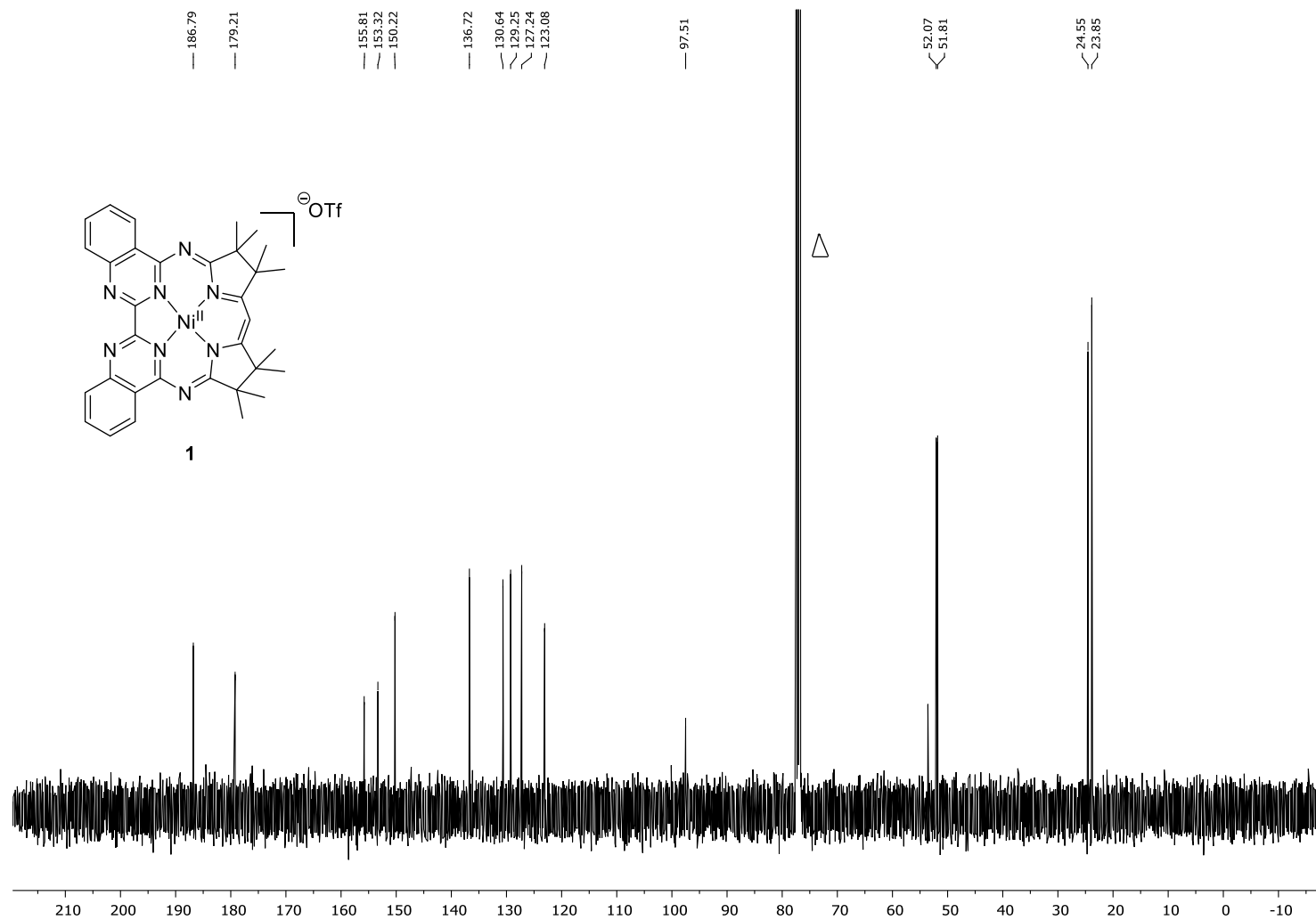


Figure S34: ¹³C NMR (101 MHz, CDCl₃) of **1**.

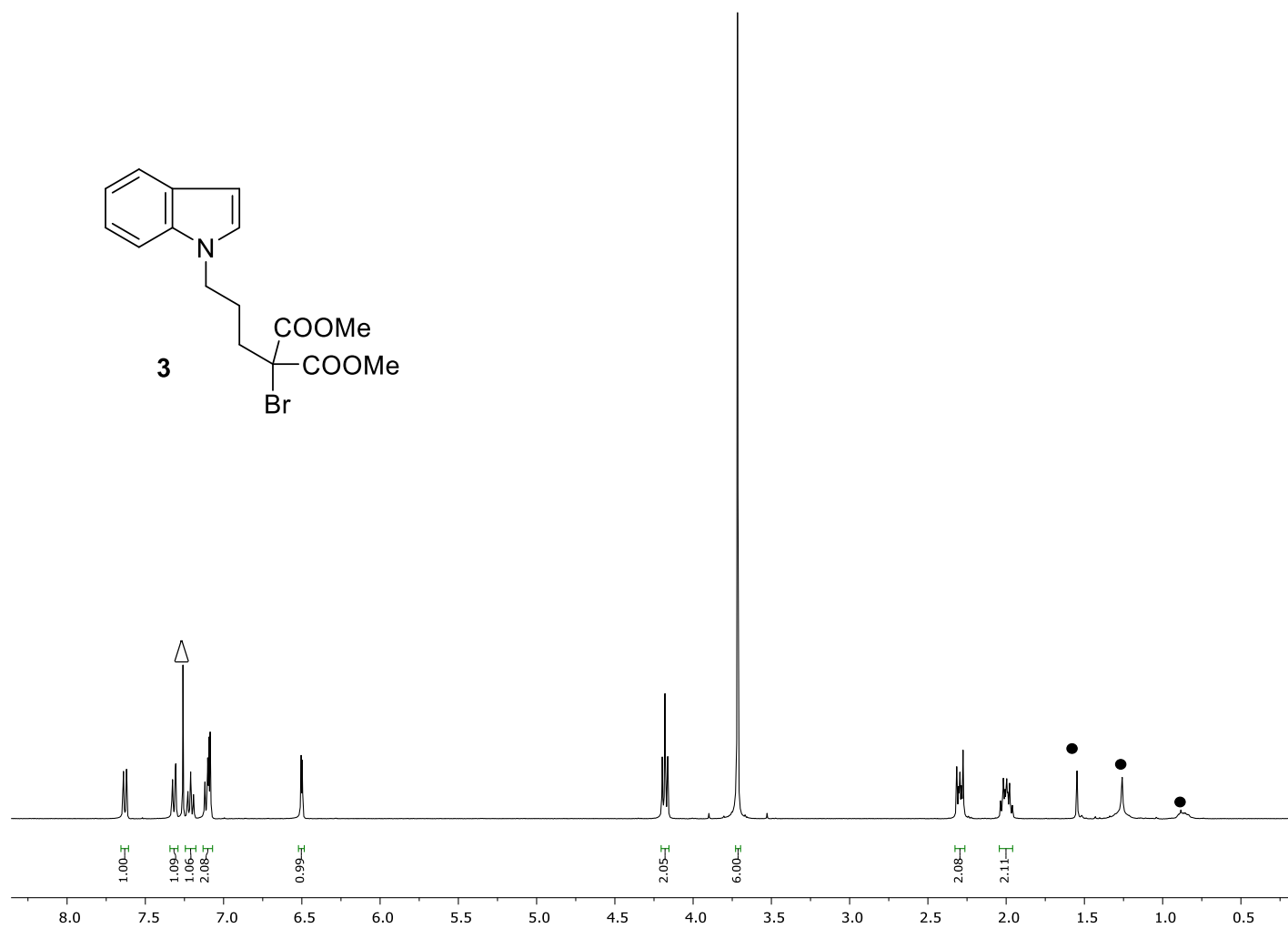


Figure S35: ¹H NMR (400 MHz, CDCl₃) of **3**; Δ= solvent peaks (CDCl₃ solvent residual signal); ● = water, grease.

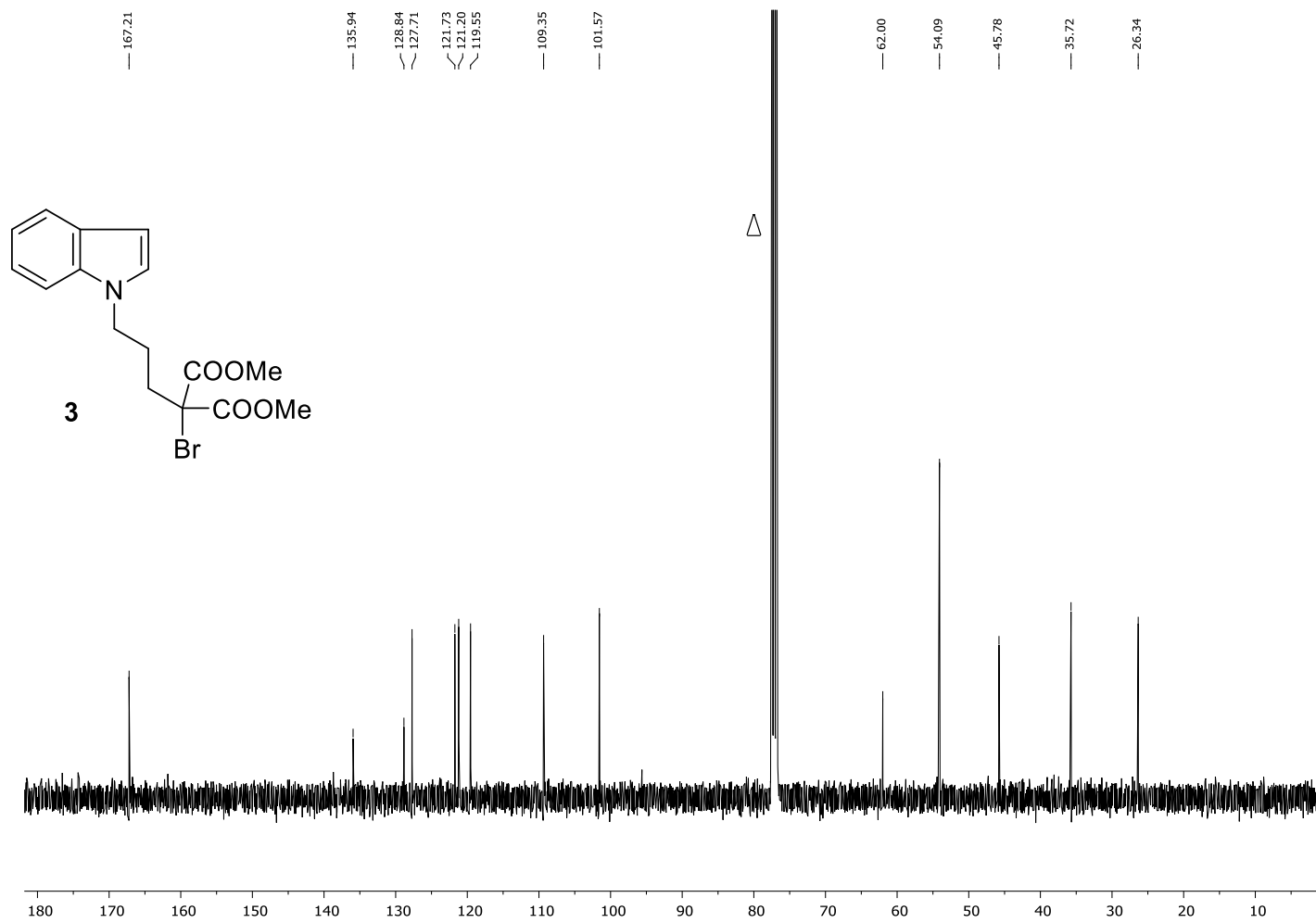


Figure S36: ^{13}C NMR (101 MHz, CDCl_3) of **3**.

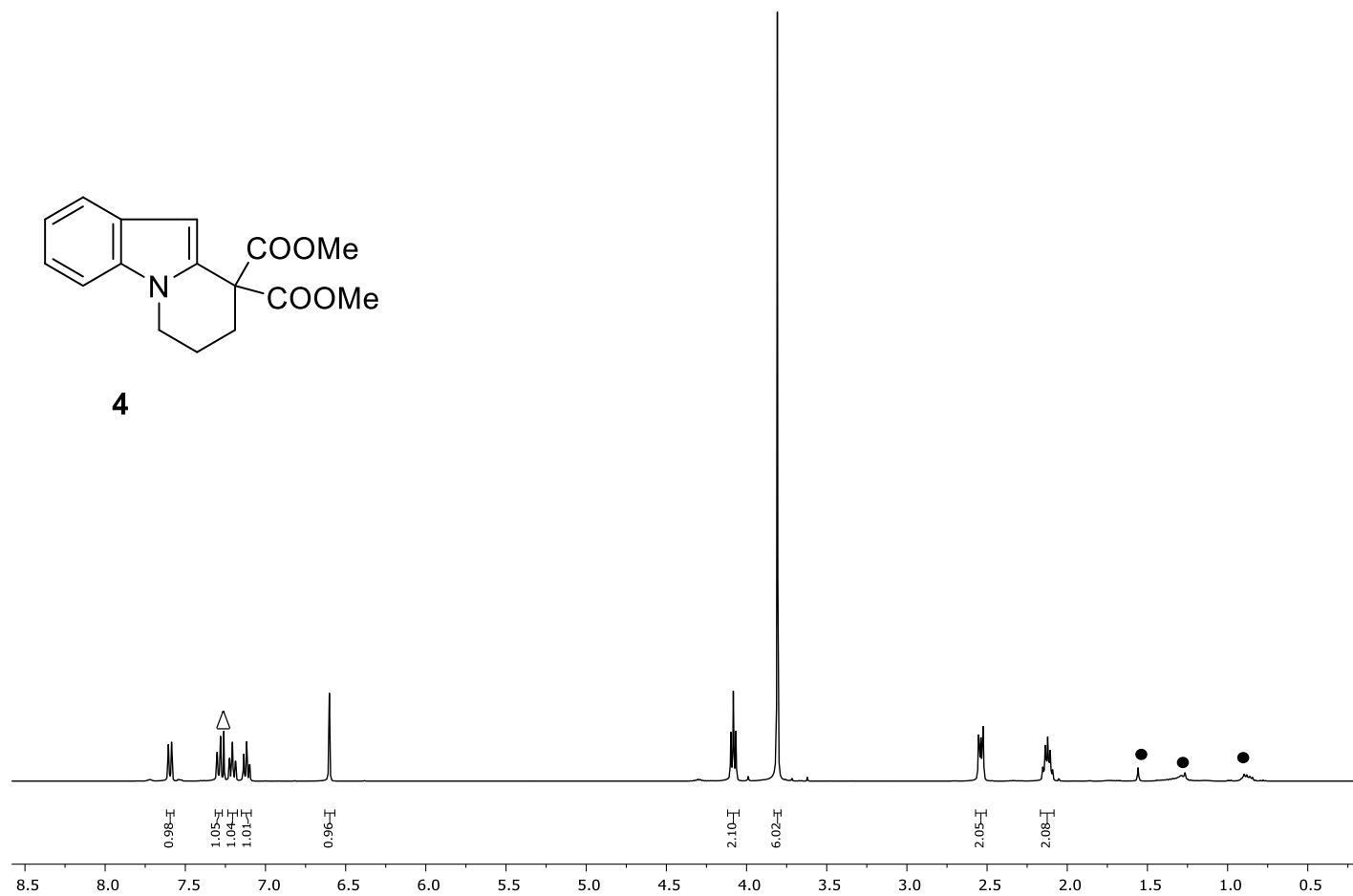


Figure S37: $^1\text{H NMR}$ (400 MHz, CDCl_3) of **4** Δ = solvent peaks (CDCl_3 solvent residual signal); • = water, grease.

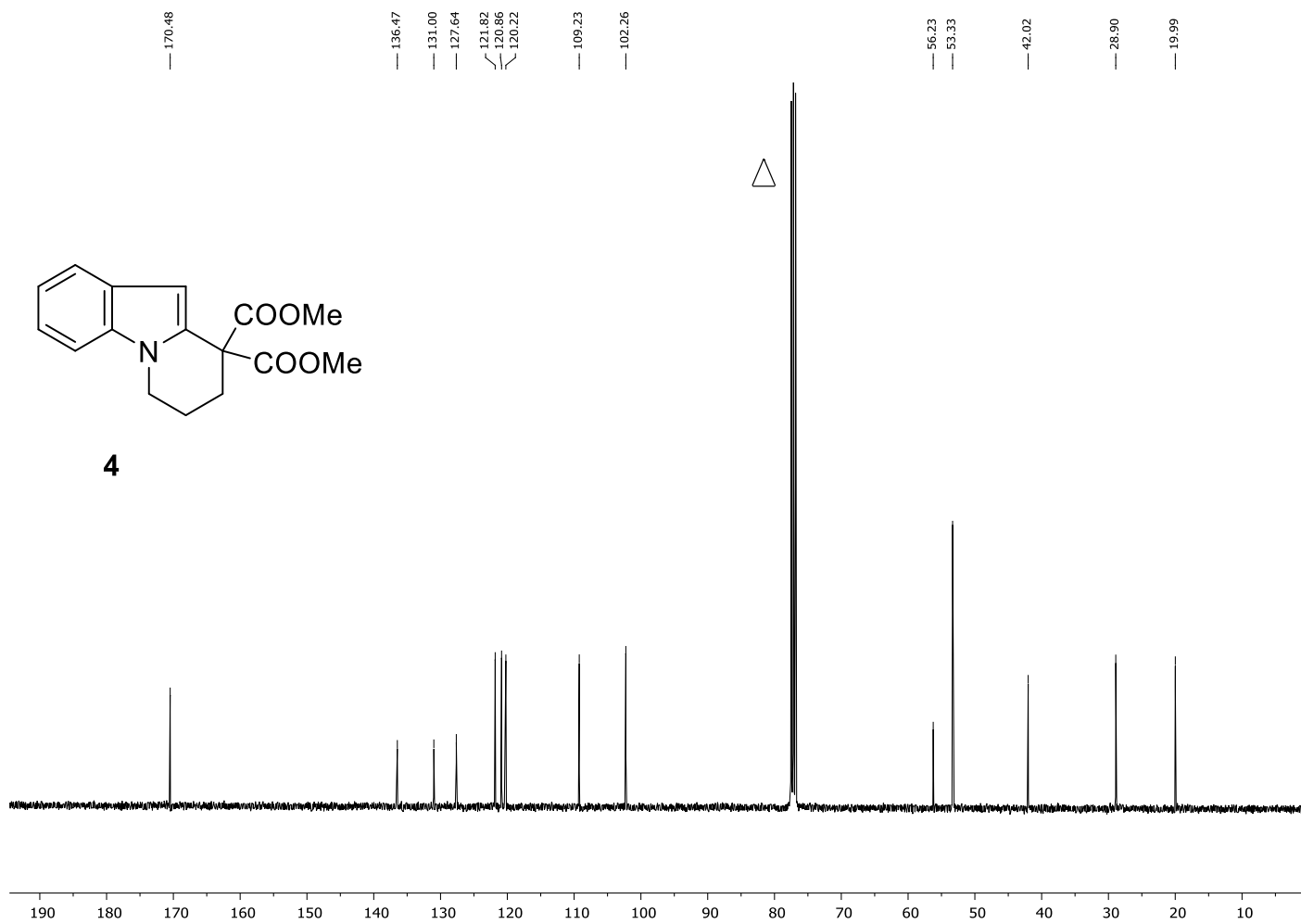


Figure S38: ^{13}C NMR (101 MHz, CDCl_3) of **4**.

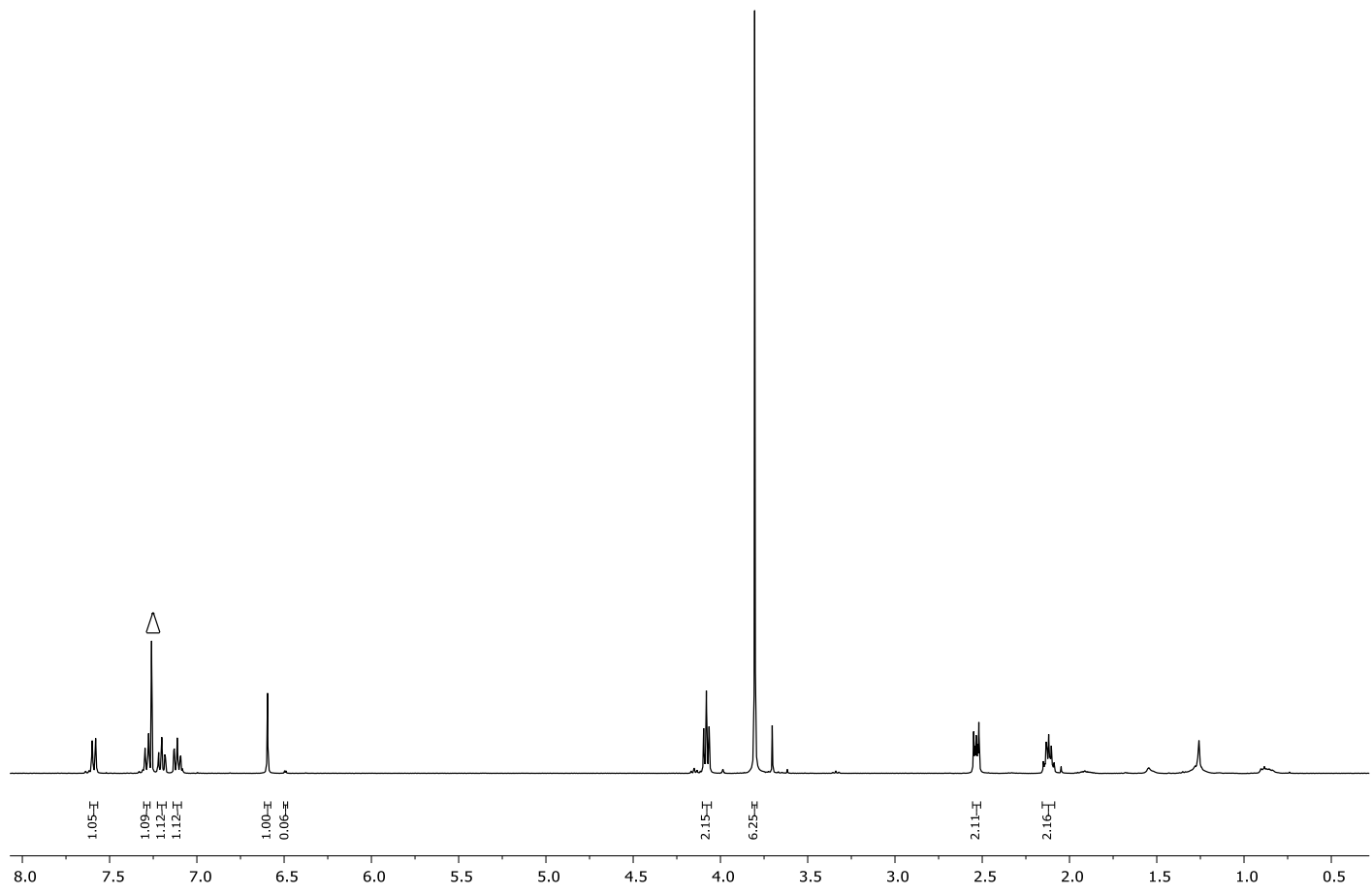


Figure S39: ^1H NMR (400 MHz, CDCl_3) of product mixture (photoredox catalysis with **1** and **3**).

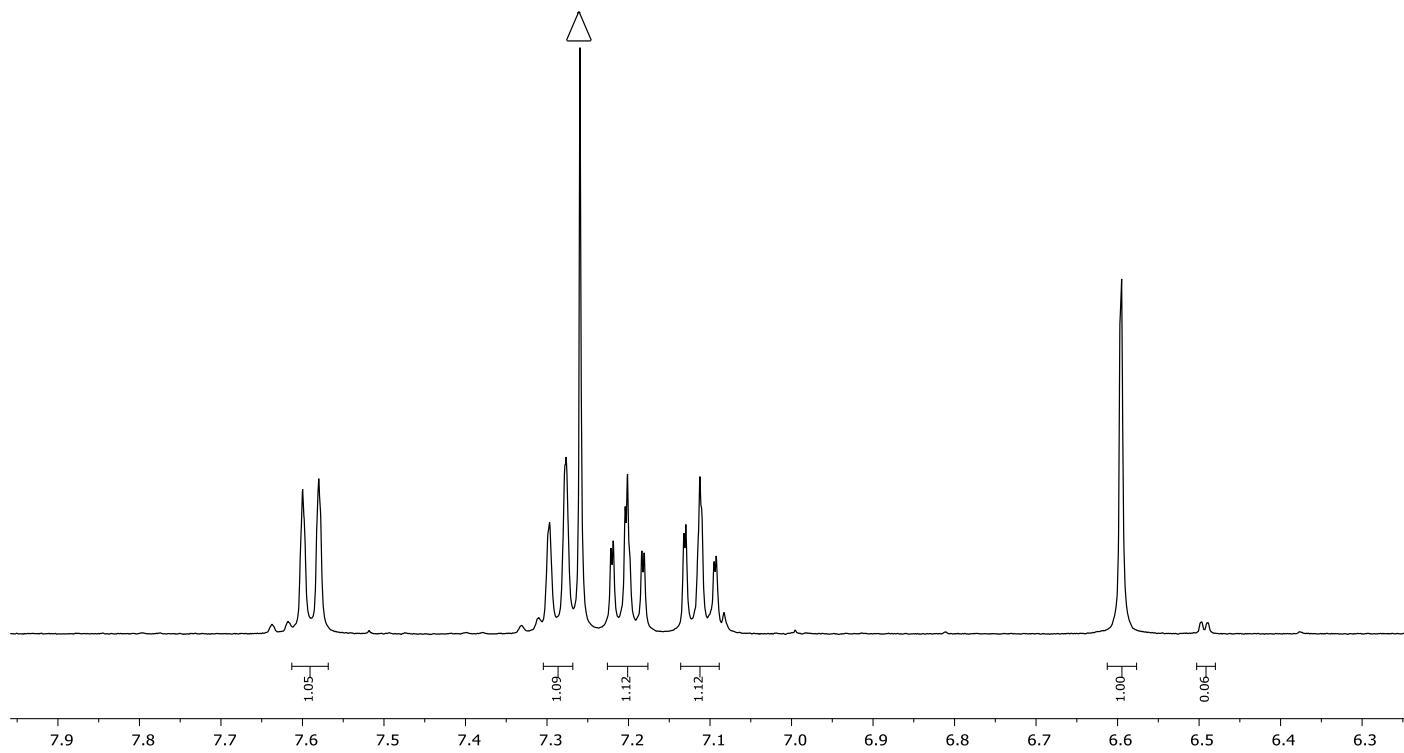


Figure S40: ¹H NMR (400 MHz, CDCl₃) of product mixture (photoredox catalysis with **1** and **3**) in the range between 6.3 ppm and 7.8 ppm.

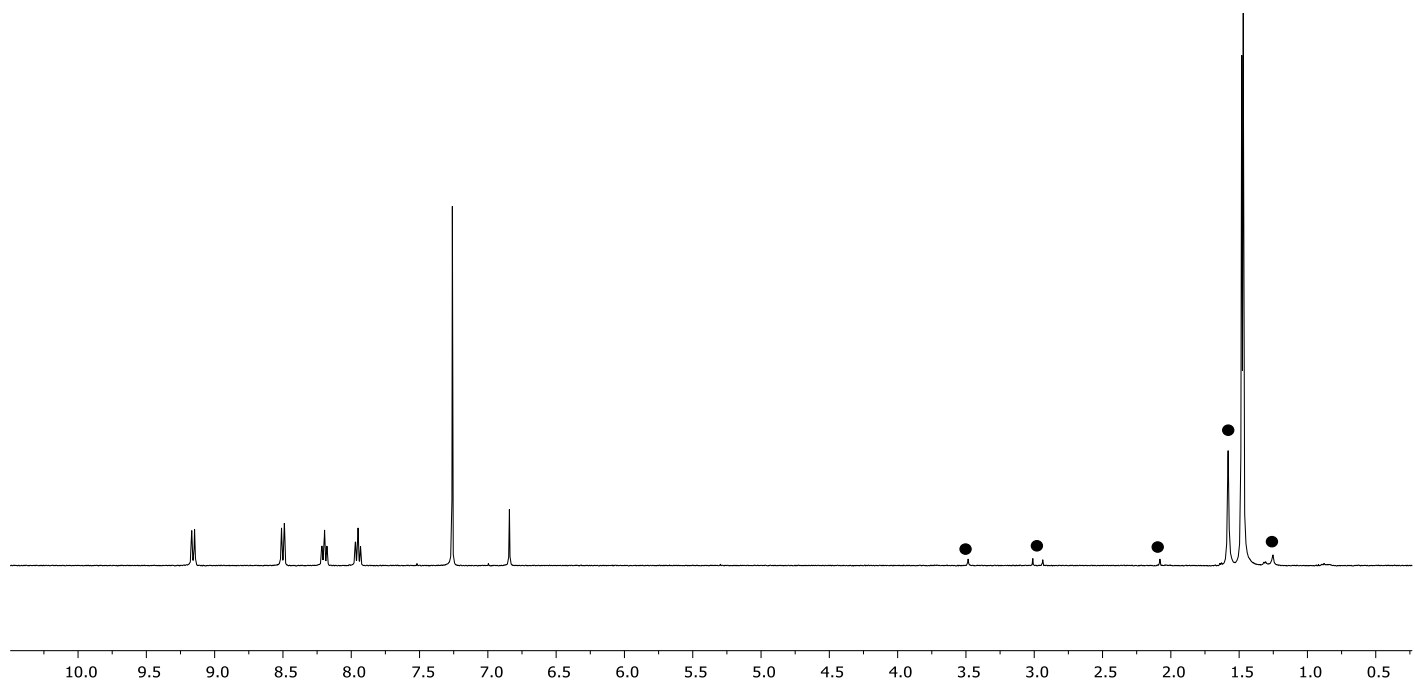


Figure S41: ^1H NMR (400 MHz, CDCl_3) of **1** after catalytic reaction; ● = water, grease, DMF, MeOH.

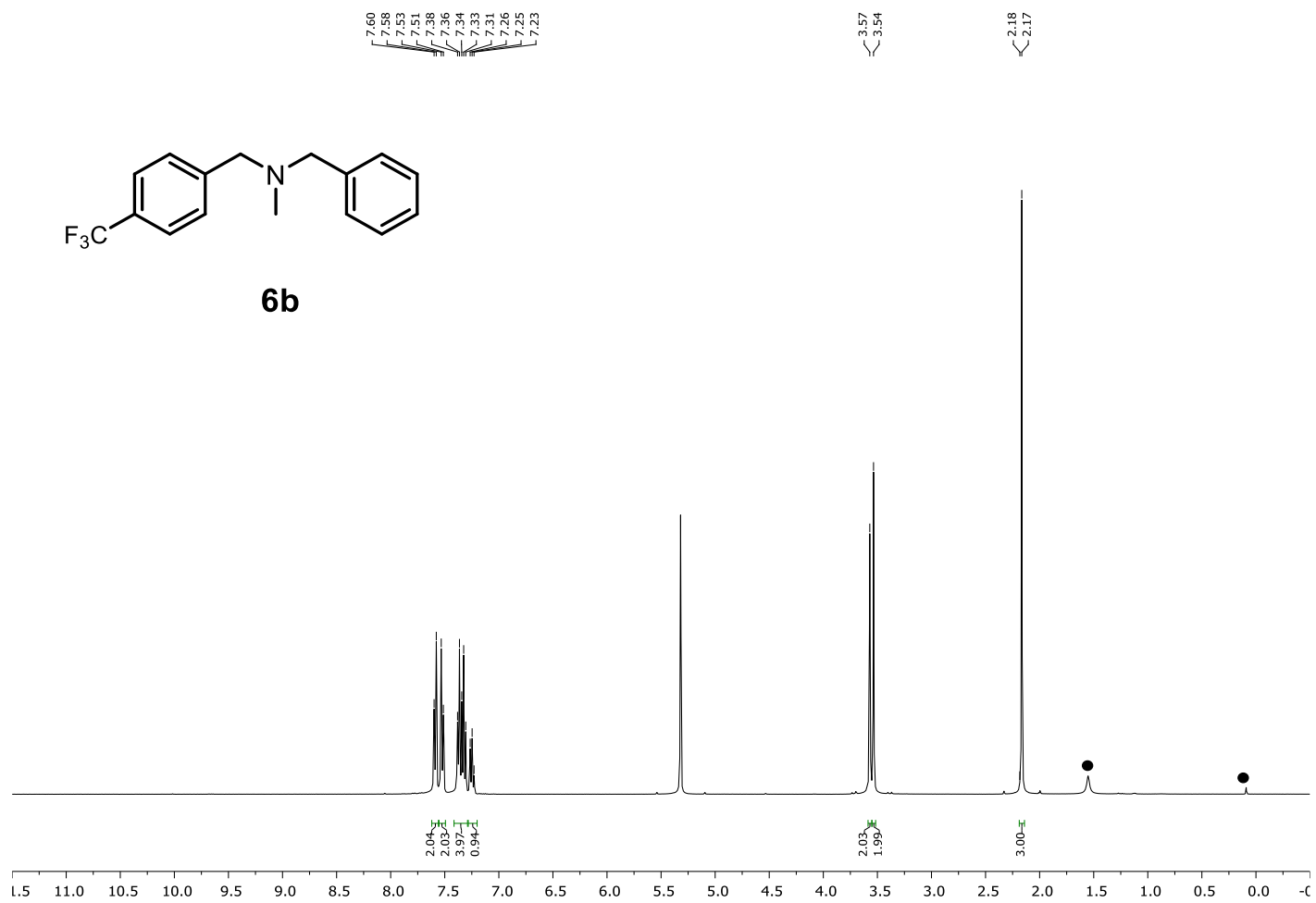


Figure S42: ¹H NMR (400 MHz, CD₂Cl₂) of **6b**; ● = water, grease.

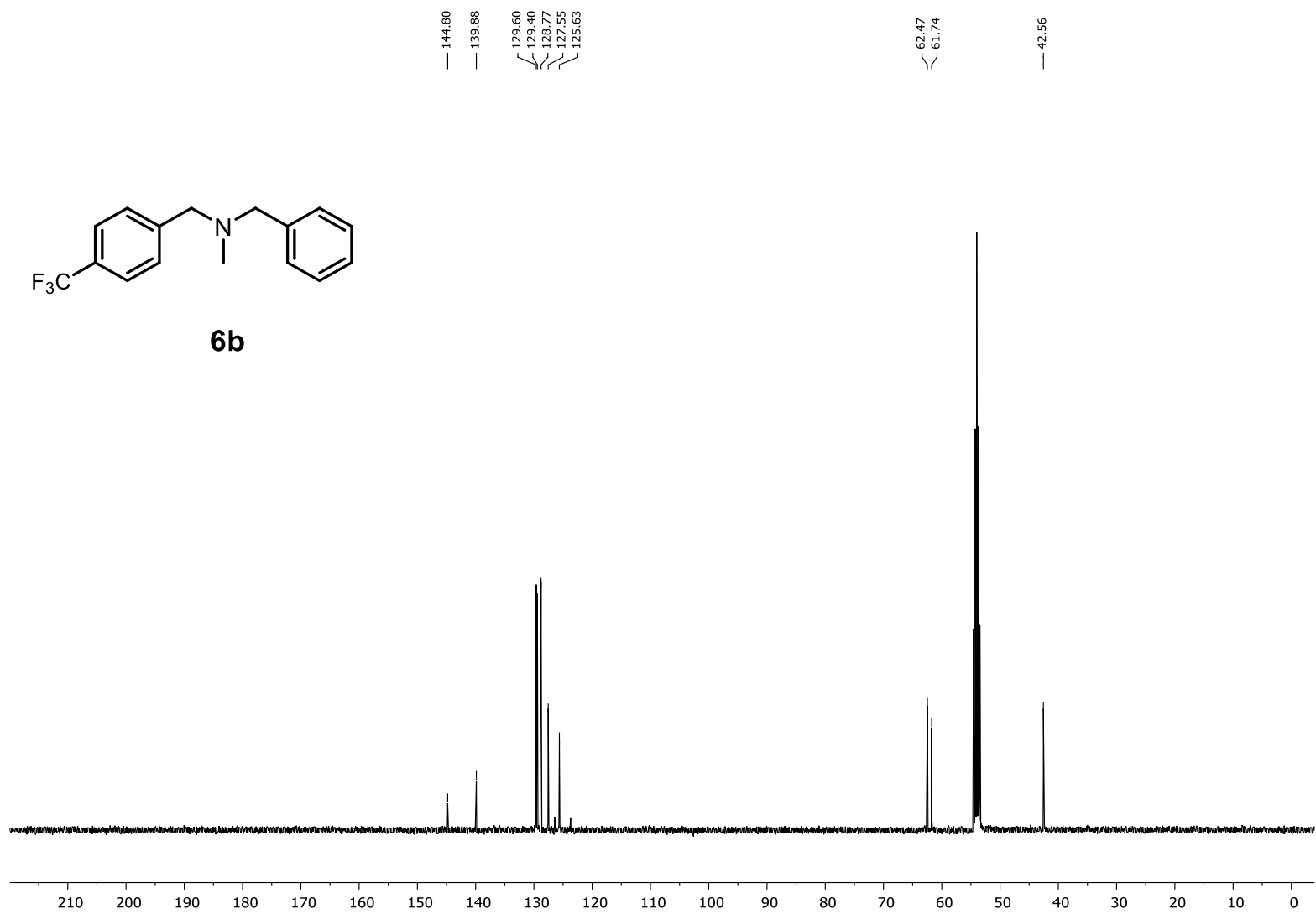


Figure S43: ^{13}C NMR (101 MHz, CD_2Cl_2) of **6b**.

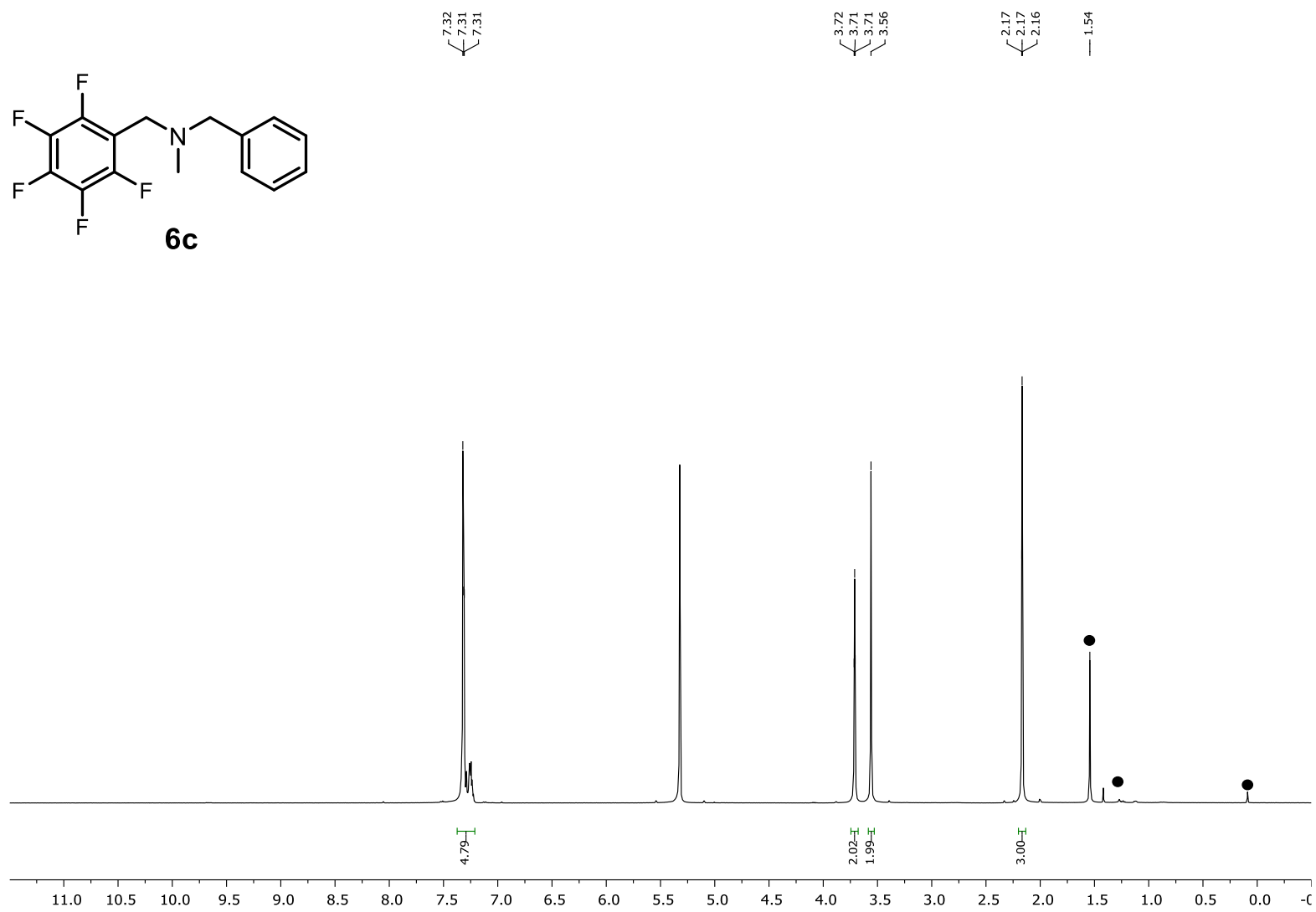


Figure S44: ^1H NMR (400 MHz, CD_2Cl_2) of **6c**, ● = water, grease.

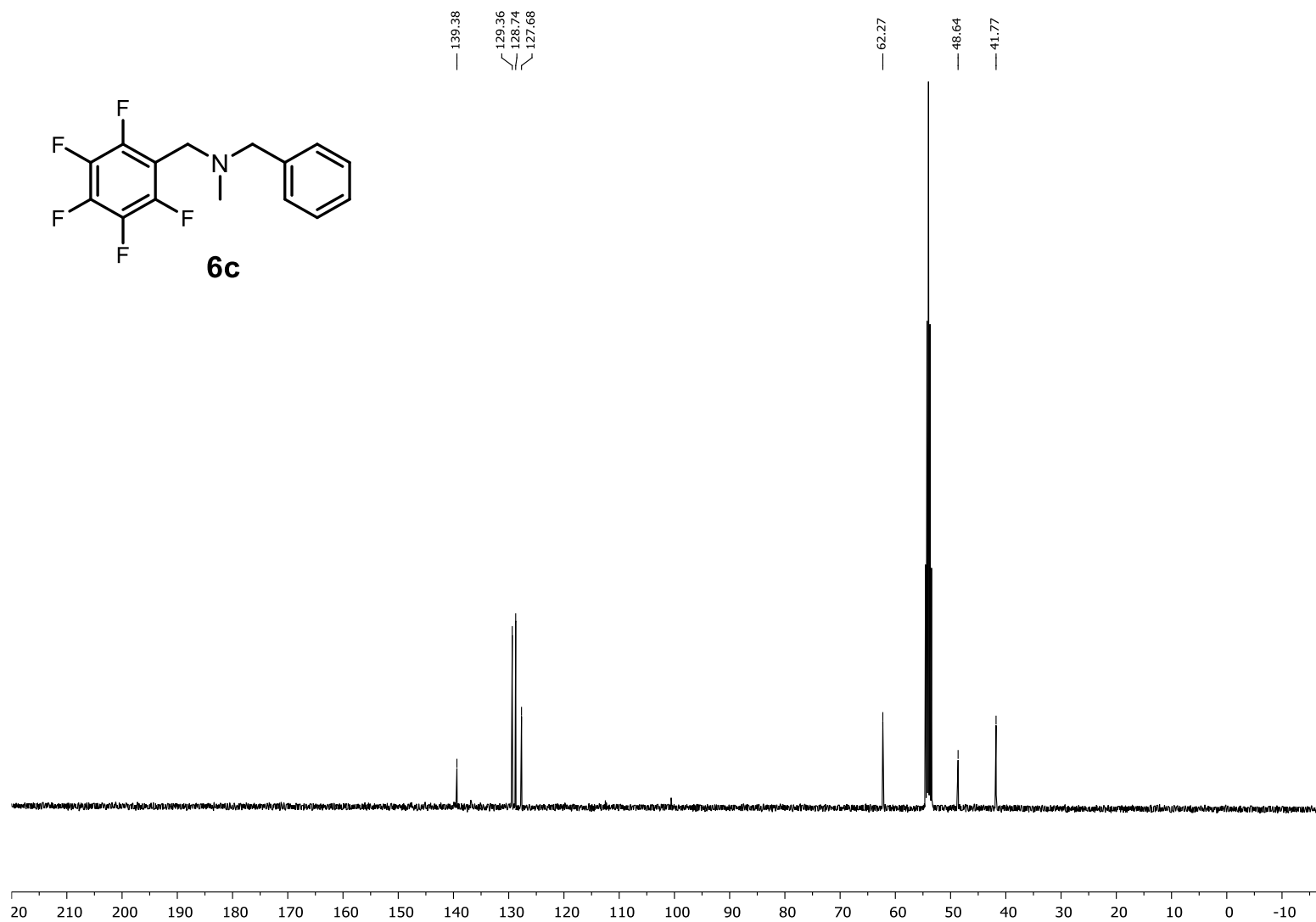


Figure S45: ^{13}C NMR (101 MHz, CD_2Cl_2) of **6c**.

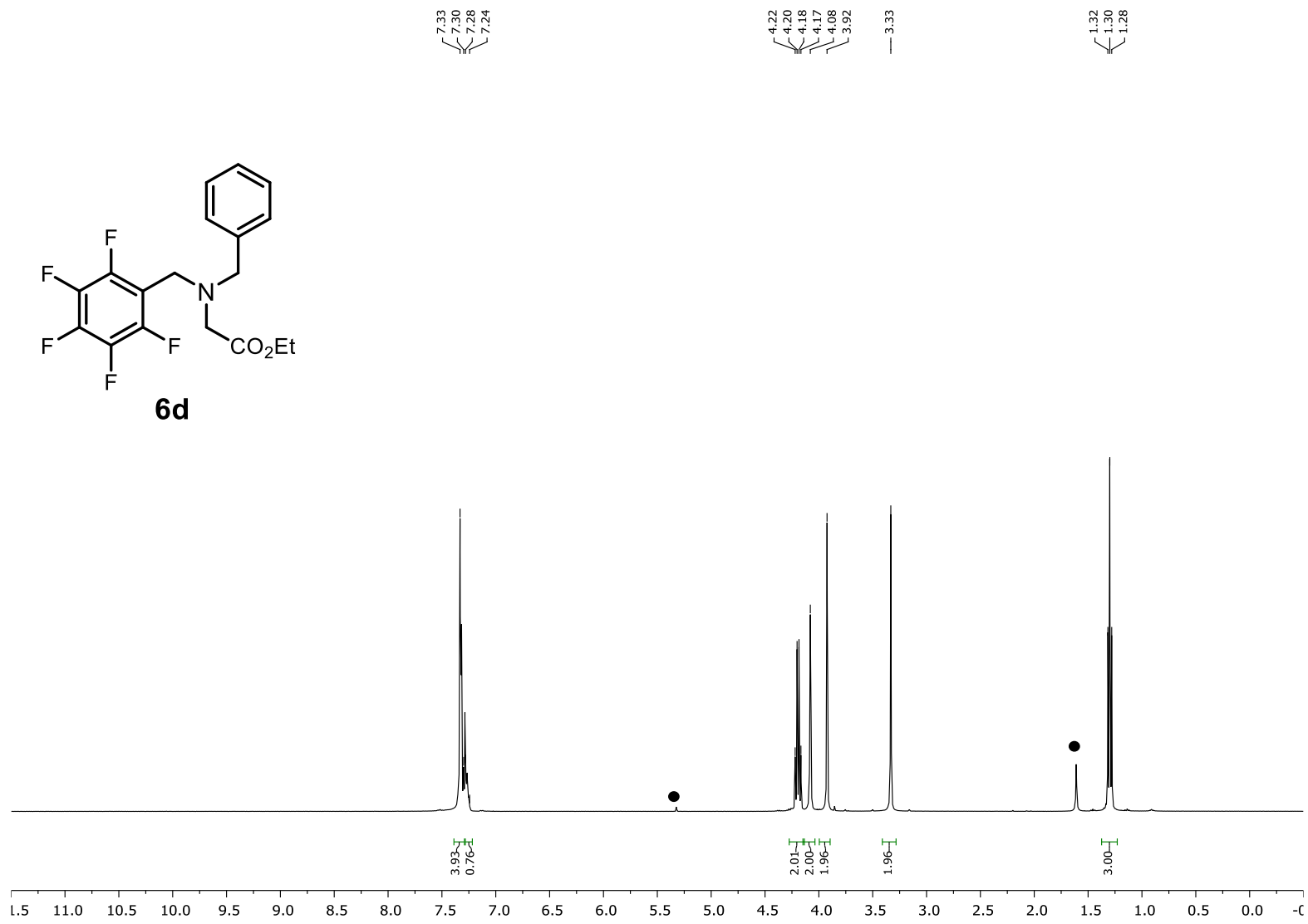


Figure S46: ¹H NMR (400 MHz, CDCl₃) of **6d**, ● = water, CH₂Cl₂.

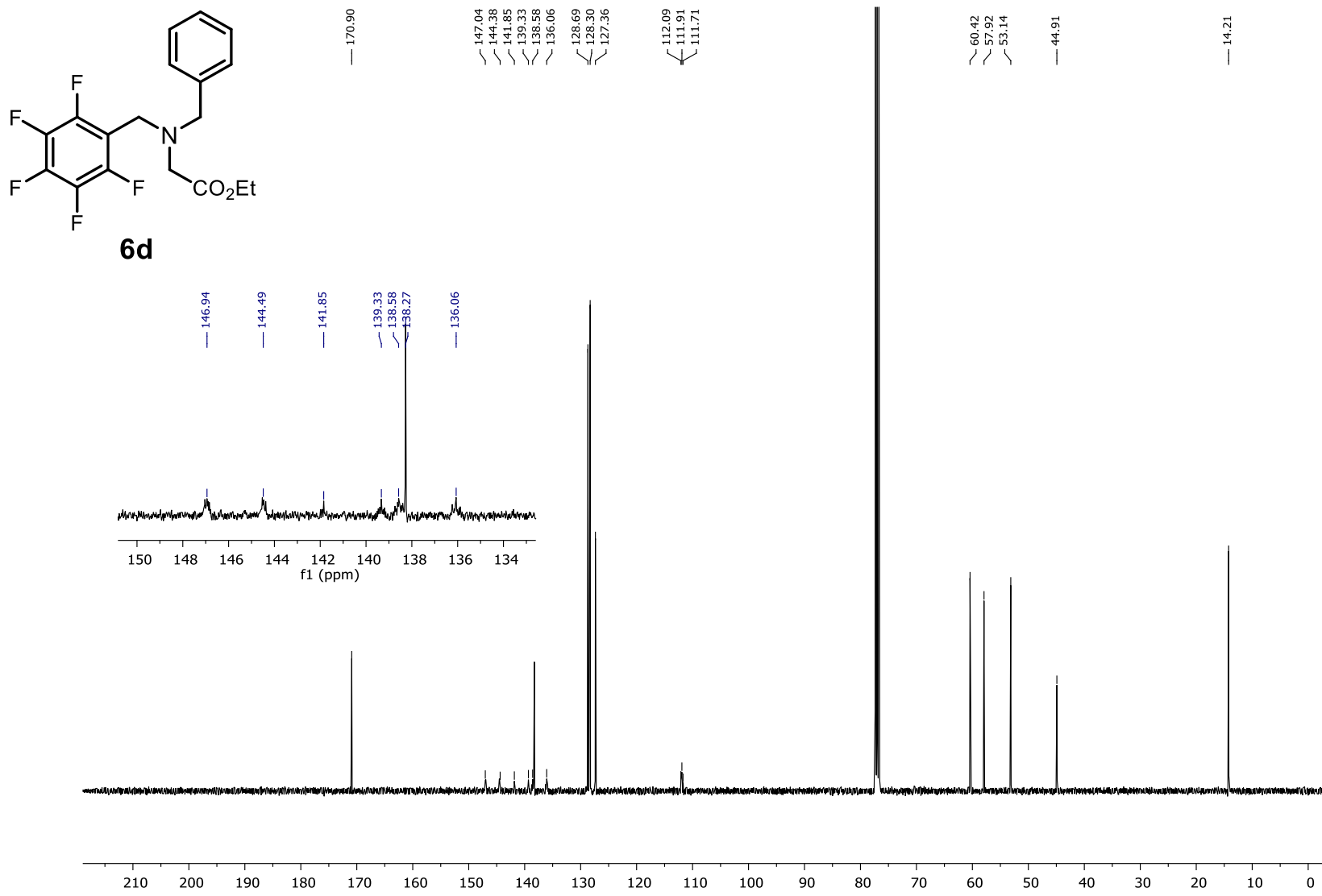


Figure S47: ^{13}C NMR (101 MHz, CDCl_3) of **6d**.

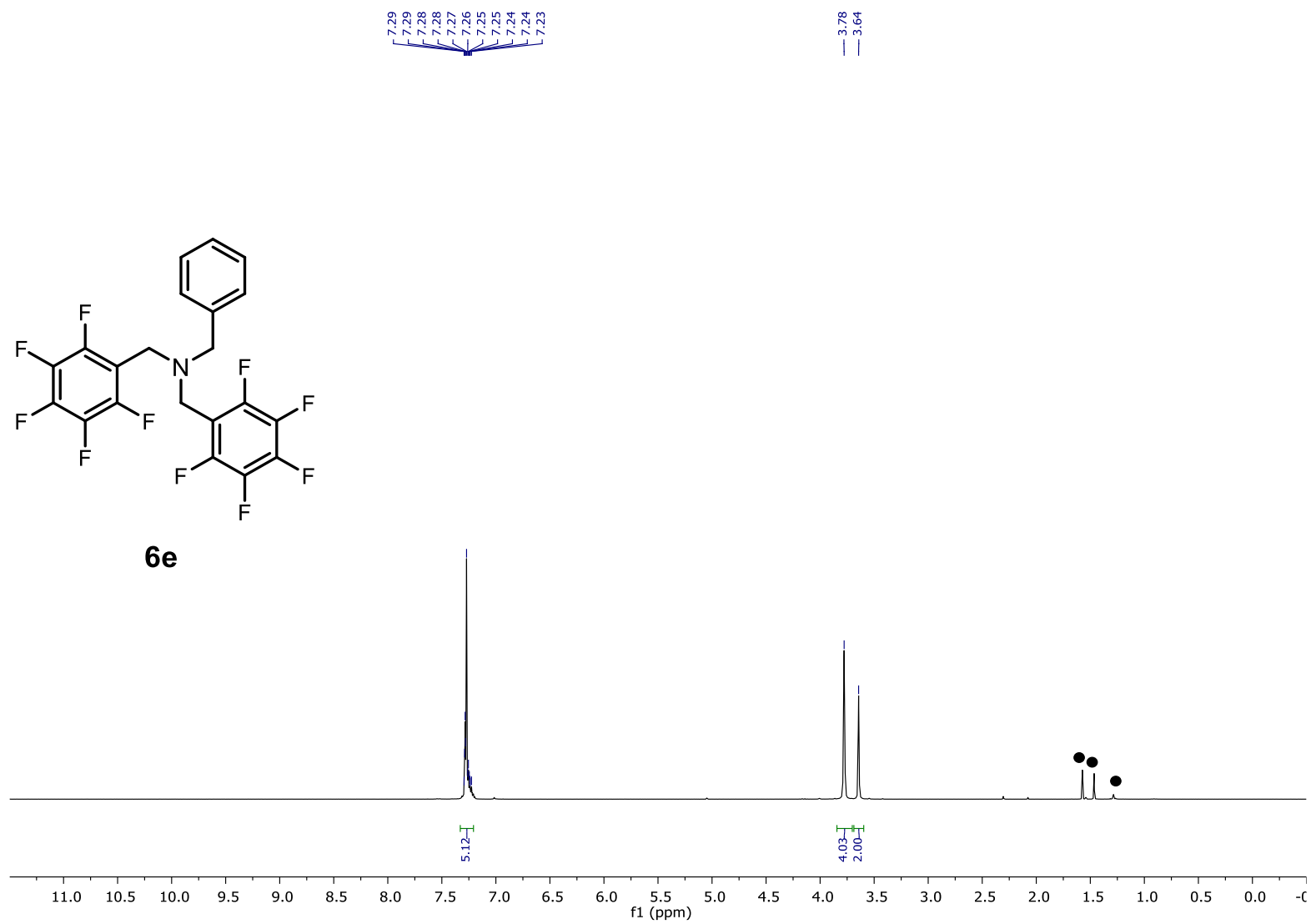


Figure S48: $^1\text{H NMR}$ (400 MHz, CDCl_3) of **6e**, ● = water, grease, cyclohexane.

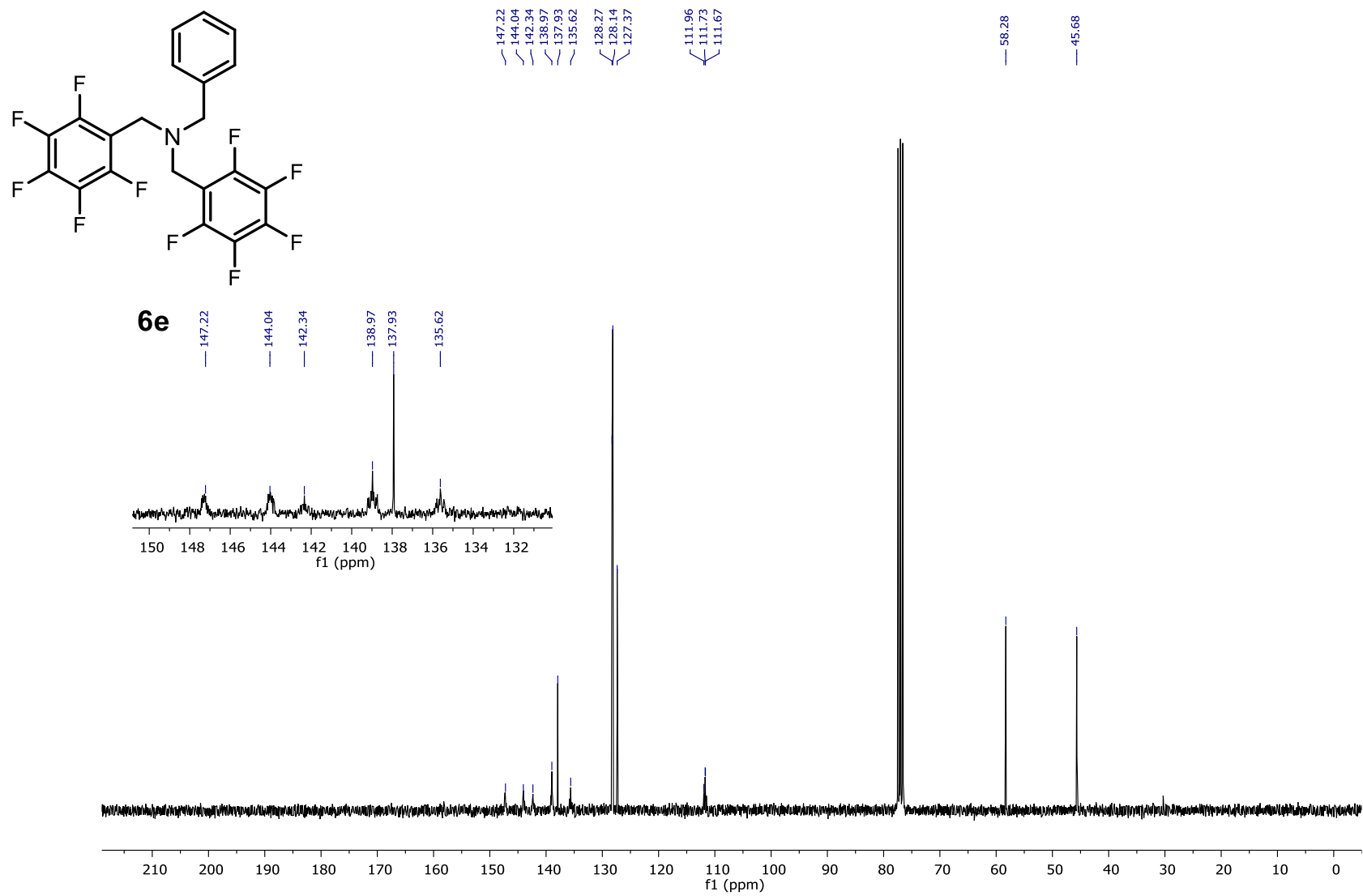


Figure S49: ^{13}C NMR (101 MHz, CDCl_3) of **6e**.

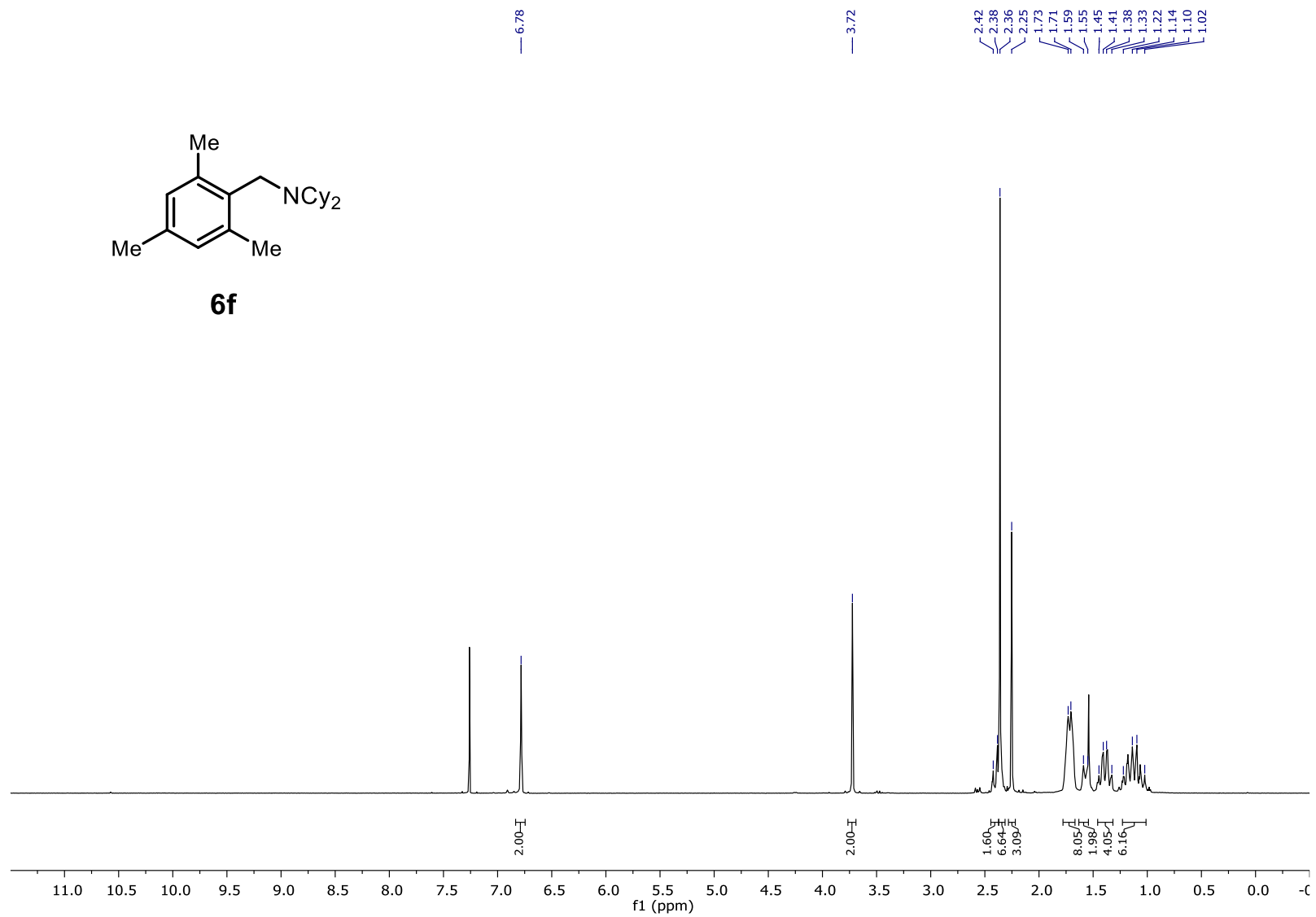


Figure S50: ¹H NMR (400 MHz, CDCl₃) of **6f**.

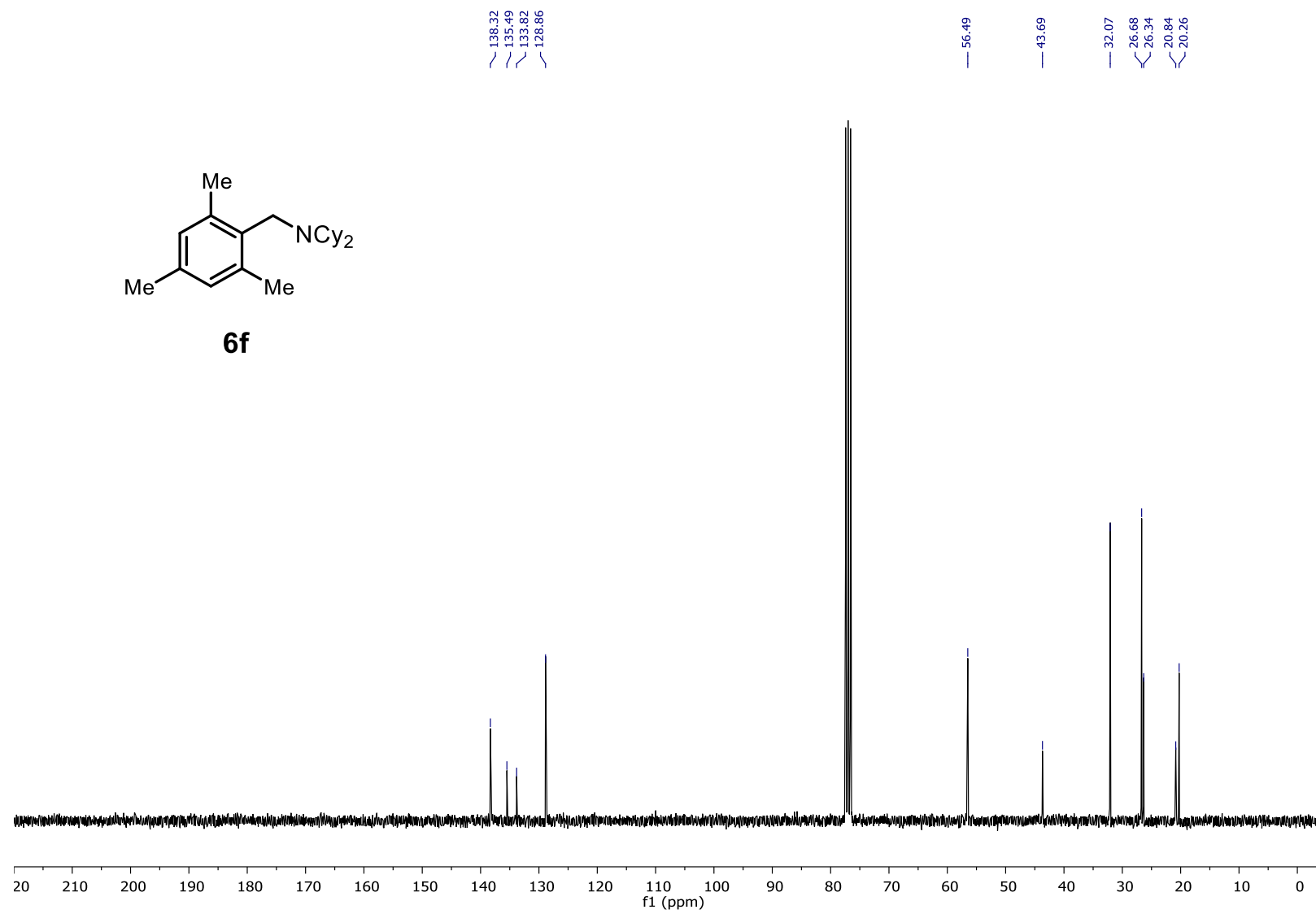


Figure S51: ^{13}C NMR (101 MHz, CDCl_3) of **6f**.

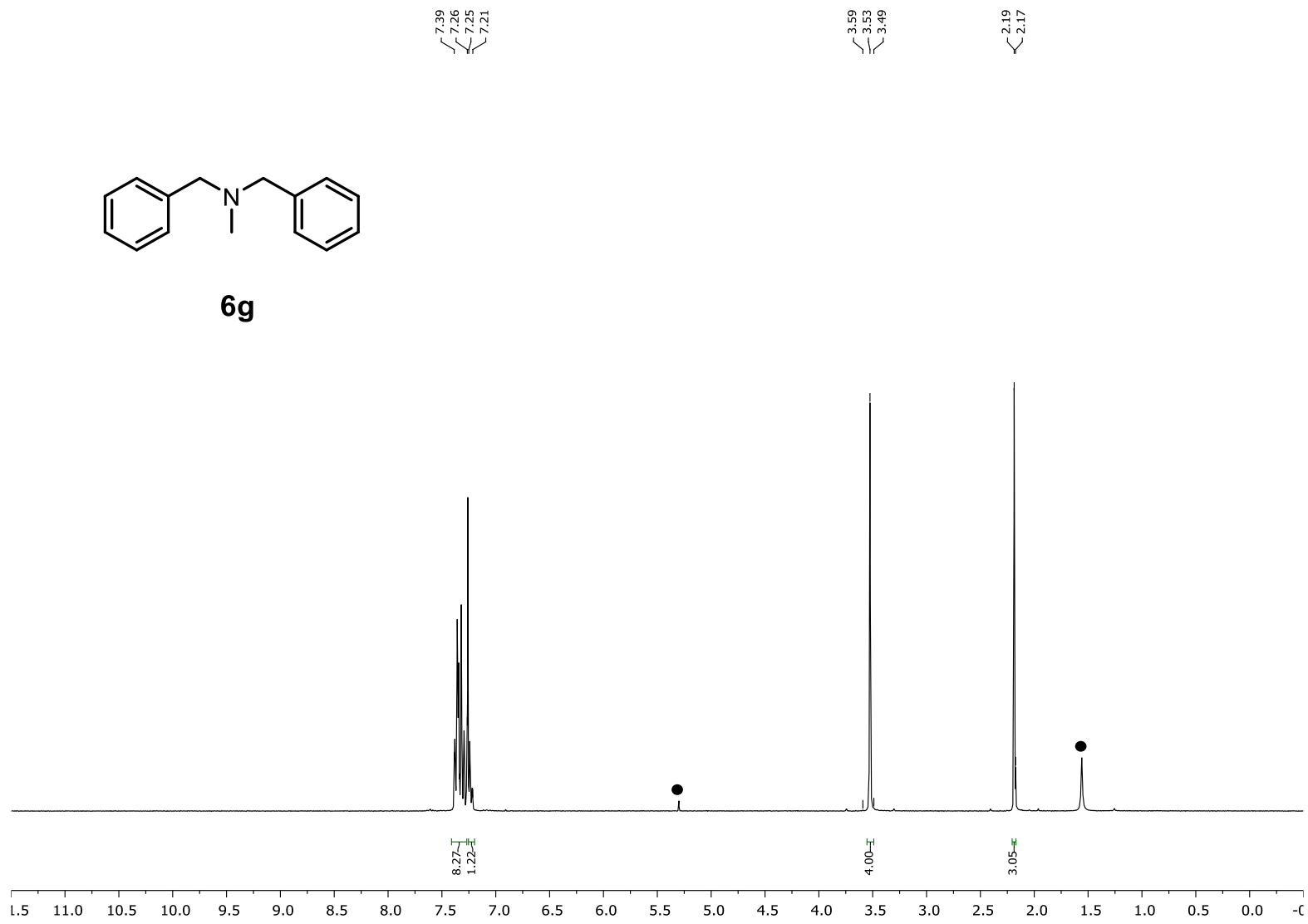


Figure S52: ^1H NMR (400 MHz, CDCl_3) of **6g**, ● = water, CH_2Cl_2 .

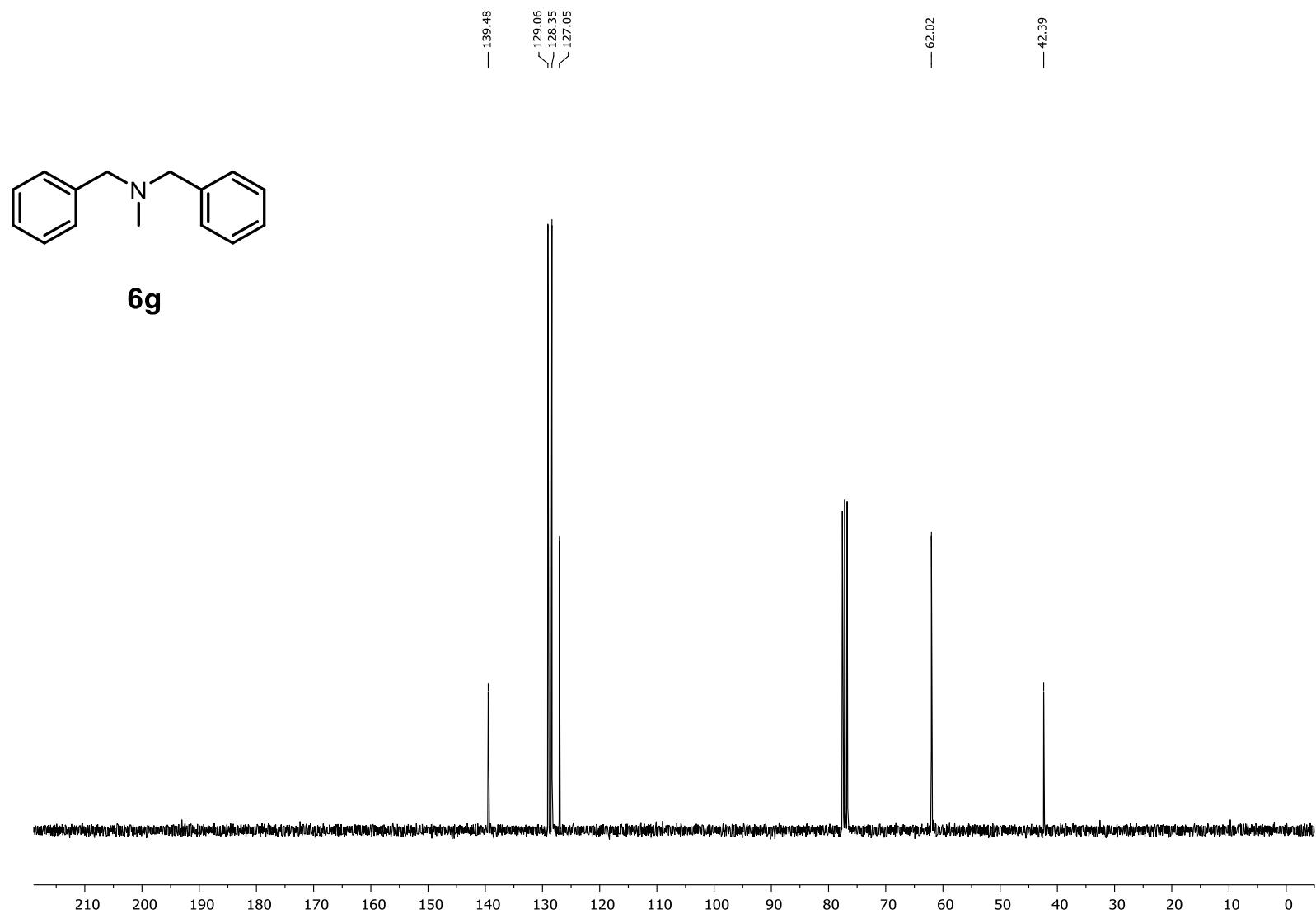


Figure S53: ^{13}C NMR (101 MHz, CDCl_3) of **6g**.

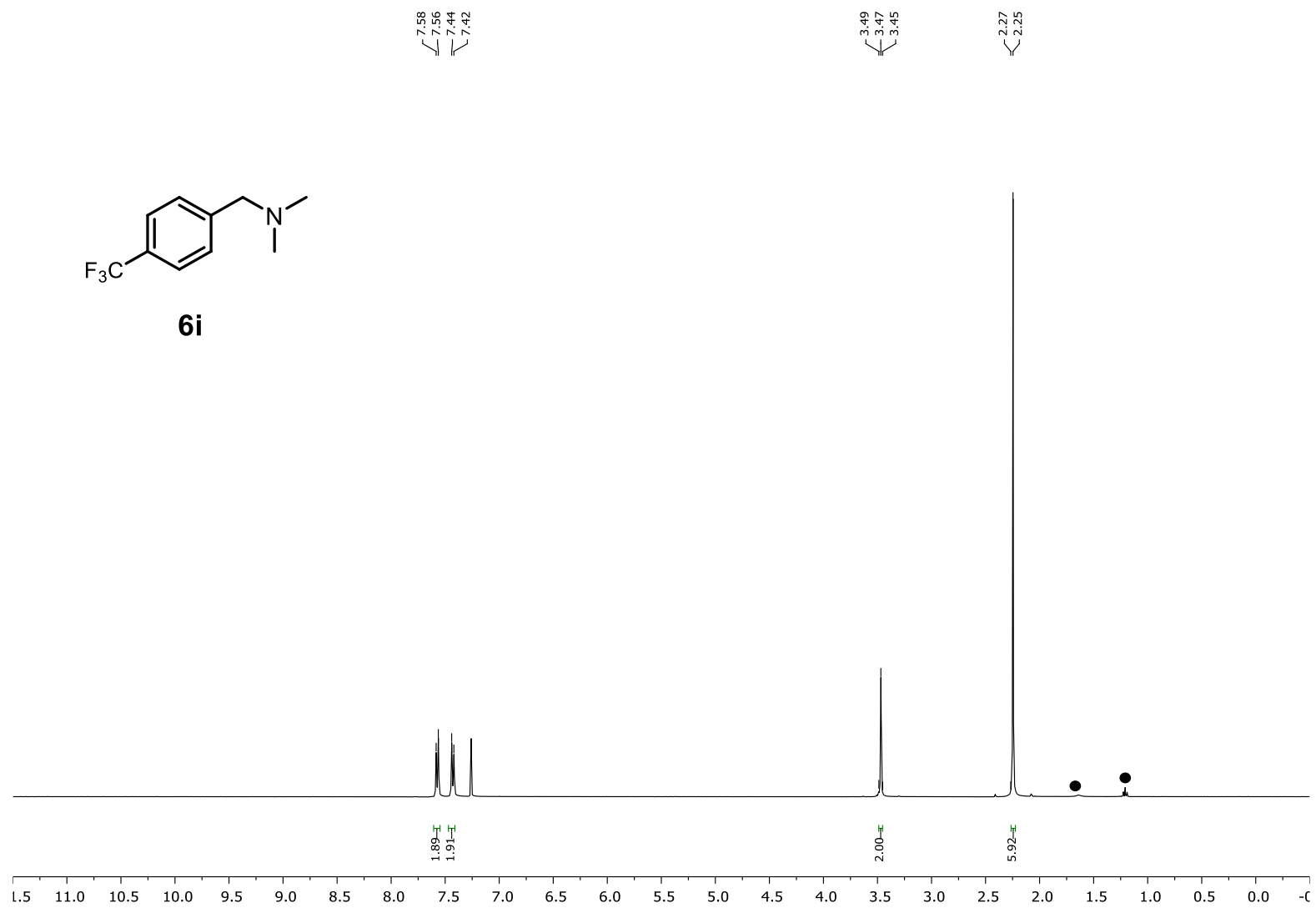


Figure S54: ^1H NMR (400 MHz, CDCl_3) of **6i**, ● = water, grease.

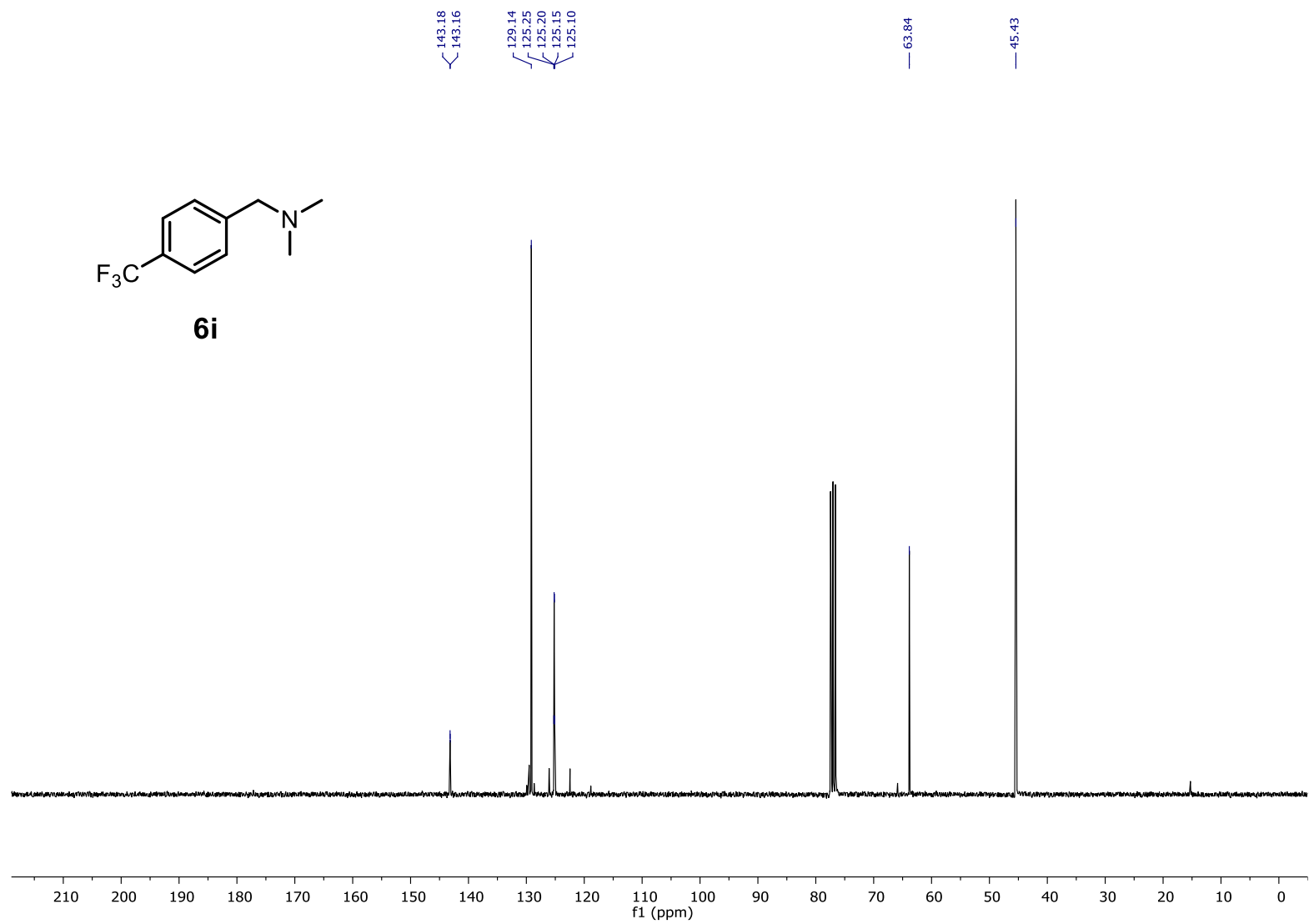


Figure S55: ¹³C NMR (101 MHz, CDCl₃) of **6i**.

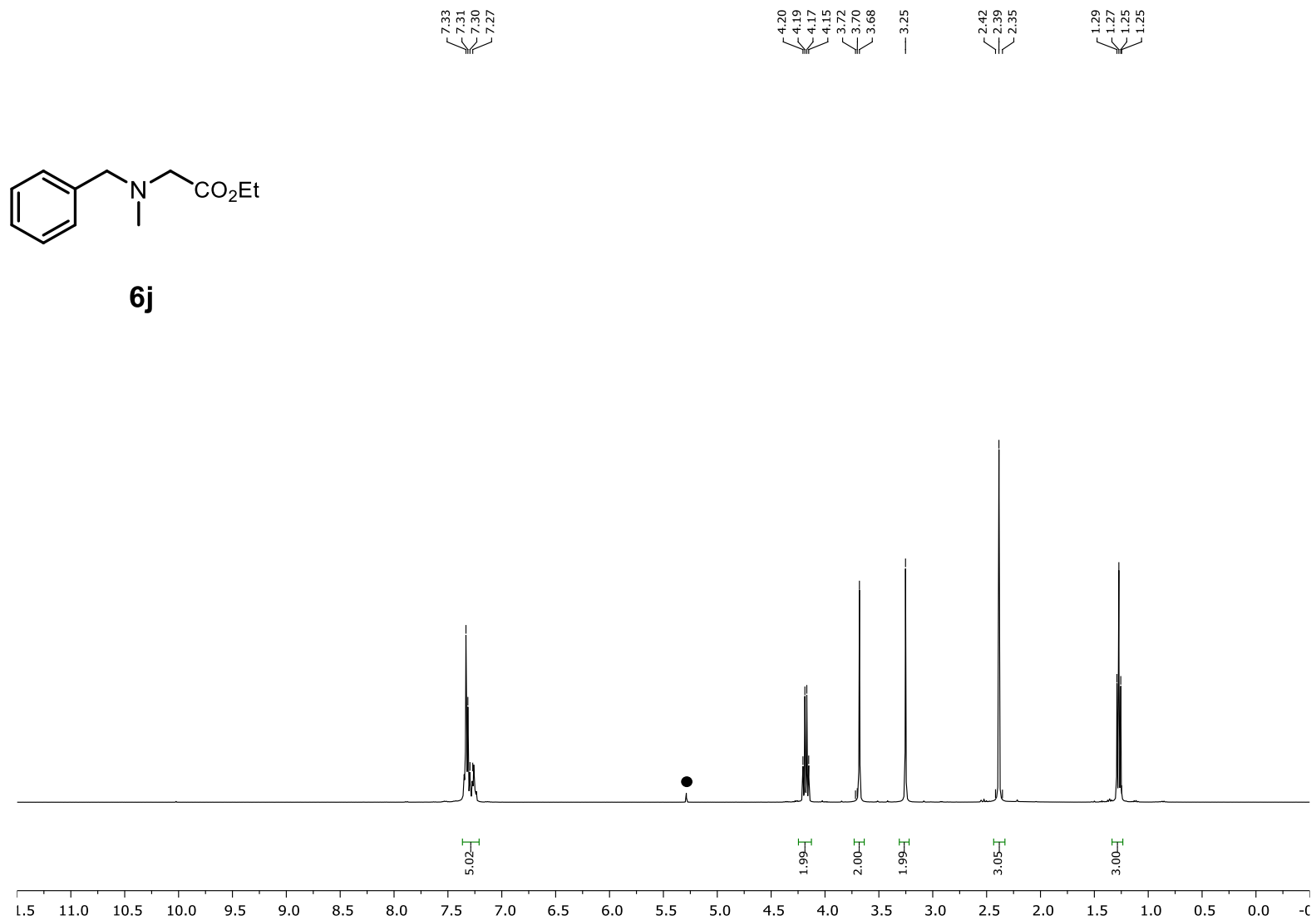


Figure S56: ^1H NMR (400 MHz, CDCl_3) of **6j**, ● = CH_2Cl_2 .

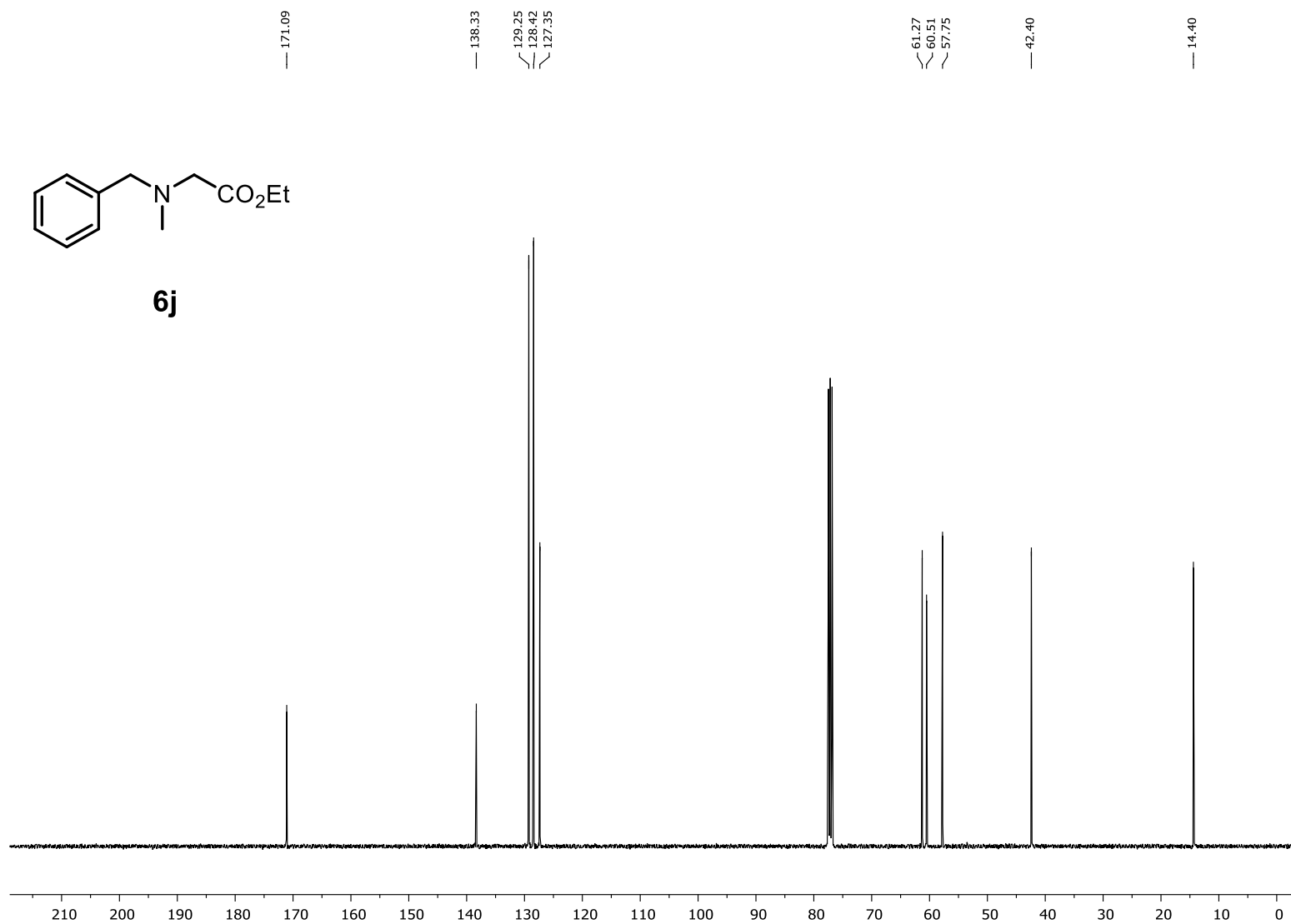
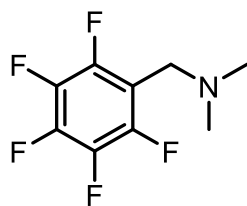


Figure S57: ¹³C NMR (101 MHz, CDCl₃) of **6j**.



6k

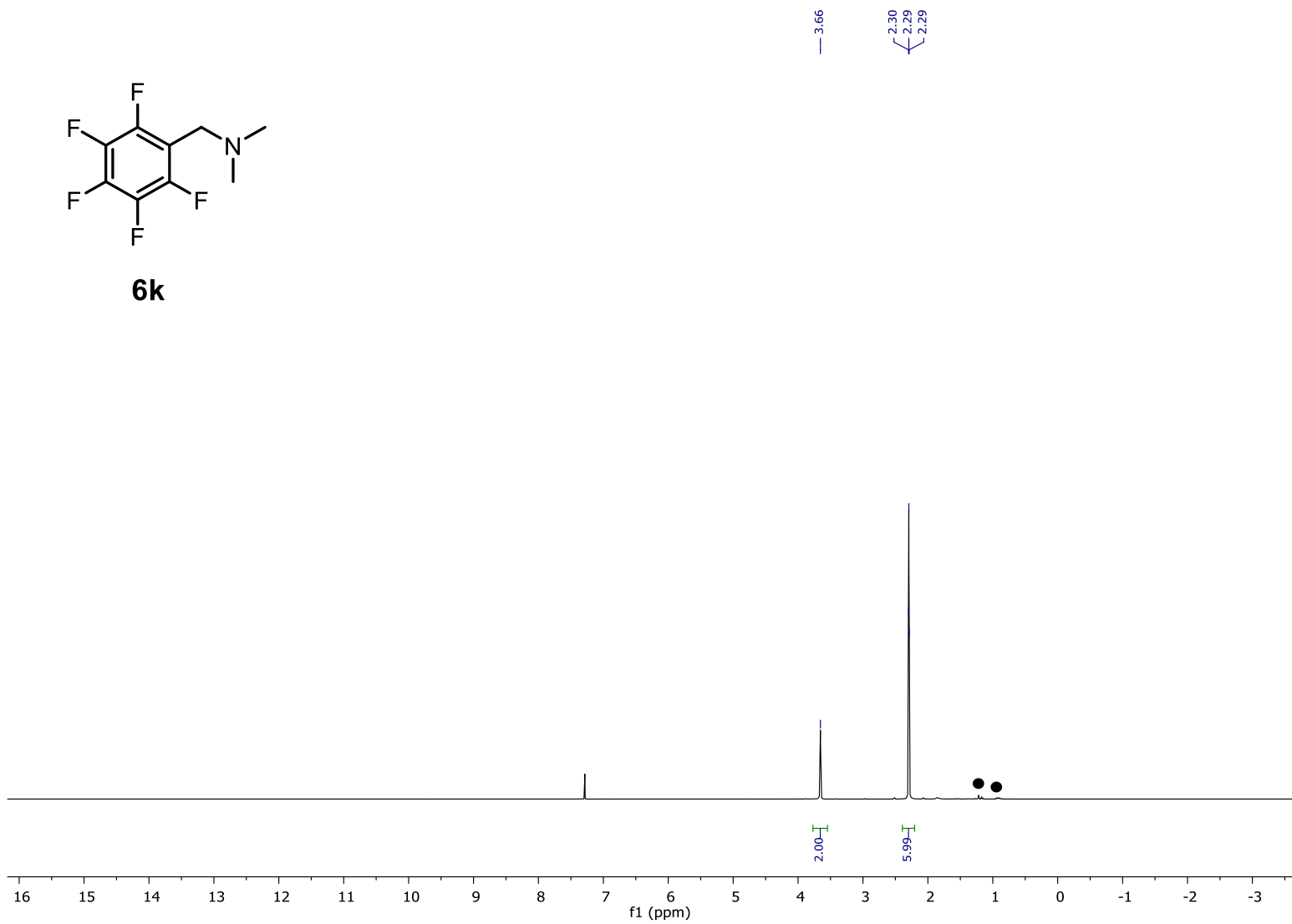


Figure S58: ^1H NMR (400 MHz, CDCl_3) of **6k**, ● = water, grease.

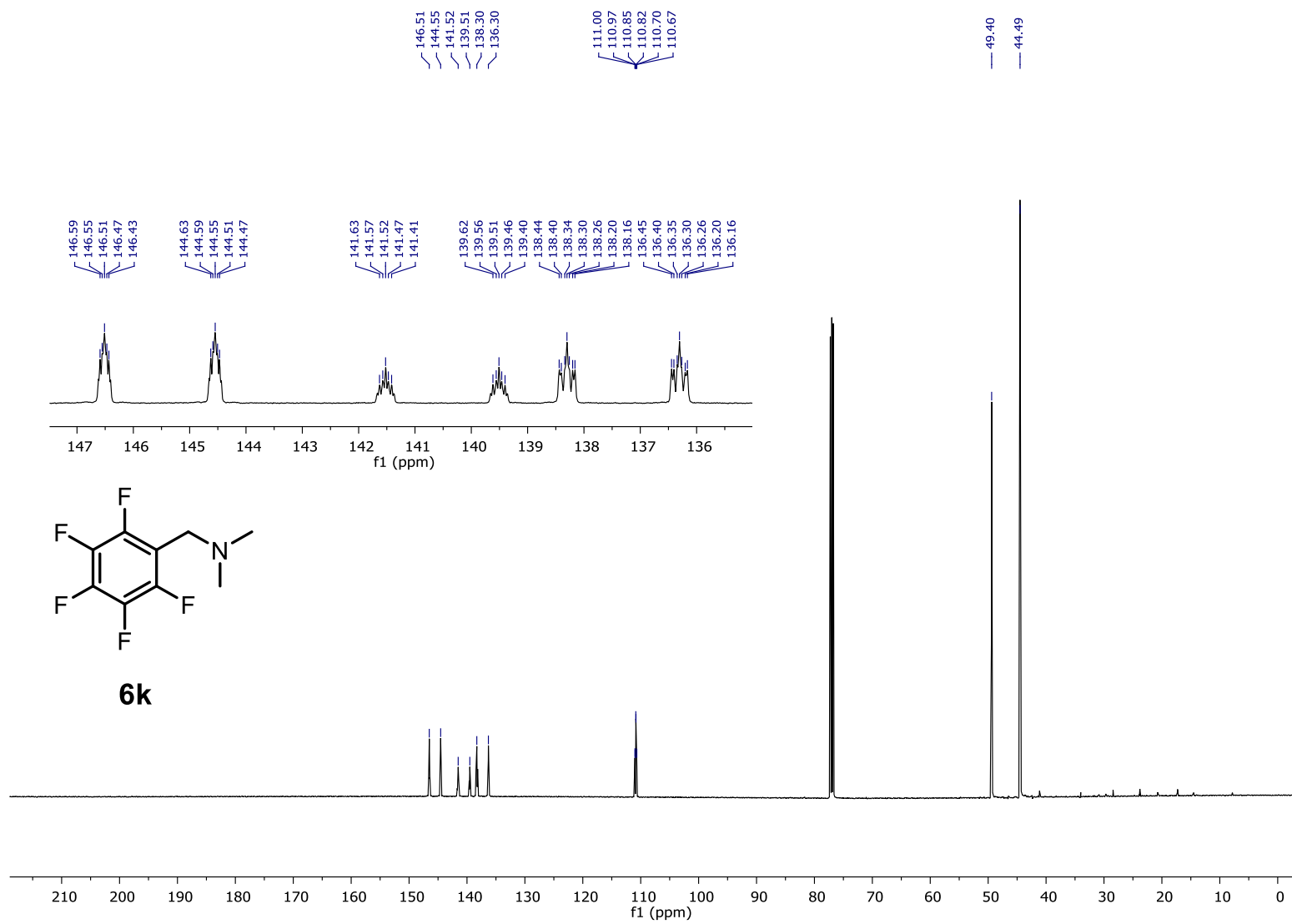


Figure S59: ¹³C NMR (126 MHz, CDCl₃) of **6k**.

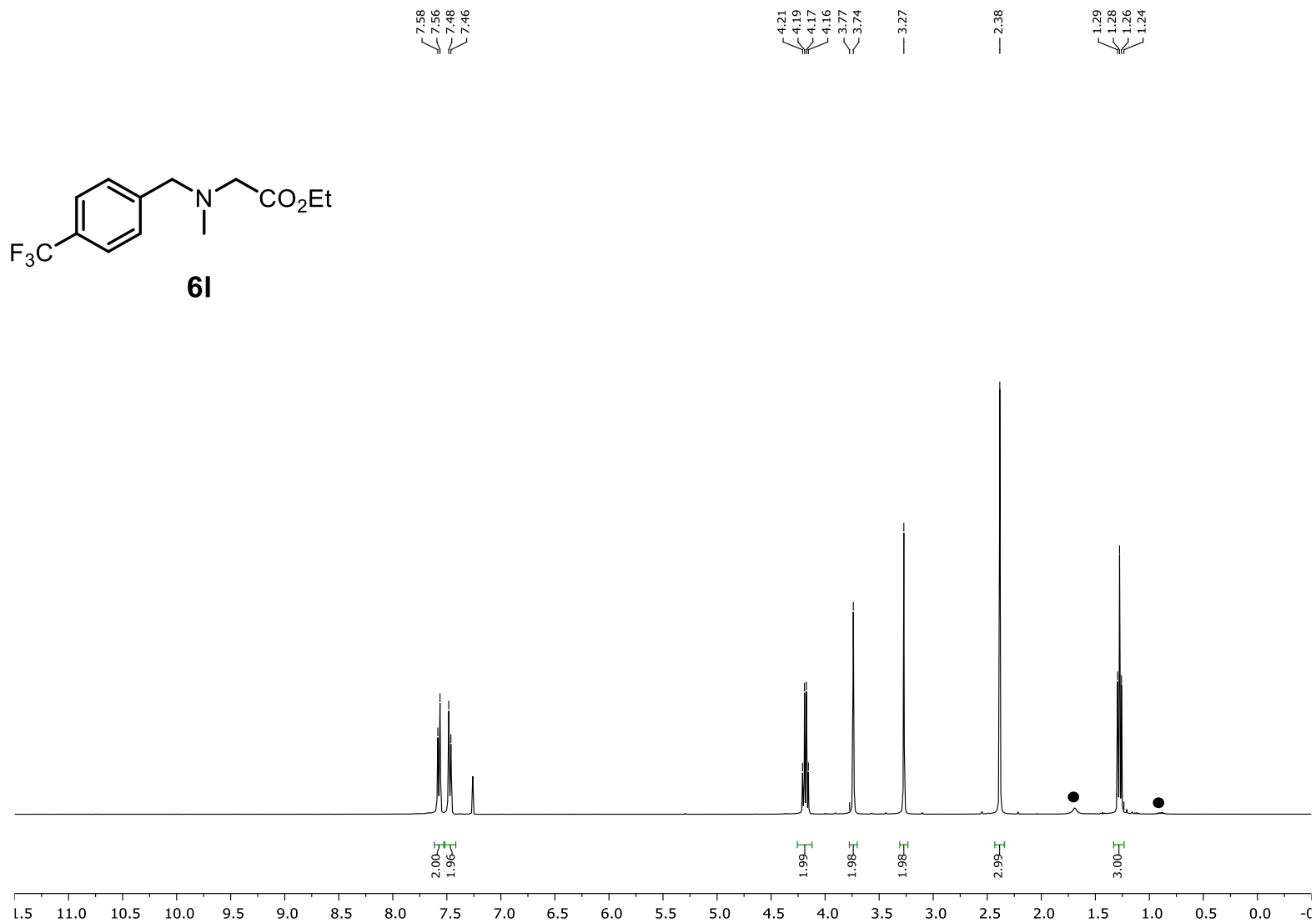


Figure S60: ^1H NMR (400 MHz, CDCl_3) of **6I**, ● = water, grease.

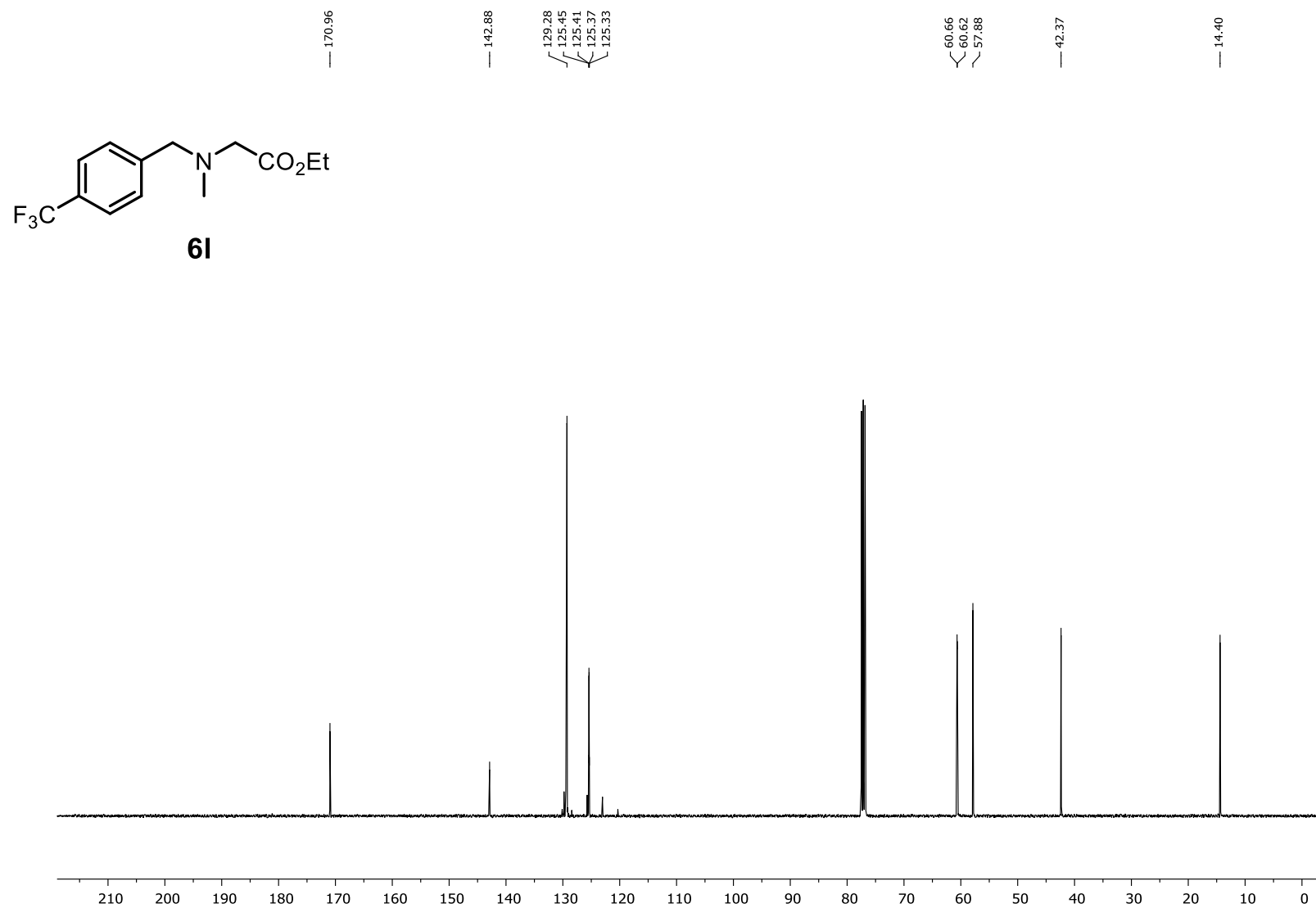


Figure S61: ^{13}C NMR (101 MHz, CDCl_3) of **6l**.

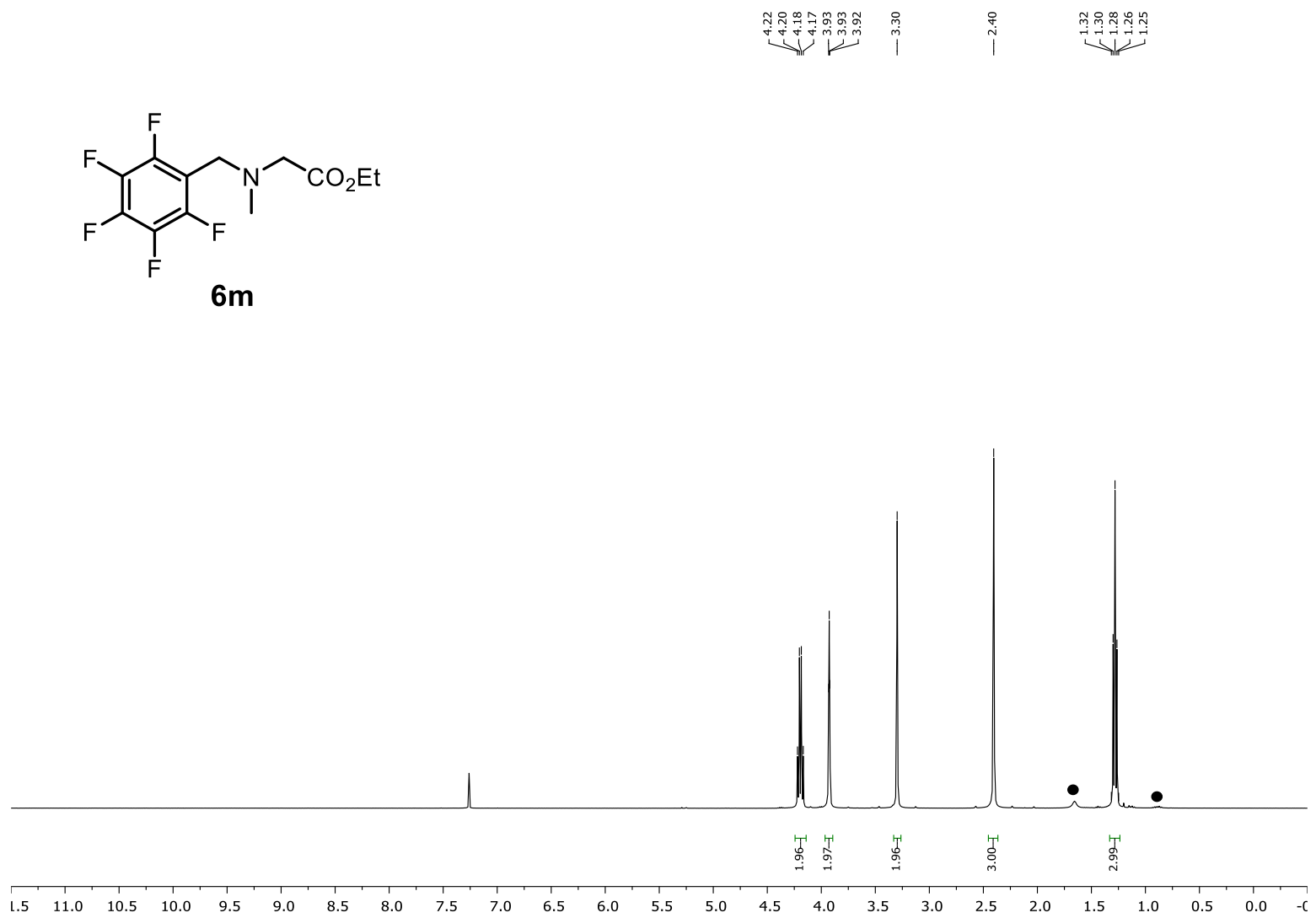


Figure S62: $^1\text{H NMR}$ (400 MHz, CDCl_3) of **6m**, ● = water, grease.

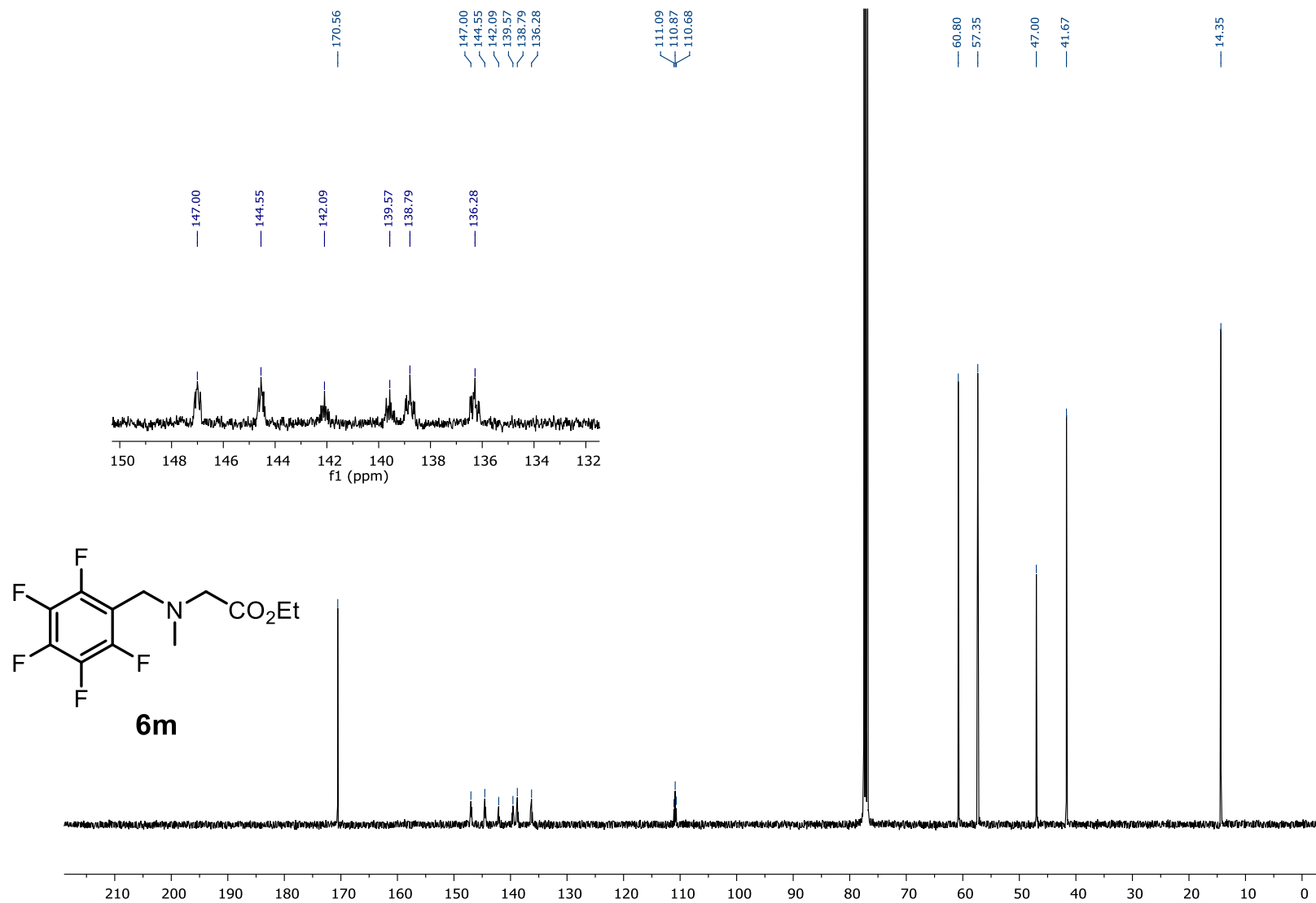


Figure S63: ¹³C NMR (101 MHz, CDCl₃) of **6m**.

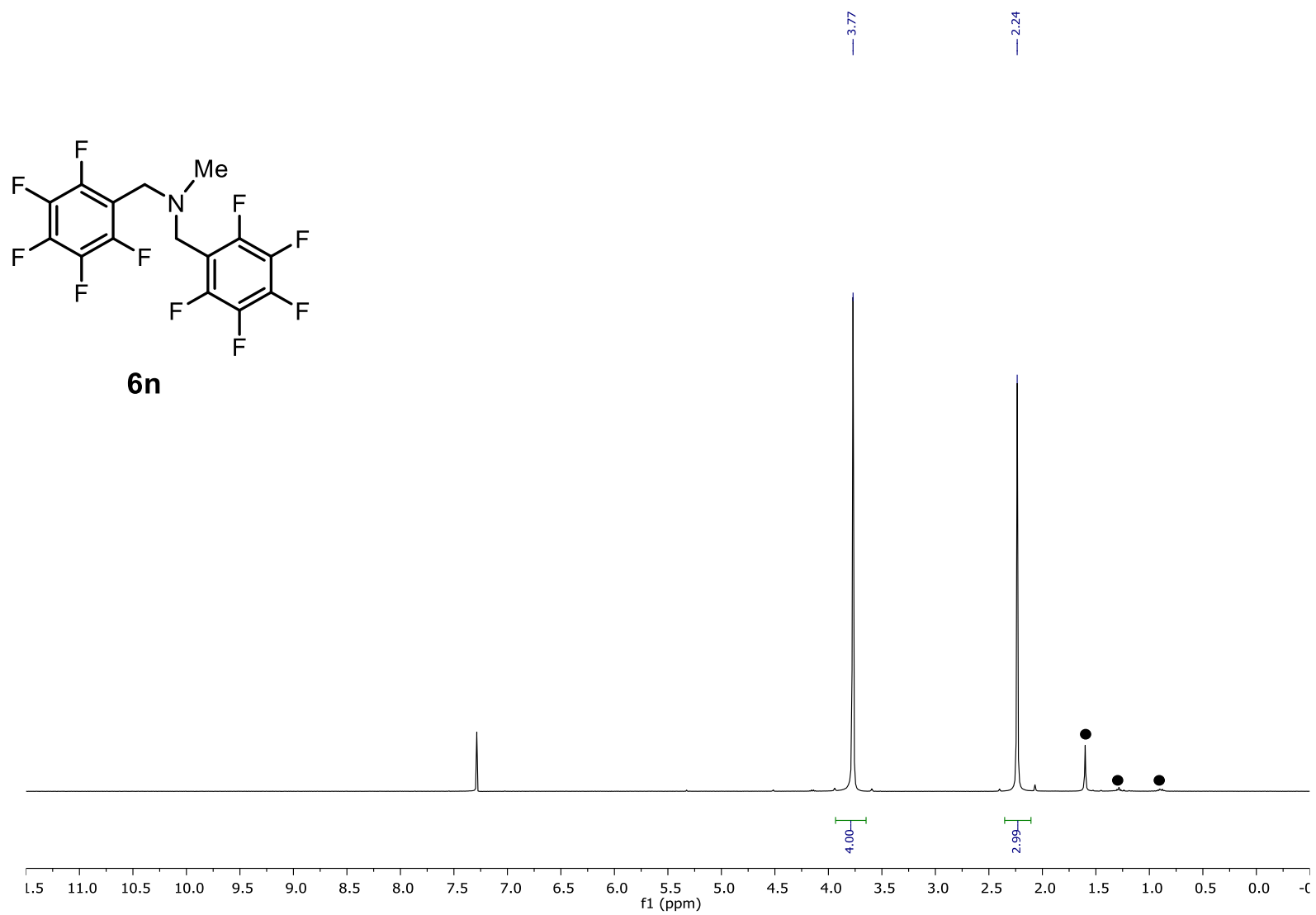


Figure S64: $^1\text{H NMR}$ (400 MHz, CDCl_3) of **6n**, ● = water, grease.

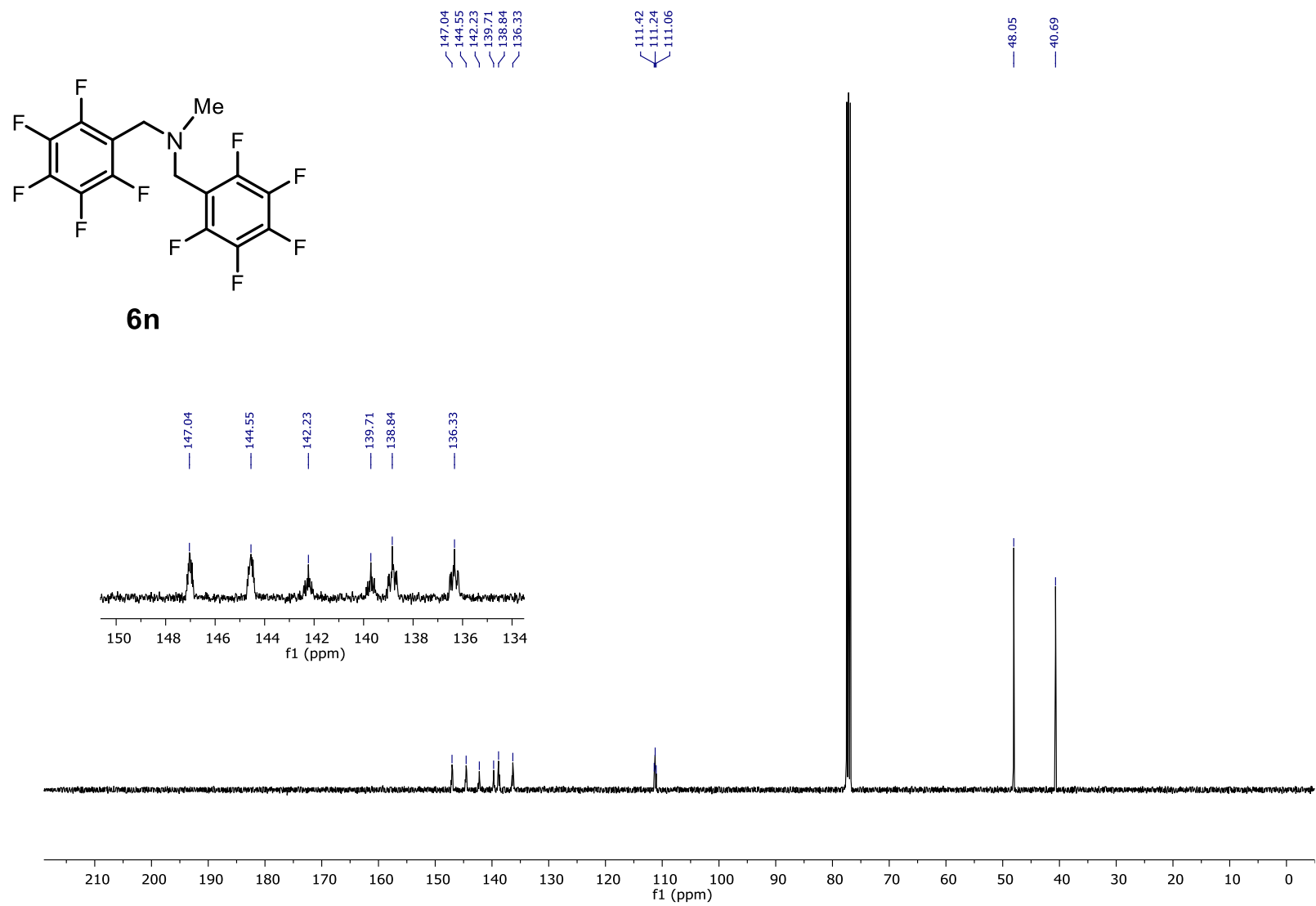


Figure S65: ^{13}C NMR (101 MHz, CDCl_3) of **6n**.

References

- [1] *APEX suite of crystallographic software, APEX 2, version 2008.4.*, Bruker AXS Inc., Madison, Wisconsin, USA (2008).
- [2] *SAINT, version 7.56a, SADABS, version 2008.1*, Bruker AXS Inc., Madison, Wisconsin, USA (2008).
- [3] Hübschle, C. B.; Sheldrick, G. M.; Dittrich, B., *SHELXLE, J. Appl. Crystallogr.* **2011**, *44*, 1281-1284.
- [4] Sheldrick, G. M., *SHELXL-2014*, University of Göttingen, Göttingen, Germany (2014).
- [5] Sheldrick, G. M., *SHELXL-97*, University of Göttingen, Göttingen, Germany (1998).
- [6] Wilson, A. J. C., *International Tables for Crystallography*, Dordrecht, The Netherlands, Kluwer Academic Publishers (1992).
- [7] Spek, A. L., *J. Appl. Cryst.* **2003**, *36*, 7-13.
- [8] Spek, A. L., *Acta Cryst.* **2009**, *D65*, 148-155.
- [9] F. Neese, Version 3.0.3 ed., Max Plank Institute for Bioinorganic Chemistry, Mühlheim an der Ruhr, Germany, **Jan 2012**.
- [10] J. P. Perdew, W. Yue, *Phys. Rev. B* **1986**, *33*, 8800.
- [11] J. P. Perdew, *Phys. Rev. B* **1986**, *33*, 8822.
- [12] A. D. Becke, *J. Chem. Phys.* **1986**, *84*, 4524.
- [13] A. D. Becke, *J. Chem. Phys.* **1993**, *98*, 5648.
- [14] C. T. Lee, W. T. Yang, R. G. Parr, *Phys. Rev. B* **1988**, *37*, 785.
- [15] A. Schäfer, H. Horn, R. Ahlrichs, *J. Chem. Phys.* **1992**, *97*, 2571.
- [16] A. Schäfer, C. Huber, R. Ahlrichs, *J. Chem. Phys.* **1994**, *100*, 5829.
- [17] K. Eichkorn, O. Treutler, H. Ohm, M. Häser, R. Ahlrichs, *Chem. Phys. Lett.* **1995**, *240*, 283.
- [18] K. Eichkorn, O. Treutler, H. Ohm, M. Häser, R. Ahlrichs, *Chem. Phys. Lett.* **1995**, *242*, 652.
- [19] R. Dennington, T. Keith, J. Milliam, Version 5.0 ed., Semichem Inc., Shawnee Mission KS, **2009**.
- [20] F. Neese, F. Wennmohs, A. Hansen and U. Becker, *Chem. Phys.*, **2009**, *356*, 98.
- [21] K. Eichkorn, F. Weigend, O. Treutler and R. Ahlrichs, *Theor. Chem. Acc.*, **1997**, *97*, 119.

- [22] C. J. van Wüllen, *J. Chem. Phys.*, **1998**, *109*, 392.
- [23] a) D. Rackel, V. Kais, P. Kreitmeier, O. Reiser, *Beilstein J. Org. Chem.* **2014**, *10*, 2157-2165; b) D. Lenhart, A. Pöthig, T. Bach, *Chem. Eur. J.* **2016**, *22*, 6519-6523
- [24] J. W. Tucker, J. M. R. Narayanam, S.W. Krabbe, C. R. J. Stephenson, *Org. Lett.* **2010**, *12*, 2, 368-371
- [25] Q. Lei, Y. Wei, D. Talwar, C. Wang, D. Xue, J. Xiao, *Chem. Eur. J.*, **2013**, *19*, 4021-4029
- [26] R. Feng, J. Yao, Z. Liang, Z. Liu, Y. Zhang, *J. Org. Chem.* **2013**, *78*(8), 3688
- [27] J. P. Barham, M. P. John, J. A. Murphy, *J. Am. Chem. Soc.* **2016**, *138*, 15482-15487
- [28] J. Michalak, H. B. Zhai, M. S. Platz, *J. Phys. Chem.* **1996**, *100*, 14028-14036
- [29] D. Lenhardt, A. Bauer, A. Pöthig, T. Bach, *Chem. Eur. J.* **2016**, *22*, 6519–6523
- [30] S. L. Murov, I. Carmichael, G. L. Hug, “*Handbook of Photochemistry*” , 2nd edition, Marcel Dekker, New York, 1993.
- [31] H. J. Kuhn, S. E. Braslavsky, R. Schmidt, *Pure Appl. Chem.* 2004, **76**, 2105–2146.
- [32] J. N. Demas, W. D. Bowman, E. F. Zalewski, R. A. Velapoldi, *J. Phys. Chem.* 1981, **85**, 2766–2771.
- [33] Y. Kaneko, Y. Nishimura, T. Arai, H. Sakuragi, K. Tokumaru, D. Matsunaga, *J. Photochem. Photobiol.* **1995**, *89*, 37
- [34] H.-C. Ku, C.-C. Wang, C.-H. Tu, *J. Chem. Eng. Data*, **2008**, *53*, 566–573
- [35] X.-H. Fan, Y.-P. Chen, C.-S. Su, *J. Chem. Eng. Data*, **2016**, *61*, 920–927
- [36] Hatchard, C. G.; Parker, C. A. *Proc. Roy. Soc. (London)* **1956**, *A235*, 518–536